STATE OF FLORIDA

Instrumentation Data Interpretation

Contract PR490902

Michael I. Hammons, Ph.D., P.E.
David Timm, Ph.D.
James Greene, P.E.

September 2007

STATE MATERIALS OFFICE

DISCLAIMER

The opinions, findings and conclusions expressed in this publication are those of the authors and do not necessarily reflect those of the State of Florida Department of Transportation.

SI (MODERN METRIC) CONVERSION FACTORS

APPROXIMATE CONVERSIONS TO SI UNITS

SYMBOL	WHEN YOU KNOW	MULTIPLY BY	TO FIND	SYMBOL
LENGTH				
in	inches	25.4	millimeters	mm
ft	feet	0.305	meters	m
yd	yards	0.914	meters	m
mi	miles	1.61	kilometers	km

SYMBOL	WHEN YOU KNOW	MULTIPLY BY	TO FIND	SYMBOL
AREA				
in^2	square inches	645.2	square millimeters	mm^2
ft^2	square feet	0.093	square meters	m^2
yd^2	square yard	0.836	square meters	m^2
ac	acres	0.405	hectares	ha
mi^2	square miles	2.59	square kilometers	km^2

SYMBOL	WHEN YOU KNOW	MULTIPLY BY	TO FIND	SYMBOL
VOLUME				
fl oz	fluid ounces	29.57	milliliters	mL
gal	gallons	3.785	liters	L
ft^3	cubic feet	0.028	cubic meters	m^3
yd^3	cubic yards	0.765	cubic meters	m^3
NOTE: volumes greater than 1000 L shall be shown in m^3				

SYMBOL	WHEN YOU KNOW	MULTIPLY BY	TO FIND	SYMBOL
MASS				
oz	ounces	28.35	grams	g
lb	pounds	0.454	kilograms	kg
T	short tons (2000 lb)	0.907	megagrams (or "metric ton")	Mg (or "t")

SYMBOL	WHEN YOU KNOW	MULTIPLY BY	TO FIND	SYMBOL
TEMPERATURE (exact degrees)				
^oF	Fahrenheit	5 (F-32)/9 or (F-32)/1.8	Celsius	^oC

SYMBOL	WHEN YOU KNOW	MULTIPLY BY	TO FIND	SYMBOL
ILLUMINATION				
fc	foot-candles	10.76	lux	lx
fl	foot-Lamberts	3.426	$candela/m^2$	cd/m^2

SYMBOL	WHEN YOU KNOW	MULTIPLY BY	TO FIND	SYMBOL
FORCE and PRESSURE or STRESS				
lbf	poundforce	4.45	newtons	N
lbf/in^2	poundforce per square inch	6.89	kilopascals	kPa

APPROXIMATE CONVERSIONS TO SI UNITS

SYMBOL	WHEN YOU KNOW	MULTIPLY BY	TO FIND	SYMBOL
LENGTH				
mm	millimeters	0.039	inches	in
m	meters	3.28	feet	ft
m	meters	1.09	yards	yd

SYMBOL	WHEN YOU KNOW	MULTIPLY BY	TO FIND	SYMBOL
AREA				
mm^2	square millimeters	0.0016	square inches	in^2
m^2	square meters	10.764	square feet	ft^2
m^2	square meters	1.195	square yards	yd^2
ha	hectares	2.47	acres	ac

SYMBOL	WHEN YOU KNOW	MULTIPLY BY	TO FIND	SYMBOL
VOLUME				
mL	milliliters	0.034	fluid ounces	fl oz
L	liters	0.264	gallons	gal
m^3	cubic meters	35.314	cubic feet	ft^3
m^3	cubic meters	1.307	cubic yards	yd^3

SYMBOL	WHEN YOU KNOW	MULTIPLY BY	TO FIND	SYMBOL
MASS				
g	grams	0.035	ounces	oz
kg	kilograms	2.202	pounds	lb
Mg (or "t")	megagrams (or "metric ton")	1.103	short tons (2000 lb)	T

SYMBOL	WHEN YOU KNOW	MULTIPLY BY	TO FIND	SYMBOL
TEMPERATURE (exact degrees)				
ºC	Celsius	1.8C+32	Fahrenheit	ºF

SYMBOL	WHEN YOU KNOW	MULTIPLY BY	TO FIND	SYMBOL
ILLUMINATION				
lx	lx	lx	lx	lx
cd/m^2	cd/m^2	cd/m^2	cd/m^2	cd/m^2

SYMBOL	WHEN YOU KNOW	MULTIPLY BY	TO FIND	SYMBOL
FORCE and PRESSURE or STRESS				
N	newtons	0.225	pound force	lbf
kPa	kilopascals	0.145	pound force per square inch	lbf/in^2

*SI is the symbol for the International System of Units. Appropriate rounding should be made to comply with Section 4 of ASTM E380.

TECHNIAL REPORT DOCUMENTATION

1. Report No.	2. Government Accession No.	3. Recipient's Catalog No.
4. Title and Subtitle Instrumentation Data Interpretation		5. Report Date September 2007
		6. Performing Organization Code
7. Author(s) Michael I. Hammons, David Timm, James Greene		8. Performing Organization Report No.
9. Performing Organization Name and Address Applied Research Associates, Inc. 5000 NW 27th Court, Suite E Gainesville, FL 32606		10. Work Unit No. (TRAIS)
		11. Contract or Grant No. PR 490902
12. Sponsoring Agency Name and Address Florida Department of Transportation 605 Suwannee Street Tallahassee, FL 32399-0450		13. Type of Report and Period Covered Final Report September 2005 to September 2007
		14. Sponsoring Agency Code
15. Supplementary Notes		

16. Abstract

The use of embedded pavement instrumentation has been an important technology in the advancement of pavement engineering. Responses measured at critical locations in the structure enable engineers to develop a fundamental understanding of the interaction between pavement response and pavement performance. Virtually every road test or accelerated pavement test facility, with the exception of the WesTrack experiment, has utilized embedded instrumentation to gain valuable mechanistic-empirical information.

While instrumentation has been used successfully, in-situ measurement of pavement response under dynamic wheel loadings can be a technically challenging and expensive task. Careful selection and installation of sensors are prerequisites for a successful instrumentation project. The selection of instruments depends upon the type of pavement and the objectives of the experiment. The instruments should be sensitive enough to produce the necessary data while reliable enough to ensure that dependable data can be obtained throughout the period of the experiment. This research provides guidelines for the sensor planning, selection, calibration and analysis required for a successful instrumentation project.

17. Key Word	18. Distribution Statement
Instrumentation, Accelerated Pavement Testing, Heavy Vehicle Simulator, Sensor, Mechanistic-Empirical Pavement Design Guide, Pavement Performance, Pavement Response	No Restrictions

19. Security Classif. (of this report)	20. Security Classif. (of this page)	21. No. of Pages	22. Price
Unclassified	Unclassified	120	

TABLE OF CONTENTS

LIST OF FIGURES

LIST OF TABLES

1 INTRODUCTION

1.1 Background

Pavement response is the reaction of a pavement to wheel load or to environmental factors such as changes in moisture or temperature. Pavement responses are often related to the development of pavement distresses such as rutting, cracking and pavement roughness. Pavement performance refers to the serviceability of pavement over time, which is quantified in terms of the extent and severity of pavement distresses such as rut depth, crack patterns, roughness, and surface friction.

Accelerated pavement testing (APT) is the application of wheel loadings to specifically constructed or in-service pavements to determine pavement response and performance under controlled, accelerated accumulation of damage (Metcalf 1996). APT allows agencies to collect response and performance data under controlled conditions more rapidly than possible using test sections placed along in-service roadways. Hugo and Martin (2004) documented the following applications of APT:

- Evaluation, validation, and improvement of structural designs
- Vehicle/pavement/environment interactions
- Evaluation of materials and tests
- Enhancement of modeling in pavement engineering
- Development and validation of rehabilitation, construction, and maintenance strategies
- Pavement engineering applications and issues
- Improvement in pavement economics and management

The Florida Department of Transportation (FDOT) recognized the benefits of APT and purchased a Heavy Vehicle Simulator (HVS), Mark IV model in 2000. Florida's APT equipment and facility, located at the State Materials Office (SMO) at Materials Research Park in Gainesville, Florida, consists of eight linear test tracks, each track measuring approximately 150 feet long by 12 feet wide. There are two additional test tracks designed with water table control capabilities with the supporting pavement foundation layers. To date, several experiments have been completed successfully at the facility, including three experiments of flexible pavements, two experiments on rigid pavements, one experiment on composite pavements, and two experiments on base course.

1.2 Objectives

The objective of this project was to assess the appropriateness of available instrumentation to measure key pavement response parameters (strains, stresses, temperatures, deflections, etc.) and to use the principles of engineering mechanics to relate these parameters to material and pavement performance. APT requires that key material and structural response parameters be measured effectively and accurately. Large volumes of data that must be efficiently processed to facilitate engineering mechanics based analysis. Key activities for this project included the following:

- Evaluate the effectiveness of current practices.
- Develop appropriate protocols/methodologies to assess the effectiveness/appropriateness (including accuracy, precision, causes of errors, effects of pavement structures, etc.) of the various instrumentation types used in APT test tracks.
- Identify materials properties and performance indicators that can be realistically measured using embedded instruments.
- Develop appropriate data analysis methodologies for instrumentation measurements.
- Develop a guide or best practice for APT test track instrumentation calibration, installation, and performance monitoring.

2 INSTRUMENTATION OVERVIEW

2.1 Data Collected at APT Facilities

Saeed and Hall (2003) identified a number of data elements commonly collected at APT sites:

- Administrative
- Load application
- Pavement description
- Material characterization
- Environmental conditions
- Pavement response
- Pavement performance

Because the focus of this research is on instrumentation for APT, we will focus on the pavement response data element and its relationship to the pavement performance data element.

2.2 Instrumentation Planning

In-situ measurement of pavement response under dynamic wheel loadings can be a technically challenging and expensive task. Careful selection and installation of sensors are prerequisites for a successful instrumentation project (Hilderbrand 2002).

It is important to distinguish between dynamic and static measurements (Loulizi et al. 2001). Dynamic measurements are made to record the effects of moving wheel loads on the pavement system. Dynamic measurements are collected as a wave with a fixed length and sampling frequency. Static measurements are made to record the effects of environment on the pavement system. Static measurements are typically made at specific time (or load repetition) intervals.

The selection of instruments depends upon the type of pavement and the objectives of the experiment. The instruments should be sensitive enough to produce the necessary data

while reliable enough to ensure that dependable data can be obtained throughout the period of the experiment (Nasser 2001). Timm et al. (2004) suggested the following criteria for evaluating pavement instrumentation:

1. Ability to measure the desired responses
2. Cost
3. Availability (i.e., delivery times)
4. Reputation for good reliability
5. Continuity with previous research efforts.

Hilderbrand (2002) and Steyn et al. (2006) developed lists of factors to be considered when executing an APT instrumentation project. The following outline of a complete APT instrumentation program was synthesized from their writings:

1. Identify the experiment objectives
   a. Define the questions that need to be answered
   b. Develop hypotheses about mechanisms that will control the behavior of the system
   c. Select the parameters that need to be monitored
2. Develop instrumentation plan
   a. Perform a theoretical calculation to predict the expected magnitude and distribution of responses
   b. Establish the requirements for sensitivity and range of the instruments
   c. Select instruments that can withstand the harsh environment
   d. Select the sensor locations
   e. Evaluate potential for sensor to alter the response in the vicinity of the sensor
   f. Develop an installation plan, including calibration and maintenance requirements
   g. Develop a data collection, processing, presentation, interpretation and reporting plan
3. Implement instrumentation plan
   a. Procure, install and calibrate instruments in accordance with the instrumentation plan
   b. Document as-built location of sensors and other factors that may affect readings from the instruments
   c. Collect, process, interpret and report data in accordance with the instrumentation plan
4. Evaluate instrumentation plan
   a. Evaluate whether the objectives of the experiment were met
   b. Improve instrumentation plans for future experiments

2.3 Identification of Instrumentation Errors

Nassar (2001) identified the following types of error in instrumentation systems:

1. Intrusive Error. The inclusion of the sensor may well change the response of the system.

2. Combination Error. Cases can arise where a sensor may respond to input other than their designed input.
3. Dynamic error. Measuring dynamic response with sensors calibrated under static conditions may give rise to error. An example would be hysteresis effects, where loading and unloading responses are different.
4. Signal conditioning errors. Error may arise in the process of amplifying and filtering a sensor's signal or in interfacing with an instrumentation system.
5. Repeatability. Systematic change from test to test may not be accounted for in the calibration process.

Accurate knowledge of sensor location within the pavement is critical during evaluation and modeling of pavement behavior. Burnham (1999) found the use of core samples to be effective in determining the orientation of sensors from PCC pavements at the Mn/ROAD project. While most sensors were found to be oriented close to design for slope and direction, he found significant differences between the design, as-built (post-construction survey) and in-situ depths of the sensors. He also found a few profound orientation problems, with one sensor rotated nearly 80 degrees from its intended orientation.

2.4 Pavement Response Data Elements

Pavement response is generally recorded in terms of deflection, strain, or pressure (stress). Pavement response data elements suggested by Saeed and Hall (2003) for APT are listed in Table 2-1.

Strain is usually measured near the bottom of HMA layers and at selected points near the center, edges, and joints of PCC slabs. Other relevant strain measures include strain at the top of granular base courses and at the top of the embankment. Vertical stress distributions through the depth of unbound base and embankment layers are used for settlement and rutting analyses; therefore, pressure sensors are typically placed in the base or embankment (Almohn et al. 2005).

Linear variable displacement transducers (LVDTs) are commonly used to measure permanent deformations. Most APT facilities collect air, pavement surface, and in-pavement temperatures. A few facilities collect temperatures in unbound and subgrade layers. Moisture content is sometimes measured in granular layers. The depth of the water table is typically monitored (Saeed and Hall 2003).

2.5 Pavement Performance Data Elements

Although pavement performance data is not the primary focus of this research, a brief discussion of pavement performance data elements is included for completeness. Pavement performance data include crack surveys and longitudinal and transverse profile measurements. These parameters are often measured manually, but some APT installations have semi-automated systems to measure certain pavement performance indicators. Table 2-2 presents typical pavement performance data elements.

Trained personnel usually perform a manual measurement of crack length and an assessment of their severity and extent. Usually, a photographic record is made to document the cracking at certain intervals of loading. Longitudinal and transverse cross sections are typically measured using rod and level or laser sensors. For rigid pavements, joint faulting measurements are made in conjunction with the profile survey (Saeed and Hall 2003).

Table 2-1. Pavement response data elements (Saeed and Hall 2003).

Data Element	Definition	Tolerances and Units
Load source	Source of the load, e.g., static, rolling (APT machine), impact (FWD), vibratory; list specific device used to load pavement, including model numbers, etc.	N/A
Load magnitude	Load imparted on pavement; list both total load and contact pressures at each wheel	± 1%, report in kN
Configuration	Number of contact areas, wheel position (spacing) of each load; a drawing is the best format to present this information	Distance: ± 1cm
Contact area	Area of the footprint of each tire on the pavement surface and the shape of the contact area	± 5cm
Loading rate	Frequency, speed, time, or other measure of how "fast" the load is applied to the pavement	Frequency: Hz Speed: kph
Response type	Deflection, strain, pressure (stress), pore pressure, etc.	N/A
Sensor type	Sensor mechanism (LVDT, MDD, etc.), type, model number, etc.	N/A
Sensor location	Location of the sensor in/on the pavement; a drawing may be the best method to display this information; include longitudinal, transverse, and depth data	± 1mm
Calibration factor	Number used to convert raw sensor readings into useable engineering units; e.g., 1.2 mV from the sensor corresponds to 0.01 m deflection	Absolute; report as *engineering units* / sensor unit
Calibration data	Date and place of last sensor calibration, technician that calibrated the sensor	N/A
Raw sensor data	Data as recorded by the sensor	Record sensor precision and units
Processed data	Data in appropriate engineering units	Record precision and units
Time stamp	Date and time of each sensor reading	Record the storage format of the timestamp
Repetitions	Number of APT loading cycles the pavement has experienced at time of data collection	Absolute
Test type	QC/QA, in-service, postmortem, etc.	N/A

Table 2-2. Pavement performance data elements.

Type of Information	Data Element	Definition
General	Survey date	Date(s) of survey
	Pretest condition	For in-service pavements, condition before APT load application and an estimate of traffic
	Number of repetitions	Number of load pulses applied to the pavement
	Survey purpose	Property being measured (smoothness, rutting, Pavement Condition Index, etc.)
	Survey method	Standard used to perform survey (ASTM D5340, etc.), or the complete documentation for the survey protocol
	Survey results	Results of the survey after the data have been reduced
	Variability	Standard deviation, range, confidence interval, standard error of estimate, etc.
	Raw data	Raw performance data should be stored and the storage format defined; e.g., distress data from a visual survey or elevation data from a roughness survey should be stored
Performance Measurement	Longitudinal profile	Elevation of the pavement surface in the longitudinal direction in relation to a datum or beam; data should be reduced to a strip chart of elevation vs. station or to an index number reflecting the condition of the pavement, such as the International Roughness Index
	Transverse cross sections	Elevation of the pavement surface in the transverse direction in relation to a datum or beam; data should be reduced to a strip chart of elevation vs. transverse location, or to an index number reflecting the condition of the pavement
	Rutting	Rutting is a special case of the transverse cross section
	Surface distresses	Surface distresses are recorded and reduced to an index number reflecting the condition of the pavement

2.6 Pavement Response Sensors

Table 2-3 contains a listing of typical pavement response data collected at APT facilities expanded from a table compiled by Saeed and Hall (2003). The types and locations of the pavement response sensors vary depending upon the type of pavement and objectives of the APT experiment. A more detailed discussion of pavement response sensors follows.

Table 2-3. Examples of pavement performance data collected at APT facilities.

APT Facility	Pavement Response			
	Strain Sensors	**Pressure Sensors**	**Multi-Depth Deflectometers (MDDs)**	**LVDTs**
CAL-APT	Top and bottom of the surface layer	None installed	Deflection of the top and bottom of AC, ATPB, AB, ASB, and subgrade (1 m)	Pavement surface deflection
CRREL-HVS	At the bottom of the surface layer	At three depths in the top half of the subgrade	Five levels, at the interface of each layer	Not installed
FHWA-PTF	Strains at the top and bottom of AC and PCC. PCC strains at corners, mid-slab, and along joints	Not installed	Not installed	Installed to measure surface deflections
INDOT/Purdue	Strains in the surface layer (top/bottom)	Not installed	Not installed	Only for UTW, surface deflection
KS-APT	At the bottom of AC in the wheel path	In the subgrade and at the interface of the granular layer and subgrade (in the wheel path)	Not installed	Dial gauges to measure surface deflection (one test only)
LTRC-PRF	Layer interface under the wheels	Layer interface under the wheels	Installed at layer interfaces	Not installed
Mn/ROAD	Bottom of AC in the wheel path. Near bottom and surface of PCC. Also on dowels.	Large diameter for bases, small for subgrade	Bottom of granular material and 2.4 m in to the subgrade	Surface deflections in the wheel path
NCAT Test Track	Longitudinal and transverse gauges located at the bottom of AC in the wheel path	Top of base and subgrade	Not installed	Not installed
OH-APLF	25 mm from the surface and bottom of PCC slabs at mid-slab and along slab edges. Dowel bars along the middle edge	Not installed	Not installed	At slab corners and along the longitudinal edge to measure surface deflections
TxMLS	Only on specially constructed test sections (evaluated at Victoria shakedown tests)	Only on specially constructed test sections (evaluated at Victoria shakedown tests)	Deflection at layer interfaces (three depths)	Not installed
Virginia Smart Road				
WES-HVS	3 locations; AC, AC/base interface	Installed on top of the subgrade	3 locations; 5 depths (layer interfaces) down to 2.1 m	2 locations; surface deflections
WesTrack	No pavement response instrumentation			

2.6.1 Strain

Strain measurements can be performed in bound and unbound materials. Usually, electrical resistance strain gauges are used in bound materials, while several types of displacement gauges are used in unbound materials (Hilderbrand 2002). Horizontal strains in HMA are usually measured to collect data related to the failure criteria used in the mechanistic-empirical pavement design procedures (Vijaynath 1999). Al-Qadi et al. (2005) measured strains in asphalt concrete to quantify their magnitude associated with thermal fatigue cracking. The two most critical locations to measure strain in flexible pavements are thought to be at the bottom of the HMA layer and at the top of the unbound granular layer (Timm et al. 2004). Some APT facilities also measure vertical strains in the top of the subgrade. In rigid pavements, horizontal strains are often measured in the center and edge of the slabs and at the joints.

Most strain sensors used to measure dynamic strains are based on the electrical resistance principle. When the sensor is stretched, the conductors in the sensor become longer and narrower, causing a corresponding increase in resistance to the flow of electrical current. A Wheatstone bridge is used to convert the change in resistance to a change in voltage. This induced voltage may be measured with a voltmeter or the resistor in the opposite leg may be adjusted to rebalance the bridge. In either case, the change in resistance that caused the induced voltage may be measured and converted to obtain the engineering units of strain.

2.6.1.1 Hot Mix Asphalt

The purpose of HMA strain sensors is to measure the dynamic strain responses at the bottom of the asphalt layer under moving traffic loads. These sensors may be deployed to measure both longitudinal and transverse strain (Timm et al. 2004, Romanoschi et al. 2004). Garg and Hayhoe (2001) found that longitudinal sensors were not particularly sensitive to the location of the moving wheel load, while transverse sensors were acutely sensitive to the position of the moving wheel. While dynamic strain measurement in HMA has been attempted with foil resistance strain gauges attached to carrier blocks or to cores extracted from the HMA, the use of H-gauges is far more common. H-gauges are manufactured by several manufacturers including Dynatest, CTL, and Kyowa. A typical H-gauge consists of an electrical resistance strain gauge embedded within a strip of glass-fiber reinforced epoxy with transverse stainless steel anchors at each end of the strip to form an H-shape (Figure 2-1). The transverse anchors are intended to ensure mechanical coupling to the HMA. It is important that the strip stiffness is approximately the same as the HMA stiffness (Hilderbrand 2004).

Because the H-gauge measures the average strain between the anchors, the length of the sensor should be three to five times the maximum aggregate size (Tabatabaee et al 1992).

H-gauges are designed to withstand the high placement temperatures of HMA and the compaction loads associated with pavement construction. They incorporate full Wheatstone bridge circuits within the sensor to reduce signal conditioning complexity. There are four active electrical resistance strain gauges incorporated in each sensor: two aligned in the longitudinal direction and two in the transverse direction. Individual

calibration sheets are provided with each sensor. The maximum range of the sensors is approximately ± 1500 με, which is well within the expected strain ranges for most flexible pavements. While Dynatest and CTL sensors generally have been reported to have good survival rates, Loulizi et al. (2001) reported that Kyowa sensors have been found to be unreliable.

Figure 2-1. Typical HMA horizontal strain sensor (H-sensor).

CTL manufactures an asphalt vertical strain sensor, shown in the photograph in Figure 2-2, which operates similarly to the horizontal H-sensors. The vertical extension on the lower surface of the sensor is useful for positioning the sensor prior to HMA placement.

Figure 2-2. CTL asphalt vertical strain sensor.

2.6.1.2 Portland Cement Concrete

Dynamic strain sensors in PCC provide elastic response verification under loads that do not damage the concrete. These sensors may be H-sensors similar to the HMA strain sensor, or may have a different geometry as shown in Figure 2-3. PML sensors, manufactured by Tokyo Sokki Kenkyujo, are intended for measuring strain in concrete or mortar under load testing. It consists of a Cu-Ni resistance strain gauge sealed between two thin resin plates. Saeed et al. (2000) reported using similar sensors in a rosette configuration, which measure strain at two orthogonal directions and at a 45° angle between the two orthogonal directions. This permits calculation of principal strains within the PCC slab.

Harvey et al. (2004) reports that it is difficult to interpret strain sensor output once damage to the PCC has occurred. The best configuration includes two of the same sensors at the top and bottom of the slab.

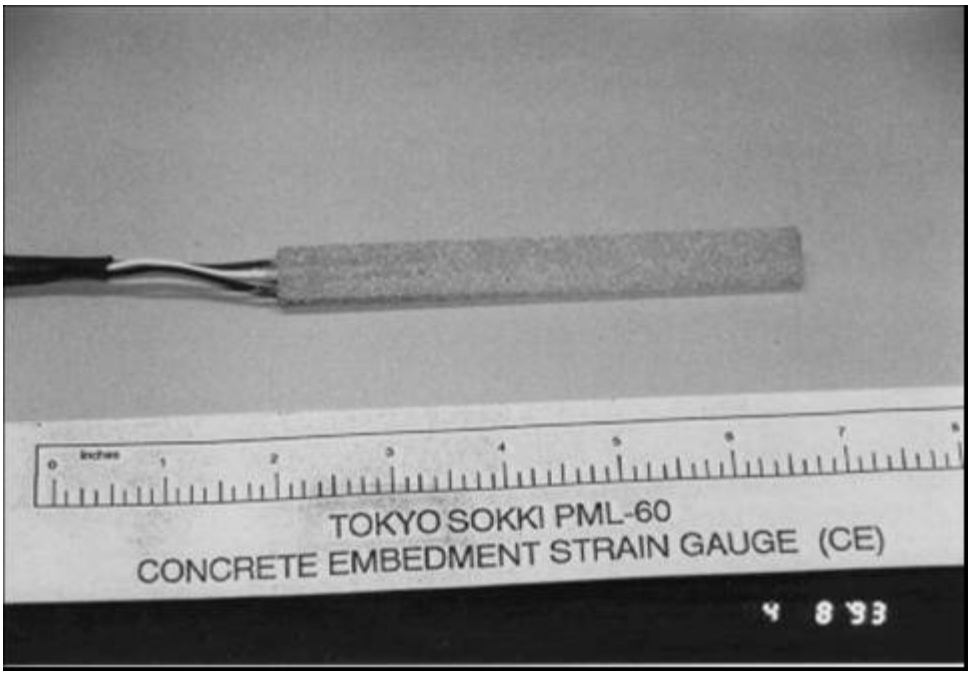

Figure 2-3. One type of PCC embedment strain sensor used at MnRoad.

Sheehan et al. (2004) installed custom-made embedment strain sensors manufactured from reinforcing bars in thin whitetopping pavement in Colorado. These sensors consisted of ½-inch long resistance strain gauges epoxied to the prepared surface of No. 3 reinforcing bars. The gauges were installed at two locations as shown in Figure 2-4: at the interface between the milled HMA surface and the thin whitetopping, and one inch above this interface. The reinforcing bars were 12 inches long at the interface, and 16 inches at 1 inch above the interface.

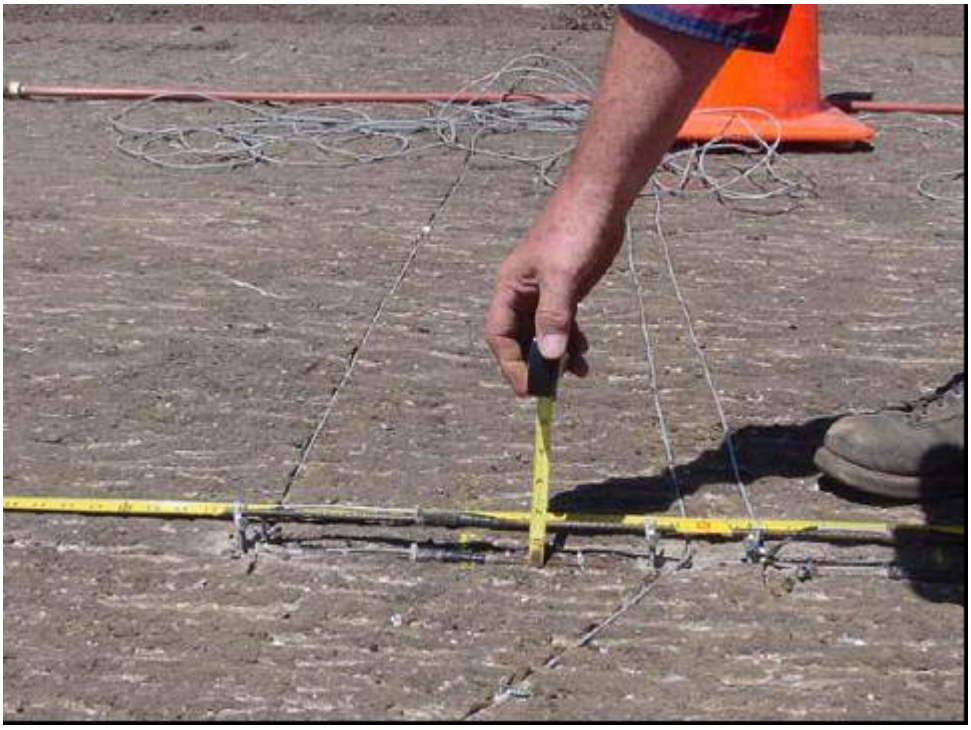

Figure 2-4. Embedment strain sensors fabricated from reinforcing bar.

Surface resistance strain gauges were also installed on the whitetopping just prior to commencement of loading (Sheehan et al. 2004). Figure 2-5 shows a photograph of these gauges, which were placed directly over the embedment gauges shown in Figure 2-5.

Figure 2-5. Surface strain gauges on surface of whitetoppping.

Carlson-type static strain sensors measure internal deformations and temperatures in PCC. These gauges are intended to provide long-term measurement of changes in slab shape due to environmental conditions, creep, shrinkage, and chemical growth. Carlson sensors consist of two coils of elastic wire enclosed in a sealed housing (Figure 2-6). When strain occurs, one coil of wire increases in length, while the other coil decreases.

The ratio of change in resistance of the two coils is correlated to strain, while the total change in resistance is related to temperature. Analysis of static strain data requires installation of two sensors in the same direction and at the same locations, with one near the top and the other near the bottom of the slab (Harvey et al. 2004). Harvey et al. (2004) have found the survivability of all static and dynamic strain sensors to be almost 100%.

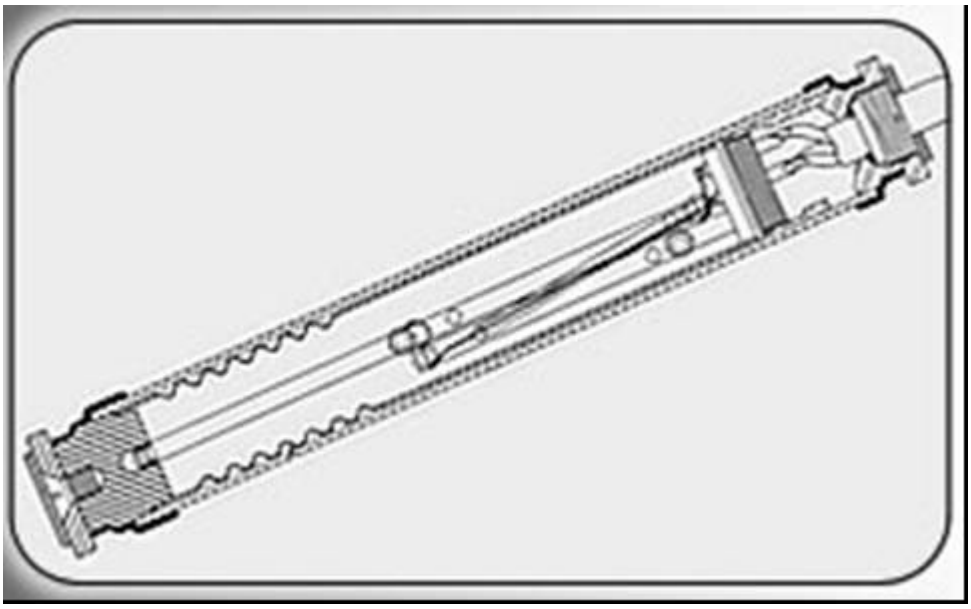

Figure 2-6. Carlson strain meter.

Vibrating wire strain sensors can be used to measure static strains in civil engineering applications. Many manufacturers market versions which are rugged enough for embedment in PCC. A vibrating wire strain sensor consists of two end blocks with a tensioned steel wire stretched between them. The end blocks move relative to one another as the concrete is strained, changing the tension in the wire. The tension in the wire is determined by an electromagnetic coil, which plucks the wire and measures its vibration frequency. Jeong and Zollinger (2004) used vibrating wire strain sensors to monitor curling and warping (static) strains in PCC slabs. Similarly, Nam et al. (2006) also employed vibrating wire strain sensors to measure the early-age behavior of continuously reinforced concrete pavements (CRCP).

2.6.1.3 Unbound Layers

Loulizi et al. (2001) used vibrating wire sensors to monitor static horizontal strains in roadbed soils at the Virginia Smart Road. They also manufactured a special sensor to accommodate aggregate sizes of 25 mm in unbound aggregate layers. The sensor consisted of a strain-gauged proving ring in series with a spring and shaft. Flanges were attached to each end of the sensor. When these flanges moved relative to one another, the tension in the spring changed thereby loading the proving ring. A polyvinyl chloride (PVC) tube protected the spring and shaft while maintaining the spring at a desired initial tension.

2.6.2 Deflection

Linear variable displacement transducers (LVDTs) are commonly used to measure deflection due to test loads (Tabatabaee and Sabaaly 1990). The LVDT is a common type of electromechanical transducer that can convert rectilinear motion into a corresponding electrical signal. LVDTs are relatively insensitive to external electrical noise, so they produce a clean response signal. However, they are intrusive, involving a hole in the soil for the connecting rod, and a metal cylinder of substantial size for the LVDT coils. Moreover, LVDTs that give the best sensitivity to dynamic strain offer a limited stroke for measuring permanent deformation, and conversely, if the stroke is large, the dynamic sensitivity is low (Janoo et al. 1999).

A single-depth deflectometer (SDD) is an LVDT installation used to measure the deflection of a single depth within the pavement, while a multi-depth deflectometer (MDD) consists of several LVDTs in a shared assembly for measuring deflections at various depths (Saeed and Hall 2003). Figure 2-7 shows a photograph of a technician installing an MDD assembly in a pavement. One of the most important components of SDD and MDD installations is establishing a reference deep enough below the pavement surface to be largely unaffected by the dynamic loads (Sargand 1994).

MDDs have been used in APT testing for a number of years (Hudson and White 2003). In rigid pavements, MDDs have been employed to measure permanent deformation of the slab and underlying layers under repeated loading. MDDs have been found to be useful for verification of the gap between the slab and base and environmental changes in the slab. However, they require a great deal of time and skill to install correctly, and the lead wire makes them difficult to use under the wheel of an APT device (Harvey et al. 2004).

Figure 2-7. Installation of a MDD.

2.6.2.1 Joint and Edge Deflection in Rigid Pavements

Joint deflection measurement devices (JDMDs) have been described by Rao and Roesler (2005) and Harvey et al. (2004). JDMDs consist of an LVDT mounted either vertically to the side of the slab at the corner or mid-edge or horizontally across a joint or crack. The vertical JDMD target is attached to the slab, and the LVDT anchored one meter deep in the shoulder away from the slab to provide an absolute measure of vertical deflection. Horizontal JDMDs provide an absolute measure of the change in joint opening. The reference values of the horizontal and vertical JDMD depends on the position of the slab at the time the device is attached (Harvey et al. 2004). Figure 2-8 shows a photograph of a crack movement gauge used at the Illinois APT site (Roesler and Kohler, public presentation, 17 May 2005).

Figure 2-8. Photograph of a JDMDD at Illinois APT.

Edge deflection measurement devices (EDMDs) are JDMDs mounted at the mid-slab edge (Figure 2-9). These have proven useful for measuring the effects of curl and load deformation and measuring permanent deformation from loading of a slab with one wheel instead of a full axle, which can cause slab rotation. However, it can be difficult to separate out curling/warping from tilting of the slab if the EDMD is only installed on one side (Harvey et al. 2004).

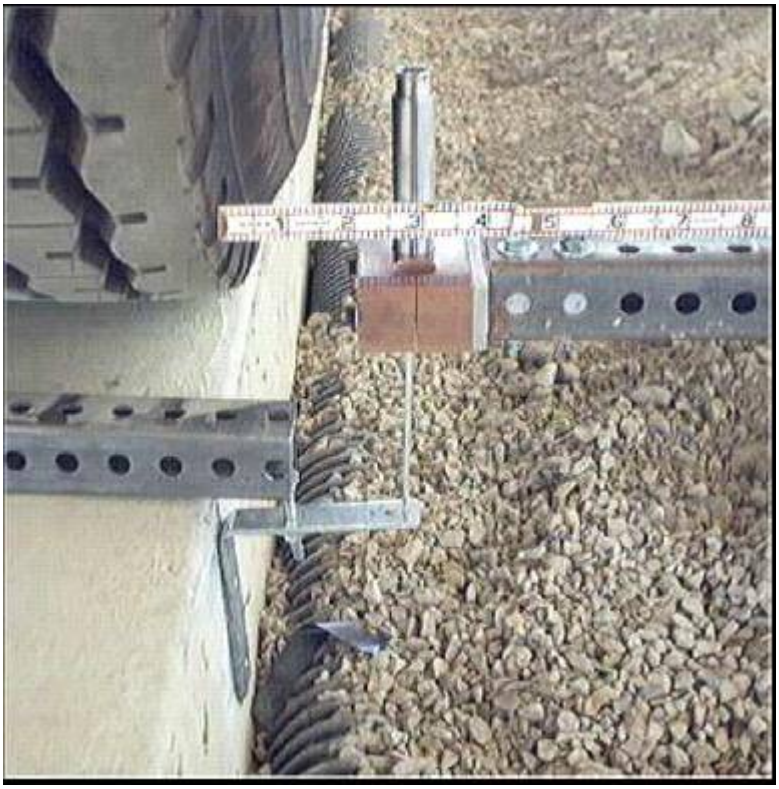

Figure 2-9. Photograph of an EDMD at Illinois APT.

2.6.3 Stress in Unbound Materials

Soil pressure sensors are installed in unbound materials to measure the dynamic stress generated under moving loads, usually in the vertical direction (Timm et al. 2004). These sensors (Figure 2-10) are typically large diameter soil stress cells consisting of two circular steel plates welded together around their rims to create a closed cell. The space between the plates is liquid filled. A steel tube connects the liquid to an electrical pressure transducer mounted several centimeters from the cell (Hossain and Wu 2003). Some APT installations use progressively larger diameter cells in the lower layers to capture stress that is laterally distributed as the pavement depth increases (Nassar 2001). Soil pressure sensors were found to have a 100% survival rate at the NCAT Test Track (Timm et al. 2004).

Figure 2-10. Typical soil pressure sensor.

The two most important requirements are the stiffness of the sensor and the ratio between its thickness and diameter (aspect ratio). The stiffness should be high compared to the material that it is to be installed in. The aspect ratio should be less than 0.2. A general problem of stress cells is their calibration, since it is difficult to establish realistic conditions for calibration in the laboratory (Hilderbrand 2002). Selig et al. (1997) also found some pressure cells to have a significant temperature dependency and electronic drift with time.

2.6.4 Soil Compression Sensors

Soil compression sensors manufactured by CTL were installed at the NCAT test track to monitor vertical deformation in an unbound base layer (Timm et al. 2004). The sensor (Figure 2-11) consists of a four-wire potentiometer with a maximum range of one inch of vertical deformation. The manufacturer claims the sensor can withstand the compaction loads associated with pavement construction.

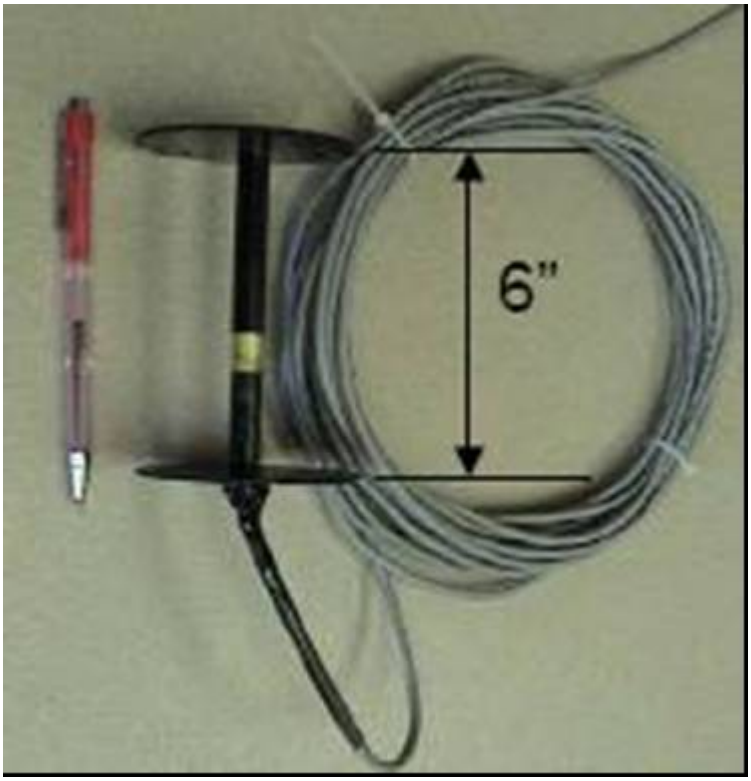

Figure 2-11. CTL soil compression sensor.

2.6.5 Environmental Sensors

Typical pavement environmental parameters include weather conditions (air temperature, precipitation, insulation, and wind), pavement temperatures, soil moisture, and depth of frost penetration. For this study, we will concentrate our efforts on moisture and temperature sensors.

2.6.5.1 Soil Moisture

The dielectric properties of soil change with moisture content (Nasser 2001). The apparent dielectric constant of a soil system is the average of the dielectric constants of the four major soil components: air, soil, bound water, and free water. Most sands, clays and organic materials have dielectric constants from 2 to 5, while water has a dielectric constant of approximately 80. The dielectric constant of air is taken to be 1 (Freeman et al. 2001, Wright et al. 2001).

Time domain reflectometry (TDR) is a method of measuring high-frequency electrical signal propagation times, typically in the nanosecond range. (Wright et al. 2001) TDR technology is applied to soils to indirectly measure the average dielectric properties of the soil system. TDR sensors consist of two or three parallel probes (Figure 2-12) separated by a few centimeters and a cable tester. The probes are inserted into the soil and act as waveguides for electrical energy initiated at the signal source, while the probe tips present a discontinuity in the wave propagation path. During a TDR scan, a fast rise time signal is propagated through the sensor. A portion of the signal is reflected at the

impedance mismatch at the top of the waveguide, while the remainder of the signal continues to propagate down the probe. When the signal reaches the end of the probe, it is reflected back along the probe. The time interval between these two reflections is recorded to measure the signal transit time. This transit time is used to calculate the wave velocity in the probe, which is related to the apparent dielectric constant of the soil (Wright et al. 2001).

Although temperature has a measurable effect on the dielectric constant of a soil system, temperature effects on TDR measurements in soil are not well understood (Wright et al 2001). The accuracy of TDR measurements depends on precise measurement of time and accurate calibration with the relative volumetric content of water around the probe. Interfering electromagnetic signals and disturbances may also influence the sensor (sowacs.com 2006). Typical accuracy for a properly calibrated probe is ±2.0 percent moisture by volume. Rainwater et al. (2006) reported that TDRs require complex instrumentation and quality calibration and may not agree with measurements taken from subgrade samples.

Troxler Electronics Laboratories, Inc., manufactures a moisture probe that estimates moisture content by measuring a frequency shift in electromagnetic waves caused by changes in soil moisture (Freeman et al. 2001). Two electrical components separated by an insulating spacer are used to generate the electromagnetic waves. The cylindrical sensors (Figure 2-12), composed of stainless steel, polypropylene, and fiberglass epoxy, are inserted into drilled holes in the soil. The manufacturer claims an accuracy of ±2.5 percent moisture.

Resistivity probes can be used to measure the depth of frost penetration in unbound layers. Because this is not an issue in Florida, the use of these sensors will not be discussed in this report.

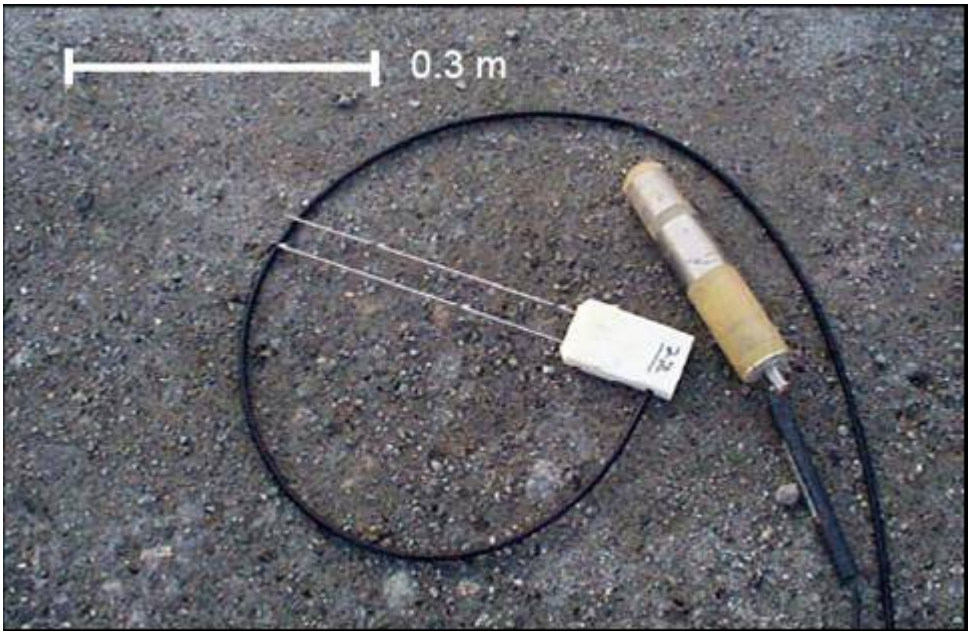

Figure 2-12. Soil moisture sensors, two-probe TDR sensor on left, Troxler on right.

2.6.5.2 Temperature

Thermocouples are widely used for temperature measurement because of their excellent service life, ease of field installation, and price. A thermocouple is a junction formed from two dissimilar metals. A temperature difference causes a temperature dependent voltage to be developed at the junction. Type K (Ni-Cr/Ni-Al) and Type T (Cu/Cu-Ni) thermocouples are often used for measurements of temperature in pavements (Nassar 1999). Type K thermocouples have an operating temperature range of -269 ^{o}C to +1260 ^{o}C, while Type T thermocouples can be used between -250 ^{o}C and +850 ^{o}C.

At the Virginia Smart Road, Loulizi et al. (2001) surrounded the exposed end of each thermocouple with copper tubing attached to the cable insulation with heat shrinkable Teflon tubing. An electrical grade epoxy was used to surround the thermocouples to serve as a barrier against environmental effects.

Thermocouples can be mounted on a "tree" as shown in Figure 2-13 to secure their location, particularly in PCC applications. (Wu and Sheehan 2002) The tree can be made of nylon or wood dowels bars. Tia et al. (2001) installed thermocouples in an unbound limerock base prior to placement of HMA by using U-shaped nails to attach the thermocouple wire to the compacted base. They also used a similar technique to attach thermocouples between lifts of HMA. Mateos and Snyder (2002) reported using thermocouples at several layers within HMA layers to obtain the mean value of pavement temperature through the thickness of the HMA section.

Figure 2-13. Thermocouples mounted to a "tree" awaiting PCC placement.

Other researchers have reported using thermistors to measure temperatures in test pavements (Sargand 1994, Freeman et al. 2001). Thermistors (Figure 2-14) are resistors constructed of semiconductor material with a resistivity that is especially sensitive to temperature. Like thermocouples, thermistors are inexpensive, easy to use, and adaptable. One advantage of thermistors is that they produce larger output voltages than thermocouples, requiring less sensitive measuring equipment. Typical survival temperatures range from -58°F to 212°F.

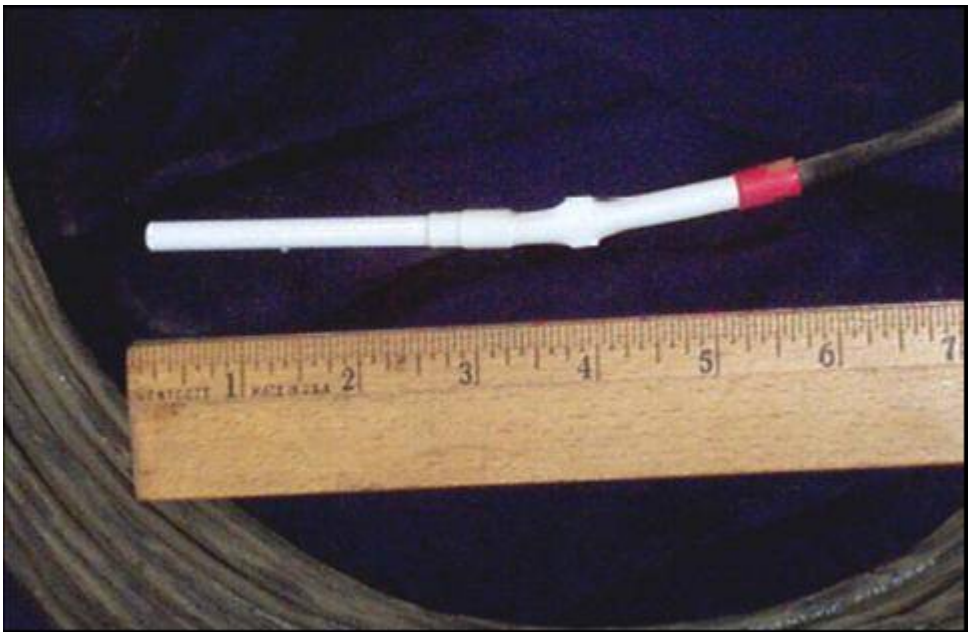

Figure 2-14. Thermistor sensor.

2.6.6 Emerging Sensor Technologies

Because the field of electronics develops continuously, technologies for measurement and instrumentation are always evolving (Steyn et al 2006). While the previously described sensors have a track record of use in APT and in-service pavement test sites, emerging sensor technologies described by researchers are summarized in the following subsections.

2.6.6.1 Inductive Coils for Measuring Strain in Unbound Materials

Janoo et al. (1999) reported using inductive coils to accurately measure triaxial strain in unbound materials at an APT site. The system consists of placing four coils at known orthogonal distances in an unbound layer. An alternating current is passed through one coil (sending coil) generating an electromagnetic field. The strength of the detected field at the receiving coils is proportional to the distance between the sending coil and receiving coil. Both dynamic and permanent strains can be measured by this system. Because the coils are sensitive to electrical and magnetic noise in the test environment, these must be reduced to acquire accurate measurements. Electrical noise was found to be from the lights and other electrical equipment, while moving metals in the vicinity of the test generated magnetic noise.

2.6.6.2 Fiber Optic-Based Strain Sensors

Fiber optic-based sensors have been used in a number of applications in civil engineering. Sharp et al. (2005) and Wang et al (2005) listed several advantages fiber optic-based sensors over other types of sensors:

- Measure both static and dynamic strains
- Provide reliable measurements with little or no noise
- Immunity to electromagnetic interference
- Small profile and light weight
- Environmental durability
- Electrical and optical multiplexing

In the past, the large-scale use of optical sensing systems has been precluded by the high cost, large system size, and high power consumption required. However, recent advances in the technology are making these options more viable (Aston University, 2006).

Sharp et al. (2005) developed a single-axis fiber optic strain sensor for HMA durable enough for placement during routine paving operations. The sensor described by Sharp et al (2005) consists of an extrinsic Fabry-Perot interferometer (EFPI). The EFPI measures the optical path length between two reflective surfaces. A broadband light source is introduced into the sensor element through an optical coupler. This light is reflected at air/glass interfaces in the sensor, and travels back through the coupler, where it is detected by a photodetector. The output is in sinusoidal form with a frequency dependent upon the gap between the air/glass interfaces within the sensor. The sensor was tested in an HMA beam using a three-point bend test, in an asphalt pavement analyzer, and finally in the field on an in-service roadway during normal paving operations. The sensors

survived the paving operations, and were able to capture the influence of the axles of a tractor-trailer.

Wang et al. (2005) reported the development of an optical fiber sensor to measure strains and temperature using the fiber Bragg grating (FBG) technology. A Bragg grating is a periodic or aperiodic perturbation of the effective absorption coefficient and/or the effective refractive index of an optical waveguide. Effectively, the FBG reflects a predetermined narrow or broad range of wavelengths of light incident on the grating, while passing all other wavelengths of the light. In a FBG sensor, the physical parameter to be measured introduces a change in the reflection wavelength of the FBG. The sensor described by Wang et al. (2005) has been mounted in HMA and PCC specimens in the laboratory and subjected to cycles of temperature and stress. However, the sensor has not been placed in an APT site or in-service roadway.

2.6.6.3 Optical Probe for In-Situ Moisture Measurement

Ghanderhari and Vimer (2005) reported on the use of optical fibers with a special cladding material to monitor subsurface moisture in pavement materials. Free water molecules in the surrounding medium permeate the nano-porous cladding of the fiber sensor, where they interact with mid-infrared light traveling within the fiber. Because water molecules are polar, they are in a constant state of vibration, resonating with the infrared portion of the electromagnetic spectrum with a unique vibration signature. This property can be exploited to give a positive indication of the presence and changes in the structure of water as incident mid-infrared energy interacts with water molecules. Data are collected using an infrared-near infrared spectrometer. To date, this technology has only been applied within concrete mortar.

3 MECHANISTIC CONCEPTS APPLIED TO SENSOR SELECTION AND LOCATION

3.1 Introduction to Mechanistic Concepts

A slow paradigm shift is occurring in the transportation industry as engineers adopt mechanistic-empirical pavement analysis, design, and evaluation. Most historical design methodologies, including the 1993 and earlier AASHTO Pavement Design Guides, have their roots in empirical techniques developed over several decades. Current and future demands on pavements caused by increased traffic volumes and unique loadings require extrapolation well beyond the existing databases. New materials and construction techniques cannot be readily evaluated and implemented due to a lack of rational methods to develop performance criteria.

Figure 3-1 shows a simplified overview of the mechanistic-empirical analysis process. The mechanistic-empirical approach, which involves relating pavement responses such as strains, stresses, and deflection to pavement performance, gives engineers a rational approach to evaluate the effects of vehicle loadings, materials, and construction techniques. Some of the important advantages of mechanistic-empirical pavement design are the following:

- A fundamentally sound theoretical basis is introduced.
- Material responses may be modeled.
- A range of wheel loadings, geometry, and traffic inputs can be modeled.
- Minimal extrapolation of model or criteria is required to cover a wide range of design and rehabilitation situations.

The mechanistic aspect has as its basis one or more analytical models founded upon the principles of mechanics. The purpose of the analytical response model is to predict pavement responses caused by applied traffic and environmental loading. Specific failure mechanisms can be addressed. Various empirical transfer functions must be used to relate model outputs to performance parameters. However, mechanistic models require a far greater number of material and system parameters than existing empirical design and evaluation methods (Loulizi et al. 2001).

While the strains can be mechanistically calculated using an analytical model, the empirically-derived constants must be determined from field or laboratory performance data. If the constants are determined from laboratory data, a “shift factor” may be required to relate laboratory performance to field performance (Timm and Newcomb 2003).

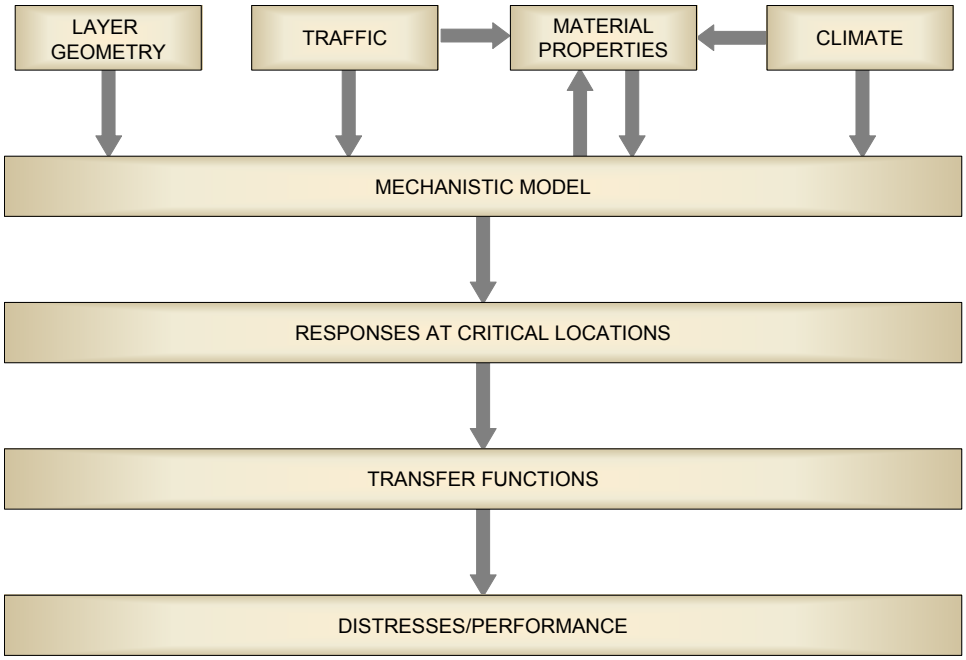

Figure 3-1. Mechanistic-empirical analysis concepts.

3.1.1 Mechanistic Models

A mechanistic model is no more than a simplified description of reality. Someone wisely said, "No model is 100 percent correct, but some are useful." This approach has allowed engineers to idealize complex phenomena using less than perfect models and use the results from those models to develop the engineered systems we utilize every day.

Man-made layers are commonly idealized as plates or elastic solids. The primary difference between plate theory and elastic layer theory is that plate theory assumes the man-made layer to be incompressible through its thickness, while elastic layer theory allows a layer to undergo compression through its thickness in response to applied loads. Plate theory (Westergaard 1926) is predominantly used for analysis of portland cement concrete (PCC) pavements, while elastic layer theory may be applied to either PCC pavements or bituminous concrete pavements.

The natural supporting layer is commonly modeled either as semi-infinite elastic half-space or as a bed of springs. The elastic half-space foundation is essentially Boussinesq's foundation characterized by an elastic modulus (E) and Poisson's ratio (υ). The bed of springs foundation, sometimes referred to as a dense liquid or Winkler foundation, assumes the layer to be made up of a set of closely-spaced springs, each of which acts independently of neighboring springs. The stiffness of the foundation is characterized by the modulus of subgrade reaction.

Table 3-1 summarizes a number of pavement structural models. The elastic layer theory was first formulated for a concentrated load and a semi-infinite half-space by Boussinesq (1885) and later generalized by Burmister (1943) for a two layer system with uniformly

distributed load acting over a circular area. Losberg (1960) developed an analytical solution that combined plate theory for the man-made layer with an elastic solid model for the natural supporting layer. Computerized solutions have made it possible to analyze a system of many layers subjected to multiple loads. Among these are the CHEVRON (Michelow 1963), BISAR (Peutz, Van Kempen, and Jones 1968), ELSYM5 (Kopperman, Tiller, and Tseng 1989), WESLEA (Van Cauwelaert, et al. 1989), and JULEA (Barker and Gonzalez 1991) programs. Khazanovich and Ioannides (1995) developed a computer code known as DIPLOMAT, an extension of Burmister's layer theory that incorporates an arbitrary sequence of elastic plates, spring beds, and isotropic elastic layers, and thus may be applied to either concrete or flexible pavement.

Table 3-1. Matrix of pavement structural response models.

		Prepared Layers	
		Elastic Layer Theory	**Plate Theory**
Natural Support Layers	Elastic Solid	BURMISTER - 1943 CHEVRON - 1963 BISAR - 1968 ELSYM5 - 1989 WESLEA - 1989 JULEA - 1991 DIPLOMAT - 1995	LOSBERG - 1960 DIPLOMAT- 1995
	Bed of Springs	DIPLOMAT - 1995	WESTERGAARD - 1926 DIPLOMAT- 1995

The finite element method is a powerful approximation technique that has been used to analyze a broad class of boundary value problems in engineering. It makes use of an approach referred to as "going from part to whole," i.e., instead of solving the problem for an entire body in one operation, the solution is approximated for discrete elements and then combined to obtain the solution for the whole. As such, the solution for the whole is, at best, no better than the approximations used for the discrete elements. With the development of the high-speed digital computer, finite element techniques have been applied to a variety of problems in pavement analysis. The finite element approach is the most powerful and versatile analysis model available today. However, the finite element modeling technique can be computationally intensive, especially if material and geometric non-linearity are modeled. A comparison of some of the key features of the various pavement response models is summarized in Table 3-2.

Table 3-2. Features of pavement response models.

Feature	Plate Theory (Westergaard)	Layered Elastic	Finite Element		
			Axisymmetric Code	Plate Theory Code	3D Code
Material models	Limited to homogeneous, isotropic, linear elastic	Limited to homogeneous, isotropic, linear elastic	Nonlinear material models limited to single load due to constraints imposed by theory of superposition	Limited to homogeneous, isotropic, linear elastic	Can be arbitrary, anisotropic nonlinear, stress-dependent temperature-dependent
Loading	Finite number of loads	Finite number of axisymmetric loads (combined using superposition)	Axisymmetric loads (combined using superposition)	Can be arbitrary	Can be arbitrary
Number of layers	Finite	Finite	Arbitrary	Finite	Arbitrary
Layer extent	Finite horizontal extent, infinite vertical extent	Finite depth, infinite horizontal extent	Finite depth, infinite horizontal extent	Finite horizontal and vertical extent	Can be finite or infinite in horizontal and vertical extent (infinite elements)
Layer contact conditions	Full slip	Can allow slip but not separation, slip model is ill-defined (no physical or mechanical correlation)	Full bond	Full bond or full slip	Can allow slip and separation, can relate to friction properties

The outputs from the pavement response model are stresses, strains, and displacements within the pavement layers. Of particular interest are the critical response variables required as inputs to the pavement distress models in the mechanistic-empirical analysis procedure. Examples of critical pavement response variables include:

- Flexible Pavement
  - Tensile horizontal strain at the bottom/top of the HMA layer
  - Compressive vertical stresses/strains within the HMA layer
  - Compressive vertical stresses/strains within the base/subbase layers
  - Compressive vertical stresses/strains at the top and within the subgrade

- Rigid Pavement
  - Tensile horizontal stresses at the bottom/top of the slab
  - Differential corner deflection

Each pavement response variable must be evaluated at the critical location within the pavement layer where the parameter is at its most extreme value. For a single wheel loading, the critical location can usually be determined by inspection. For example, the critical location for the tensile horizontal strain at the bottom of the HMA layer under a single wheel load is directly beneath the center of the wheel. For multiple wheels and/or axles, the critical location will be a function of the wheel load configuration and the pavement structure.

3.1.2 Transfer Functions

Transfer functions are required to relate the output of mechanistic models to pavement performance or load repetitions required to reach a limit state. Seeds (2003) states that transfer functions are the most important part of the mechanistic-empirical pavement design procedure. Various transfer functions have been developed by researchers for each of the pavement performance measures, typically through statistically-based correlations of pavement response with observed performance of laboratory test specimens, full-scale road test experiments, or by both methods (Seeds 2003, Priest 2005). While full-scale APT is a better representation of in-service performance than laboratory testing, it still requires a "shift", or transfer, to predict field performance (Hugo and Epps 2004). Many of these differences can be attributed to differences in loading time, loading frequency, traffic distribution, aging, and environmental conditions between APT and actual field conditions.

Transfer functions must be carefully calibrated so that the predicted distress will match with field observations. The Federal Highway Administration's (FHWA) Long Term Pavement Performance (LTTP) studies provide arguably the best opportunity to calibrate transfer functions developed from APT to actual field conditions. The LTPP studies, launched in 1987, involve long-term field experiments monitoring more than 2,400 asphalt and Portland cement concrete pavement test sections across the U.S. and Canada. The goal of the study was to determine how and why pavements perform as they do.

3.1.3 Overview of the Mechanistic-Empirical Pavement Design Guide

The Mechanistic-Empirical Pavement Design Guide (MEPDG) represents a major change in the way design is performed. The MEPDG, originally developed under NCHRP Project 1-37A and updated under NCHRP Project 1-40D, uses mechanistic-empirical principals for pavement design and is different from existing empirical

procedures. The MEPDG includes performance models calibrated and validated using data from the LTPP study. Using mechanistic-empirical principles allows for reliable and cost effective pavement designs. However, proper calibration is essential to obtain accurate results. The MEPDG design manuals, software, climatic data, and other publications describing updates are available through the NCHRP at http://www.trb.org/mepdg/. The design process for new and rehabilitated pavement structures includes consideration of the following:

- Foundation/subgrade
- Existing pavement condition
- Paving materials
- Construction factors
- Environmental factors (temperature and moisture)
- Traffic loadings
- Subdrainage
- Shoulder design
- Rehabilitation treatments and strategies
- New pavement and rehabilitation options
- Pavement performance (key distresses and smoothness)
- Design reliability
- Life cycle costs

The flexible pavement performance measures considered in the MEPDG include permanent deformation (rutting), fatigue cracking (both bottom-up and top-down), thermal cracking, and smoothness (International Roughness Index or IRI). If the trial design does not satisfy the performance criteria, the design is modified and reanalyzed until the design does satisfy all criteria. The designs that meet the applicable performance criteria are then considered feasible from a structural and functional viewpoint and can be further considered for other evaluations such as life cycle cost analysis.

The MEPDG uses the JULEA multilayer elastic theory model of the flexible pavement response, and a plate-theory finite element model representation of rigid pavement systems. To reduce computer run time, a matrix of thousands of finite element runs was used to develop a series of neural networks that accurately reproduce the results given by direct finite element analysis.

In the case of mixed traffic with various axle configurations, identifying the location of the maximum response can be problematic. However, in the case of APT testing with a super single wheel, the maximum response should be located directly beneath the center of the tire. In the case where wander is incorporated into the APT experiment, the maximum response would be expected to be at the center of the path of the tire. In the case of dual tires, the maximum response would be expected either directly beneath the path of one of the tires or midway between the two tires. The actual location of the critical response will depend upon the distress model and type of measurement.

Calculated pavement responses are translated into pavement surface distresses using transfer functions. These transfer functions were developed through a regression of the LTPP database and pavement performance information supplemented by several specific full scale pavement studies and do not necessarily represent local pavement material and performance. The MEPDG allows for modification of the response models to account for local materials and conditions.

3.2 Mechanistic Concepts Applied to Flexible Pavements

The flexible pavement response model used in the MEPDG generates strains, stresses and displacements within the pavement system using multilayer elastic theory. Pavement distresses throughout the design life are calculated using models that relate the pavement response at critical locations to fatigue cracking and permanent deformation. The critical locations for measuring response in flexible pavements are listed in Table 3-3. Additional measurements that may be beneficial to understanding the pavement response include the mid-depth temperature of the HMA and moisture content of unbound layers.

Table 3-3. Critical mechanistic measurements for flexible pavements.

Distress Type	Critical Measurement	Critical Location
HMA fatigue cracking (bottom-up or "alligator" cracking)	Horizontal tensile strain	Bottom of the HMA layer
HMA fatigue cracking (top down cracking)	Horizontal tensile strain	Top of the HMA layer Bottom of the HMA layer
HMA rutting	Vertical compressive strain/stress	Within HMA layer
Rutting of unbound layers	Vertical compressive stress/strain	Within unbound layer
Rutting of natural subgrade	Vertical compressive stress/strain	Top and within subgrade

3.2.1 Fatigue Cracking

Load induced fatigue cracking is generated from tensile and shear stresses induced by repeated traffic loads. Cracks initiate at points where stresses and strains are critical and then migrate through the entire HMA depth. The stiffness of an HMA mix greatly influences fatigue cracking resistance. Greater mix stiffness typically reduces strains associated with the initiation of fatigue cracking for conventional HMA pavements. However, a resilient mix with greater flexibility may offer better fatigue cracking resistance for thin HMA pavements supported with a weak subgrade. Photographs of fatigue cracking are shown in Figure 3-2.

Figure 3-2. Photograph of fatigue cracking.

3.2.1.1 Bottom-Up Cracking

Bottom up cracking is initiated by tensile strains that develop at the bottom of the HMA. Essentially, HMA bends when a load is applied and tensile strains are induced at the bottom of the layer. Upon repeated loading, the tensile strains and stresses initiate cracks that propagate to the surface as illustrated in Figure 3-3. This distress is first observed as short transverse cracks in the wheel path. At advanced stages, bottom-up cracking is often referred to as “alligator” cracking, a reference to the interconnected pattern the cracks form. Excessive tensile strains and stresses may form at the bottom of the HMA due to several factors such as inadequate HMA thickness and stiffness, greater wheel loads and tire pressure and insufficient underlying support.

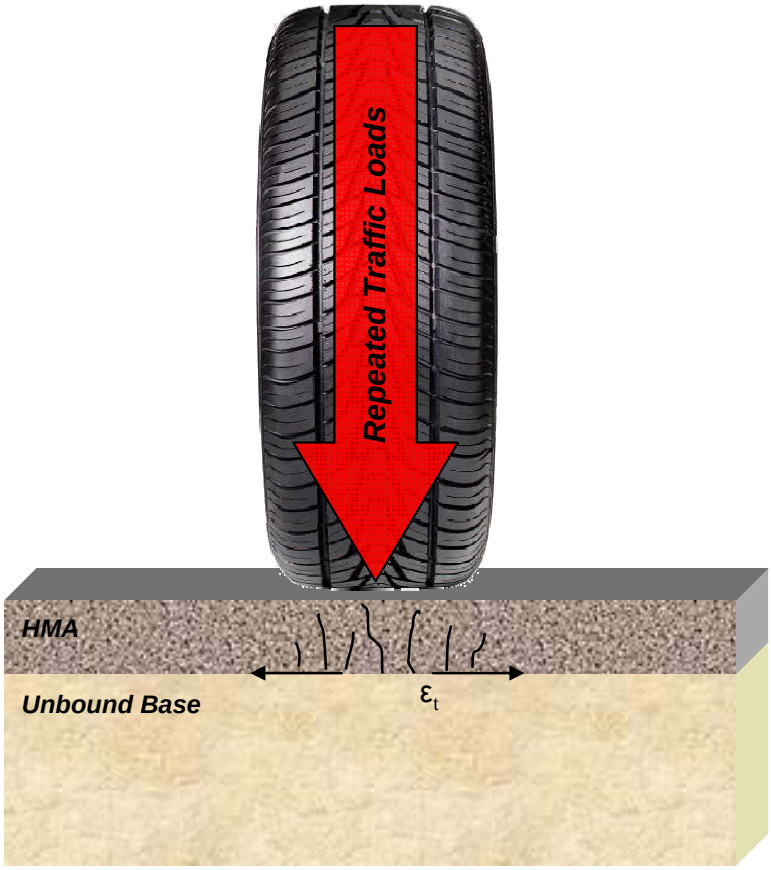

Figure 3-3. Illustration of bottom-up cracking mechanics.

The MEPDG has adopted a version of the Asphalt Institute's MS-1 approach to model bottom-up cracking. The MS-1 model is shown below:

$$N_f = Ck_1\left(\frac{1}{\varepsilon_t}\right)^{k_2}\left(\frac{1}{E}\right)^{k_3}$$

where N_f = number of load repetitions until fatigue failure
ε_t = tensile strain at critical location
E = HMA stiffness
C = Laboratory to field adjustment factor
k_1, k_2, k_3 = regression constants

3.2.1.2 Top-Down Cracking

Cracks that initiate from the surface, normally in or near the wheel paths, are referred to as top-down cracking. The sources of top-down cracking are more complex than bottom-up cracking but are thought to result from a combination of tire-pavement interaction, environmental conditions and mixture properties. More specifically, factors that likely contribute to top-down cracking are stiffness gradients from aging and temperature, thermal stresses and increased magnitudes of tire pressure and loads. Moisture damage

and segregation are also thought to contribute, or at least exacerbate top-down cracking (Christensen 2004). Top-down cracking mechanics are illustrated in Figure 3-4.

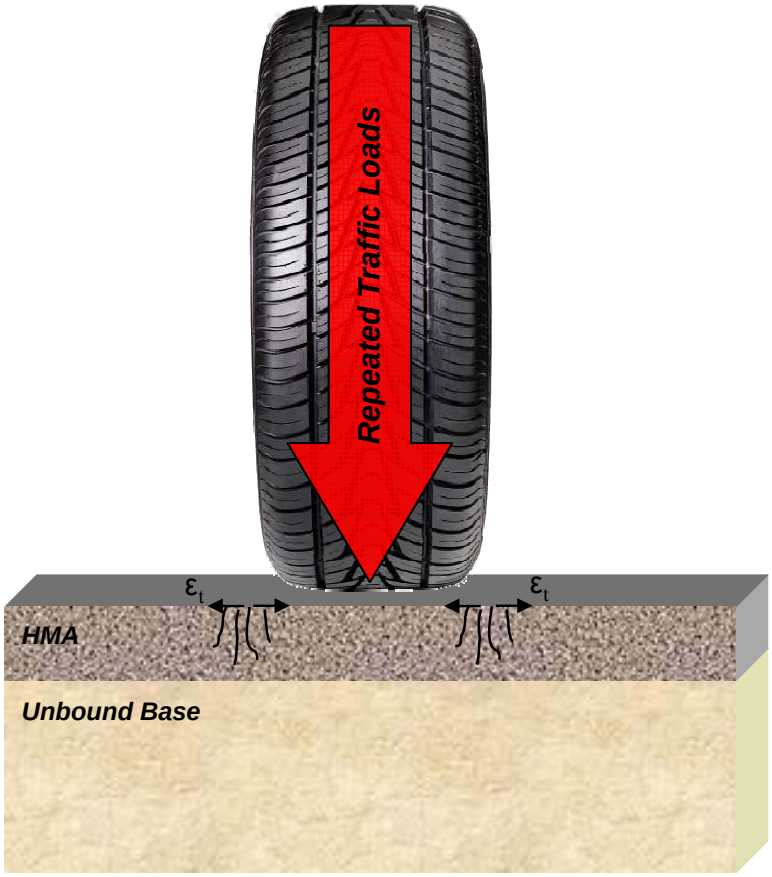

Figure 3-4. Illustration of top-down cracking mechanics.

The University of Florida has developed a mechanistic-empirical model to evaluate flexible pavements for top-down cracking (Wang et al. 2007). The model predicts crack initiation and propagation using principles of viscoelastic fracture mechanics. Figure 3-5 shows the primary components of the model. A comprehensive evaluation of Florida field test sections revealed that no single material property or characteristic could be used to reliably predict top-down cracking. Thus, the Florida model also includes the influence of pavement structure, including stiffness and thickness.

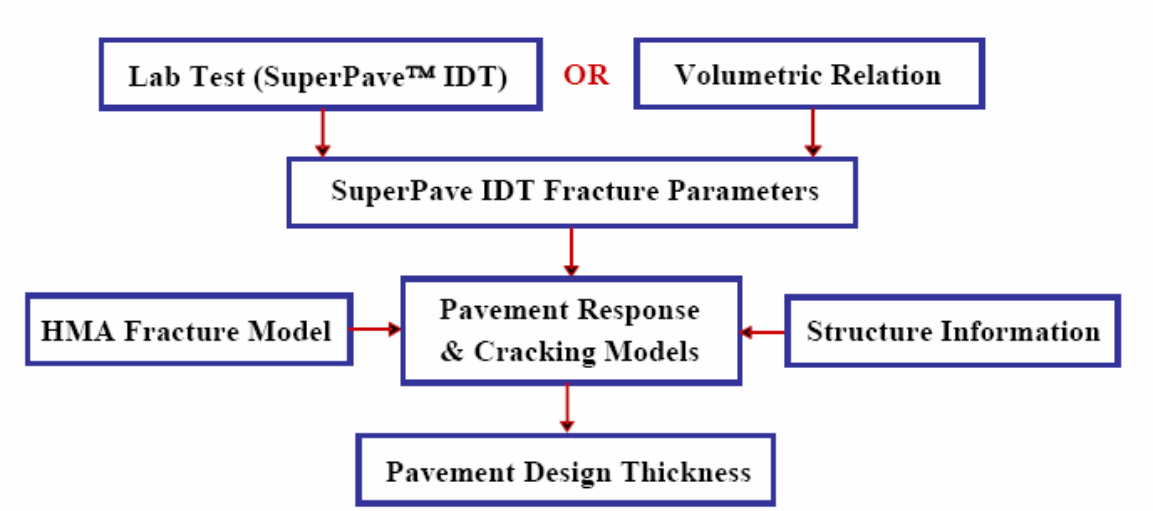

Figure 3-5. Framework for Florida top-down cracking evaluation model (after Wang et al. 2007)

The model links HMA damage to accumulated dissipated creep strain energy (DCSE), which depends upon the maximum tensile strength and resilient modulus of the mix. Figure 3-6 illustrates an indirect tensile test on an HMA pill. The dark shaded area defined in the stress-strain curve to the right defines damage threshold or limit ($DCSE_f$). The model hypothesizes that damage below this limit is healable, while damage above the limit will initiate a macro-crack or cause the macro-crack to propagate if it already exists.

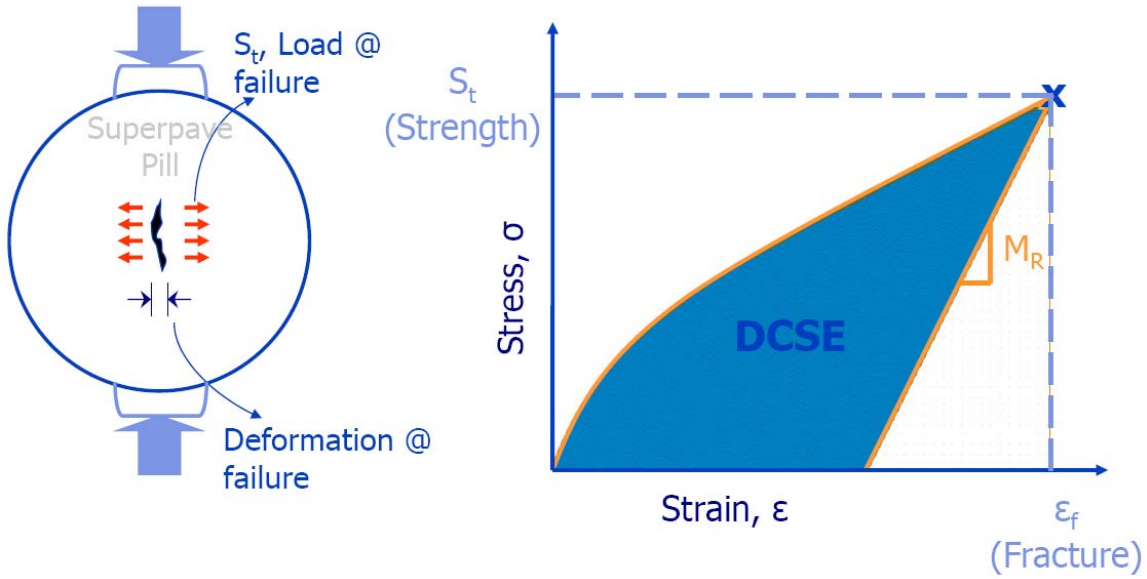

Figure 3-6. Threshold DCSE calculation.

The Florida researchers identified a set of criteria that can predict top-down cracking based upon an Energy Ratio (ER) defined as

$$ER = \frac{DCSE_f}{DCSE_{\min}}$$

where $DCSE_{min}$ is the minimum dissipated creep strain energy required to produce a 2-inch crack. The properties required to determine $DCSE_{min}$ include dynamic modulus, creep compliance power law parameters, and tensile strength. These values can either be measured from tests conducted on the mix, or alternatively they may be estimated from binder properties, mixture volumetric properties, and aggregate gradation.

As previously stated, tensile stresses in HMA are important for cracking performance. More specifically, there is a direct relationship between $DCSE_{min}$ and tensile stress in the HMA, which in turn depends upon the pavement materials, structure and loading. The Florida model uses a layered-elastic pavement response model to make a mechanistic prediction of tensile stress in the asphalt at the bottom of the HMA layer. There are at least two structural parameters which can be changed to improve top-down cracking resistance: increase the HMA thickness or increase the stiffness of the supporting base layer.

3.2.2 Permanent Deformation

Permanent deformation, or rutting, occurs with increasing load applications and is caused by a combination of volumetric change and shear deformation of the pavement materials. Rutting usually appears as longitudinal depressions in the wheel paths, as shown in Figure 3-7, and is sometimes accompanied by lateral upheaval. The rate of permanent deformation is influenced greatly by aggregate type, binder stiffness, mixture properties, load patterns and environmental conditions.

Figure 3-7. Photograph of HMA permanent deformation.

There are primarily three stages of permanent deformation for any material subjected to traffic and environmental loads. Permanent strains rapidly accumulate due to volumetric change, or material densification, in the primary stage. The permanent strain rate decreases and stabilizes in the secondary stage. Finally, strain rates again rapidly increase in the tertiary stage as shear failure occurs and the mixture flows to rupture. The MEPDG utilizes an approach that models the secondary stage and extrapolates the primary stage through the secondary stage trend. The tertiary stage is not predicted as this stage is typically difficult to model, is time consuming, and rut depths in this stage are for the most part greater than what would typically be tolerated in practice.

The MEPDG assumes that chemically stabilized materials, bedrock, PCC fractured slabs, and rigid pavements do not deform permanently and do not contribute to the overall permanent deformation of the pavement system.

Total permanent deformation is estimated from vertical compressive vertical strains from the mid depth of each pavement layer and load repetitions, as represented in Figure 3-8.

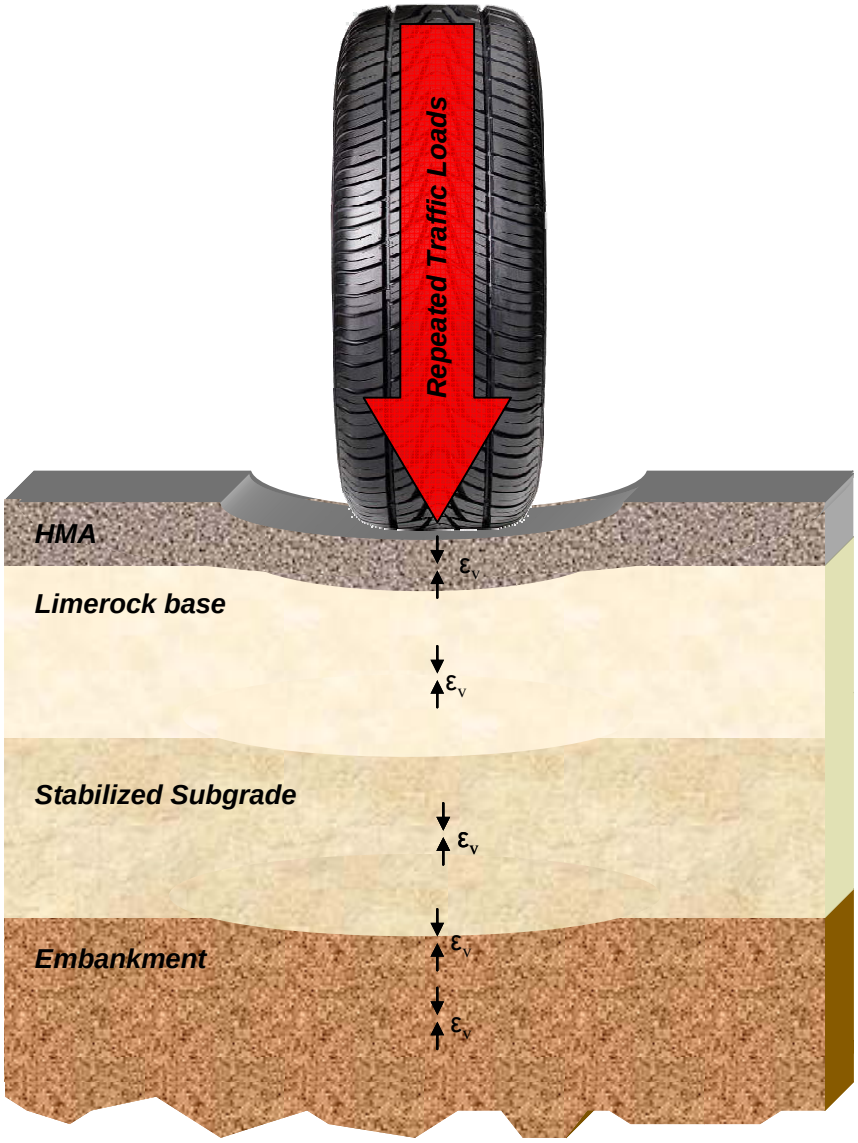

Figure 3-8. Illustration of HMA permanent deformation mechanics.

3.2.2.1 HMA Permanent Deformation

Vertical strain and temperature within the HMA are critical components for the permanent deformation model found in the MEPDG. The general uncalibrated relationship used in the MEPDG for prediction of HMA permanent deformation is defined as:

$$\frac{\varepsilon_p}{\varepsilon_r} = a_1 T^{a2} N^{a3}$$

where ε_p = accumulated permanent strain at N repetitions of load (in/in)
ε_r = resilient strain of the HMA material as a function of mix properties,

temperature and time rate of loading (in/in)
T = mix temperature (degrees Fahrenheit)
N = number of load repetitions
a_i = non-linear regression coefficients

The total permanent deformation is calculated as follows:

$$PD = \sum_{i=1}^{nsublayers} \varepsilon_p^i h^i$$

where PD = permanent deformation
nsublayers = Number of sub-layers
$\varepsilon_p{}^i$ = Total plastic strain in sub-layer i
h^i = Thickness of sub-layer i

In the past, many mechanistic-empirical methods related permanent deformation to excessive vertical strains on top of the subgrade. It was thought that a well designed pavement would resist rutting if vertical strains on top of the subgrade were limited. Typically, the HMA response for these models was measured at the bottom of the layer with an H-sensor, or at the top of the underlying unbound layer with a soil pressure gauge. However, it is now widely accepted that total permanent deformation is the cumulative rut of each layer and therefore, the model incorporated in the MEPDG for permanent HMA deformation utilizes the vertical strain within the HMA. Currently, documentation regarding the use of compressive strain gauges within HMA is limited and reliability and constructability of these gauges are unknown. It is recommended that vertical compressive strain gauges be considered in future instrumentation plans.

3.2.2.2 Unbound Materials Deformation (Rutting)

The MEPDG also models permanent deformation for unbound materials below the HMA. The general form of the model used before national calibration is:

$$\delta_a(N) = \beta_1 \left(\frac{\varepsilon_0}{\varepsilon_r} \right) e^{-\left(\frac{\rho}{N}\right)^{\beta}} \varepsilon_v h$$

where δ_a = permanent deformation for the layer/sublayer (in)
N = number of traffic repetitions
$\varepsilon_0, \beta, \rho$ = material properties
ε_r = resilient strain imposed in laboratory to obtain material properties $\varepsilon_0, \beta, \rho$ *(in/in)*
ε_v = average vertical strain in the layer (in/in)
h = thickness of layer/sublayer (in)
β_1 = calibration factor for the unbound granular and subgrade materials

Permanent deformation is calculated from the response measured at mid depth of each layer except the subgrade. However, subgrade layers are often thick and sometimes

considered to have an infinite depth. Therefore, vertical strains are estimated at the top of the subgrade and at a depth of six inches from the interface, as opposed to mid depth.

3.3 Mechanistic Concepts Applied to Rigid Pavements

The rigid pavement response model generates strains, stresses and displacements within the pavement system using plate theory. Pavement distresses throughout the design life are calculated using models that relate the pavement response at critical locations to transverse cracking and faulting for jointed concrete pavements and punchouts for continuously reinforced concrete pavements. The critical locations for measuring response in rigid pavements are listed in Table 3-4. Additional measurements that may be beneficial to understanding the pavement response include those that characterize the foundation support, such as pressure gauges and moisture sensors. Figure 2-8 illustrates a typical rigid pavement instrumented to measure critical and supplemental responses required for the MEPDG models.

Table 3-4. Critical mechanistic measurements for rigid pavements.

Pavement Type	Distress Type	Critical Measurement	Critical Location
JPCP	Transverse cracking (bottom-up)	Horizontal tensile strain	Bottom of slab near longitudinal edge, midway between transverse joints
JPCP	Transverse cracking (top-down)	Horizontal tensile strain	Top of slab near longitudinal edge, midway between transverse joints
JPCP	Faulting	Vertical deflection	Differential deflection across joints near corner
CRCP	Punchouts	Horizontal tensile strain	Top of slab near transverse cracks some distance from longitudinal joint

3.3.1 Transverse Cracking

Transverse cracks develop on all rigid pavement types and can initiate from the surface (top-down) or bottom (bottom-up) of the slab. For both conditions, the crack typically initiates near the longitudinal edge midway between transverse joints as repeated loading leads to excessive stress. Dry shrinkage of the concrete, curling and warping, late or inadequate joint sawing and repeated traffic loading all contribute to the formation and widening of transverse cracks. A photograph of transverse cracking is shown in Figure 3-9.

Figure 3-9. Photograph of JPCP transverse cracking.

3.3.1.1 Bottom-up transverse cracking

Bottom-up transverse cracking initiates when repeated traffic loading near a longitudinal joint creates a critical bending stress at the bottom of a slab. The critical stress is typically located midway between transverse joints. The stress at the bottom of the slab becomes even greater when the slab experiences a large positive temperature gradient (top of the slab is warmer than the bottom). During the daytime, the surface temperature of the concrete increases and tends to elongate. Any forces resisting the free movement of the concrete, including the self weight of the slab and in particular traffic loads, result in increased tensile stress at the bottom of the slab. In extreme instances, the convex curvature due to high temperature gradients may result in a void at the center of the slab. Bottom-up transverse cracking may be limited by minimizing slab movement due to environmental and traffic loads. Figure 3-10 illustrates the mechanics of bottom-up transverse cracking.

Allowable load repetitions for fatigue cracking may be calculated using the following equation:

$$\log(N) = c_1 \left(MR / \sigma \right)^{c_2}$$

where N = allowable number of load applications
MR = modulus of rupture, psi
σ = applied stress at critical location
$c_{1,2}$ = calibration constants

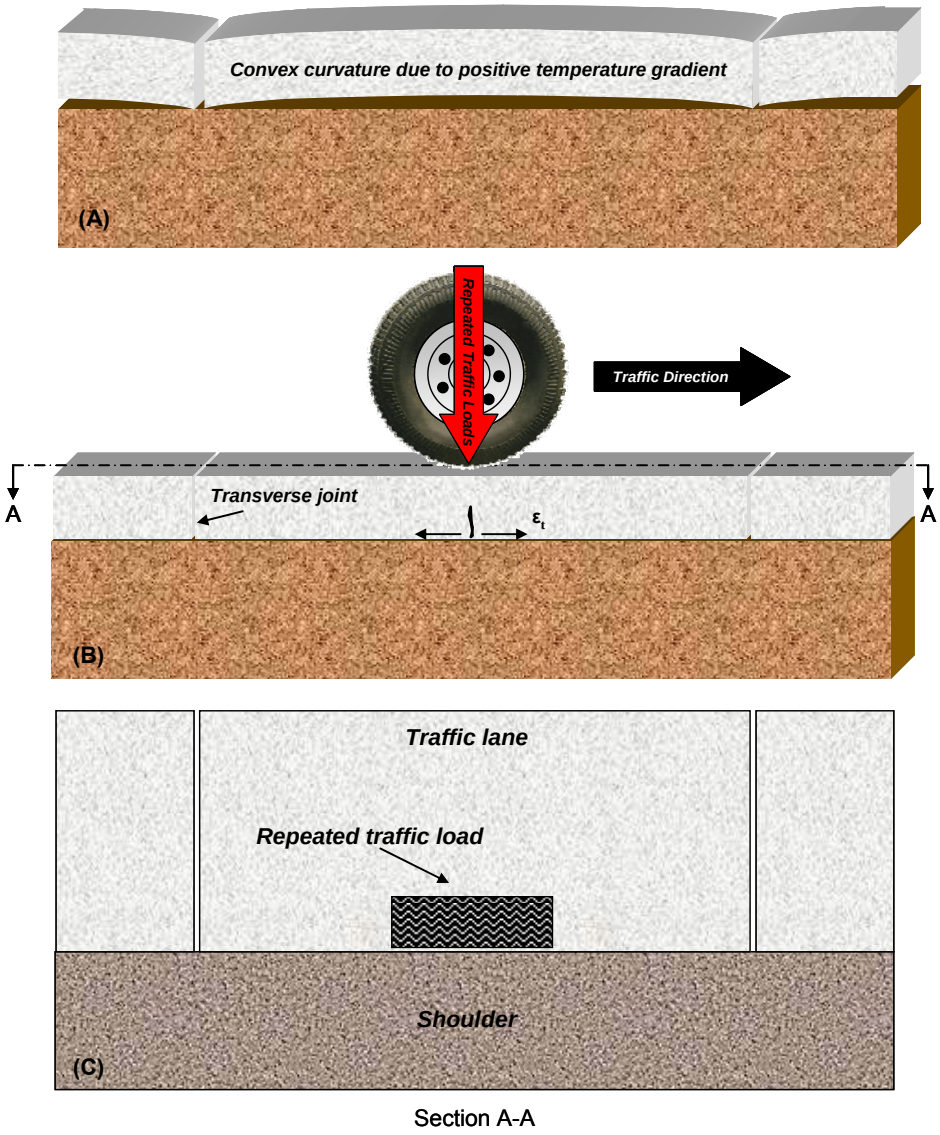

Figure 3-10. Illustration of bottom-up JPCP transverse cracking.

3.3.1.2 Top-down transverse cracking

Repeated traffic loads of specific axle spacing near a longitudinal joint during a large negative temperature gradient (top of the slab is cooler than the bottom) produces a critical stress at the top of the slab. An axle configuration that loads each end of the slab simultaneously while the slab is experiencing a concave curvature due to the concrete thermal gradient, as shown in Figure 2-11(A), is required to produce the critical stress to initiate top-down cracking at mid slab. Extreme negative temperature gradients may result in voids beneath the edges of the slab. Top-down cracking near the corners may be initiated as traffic loads the pavement as the edges are curved upwards and subgrade support is reduced. As with bottom-up cracking, top-down transverse cracking may be limited by minimizing slab movement due to environmental and traffic loads. Figure 3-11 illustrates the mechanics of top-down transverse cracking. Allowable load repetitions for

top-down cracking are calculated using the same model as bottom-up cracking. The loading requirements for mid slab top-down cracking are impossible to reproduce using a single wheel accelerated pavement testing device.

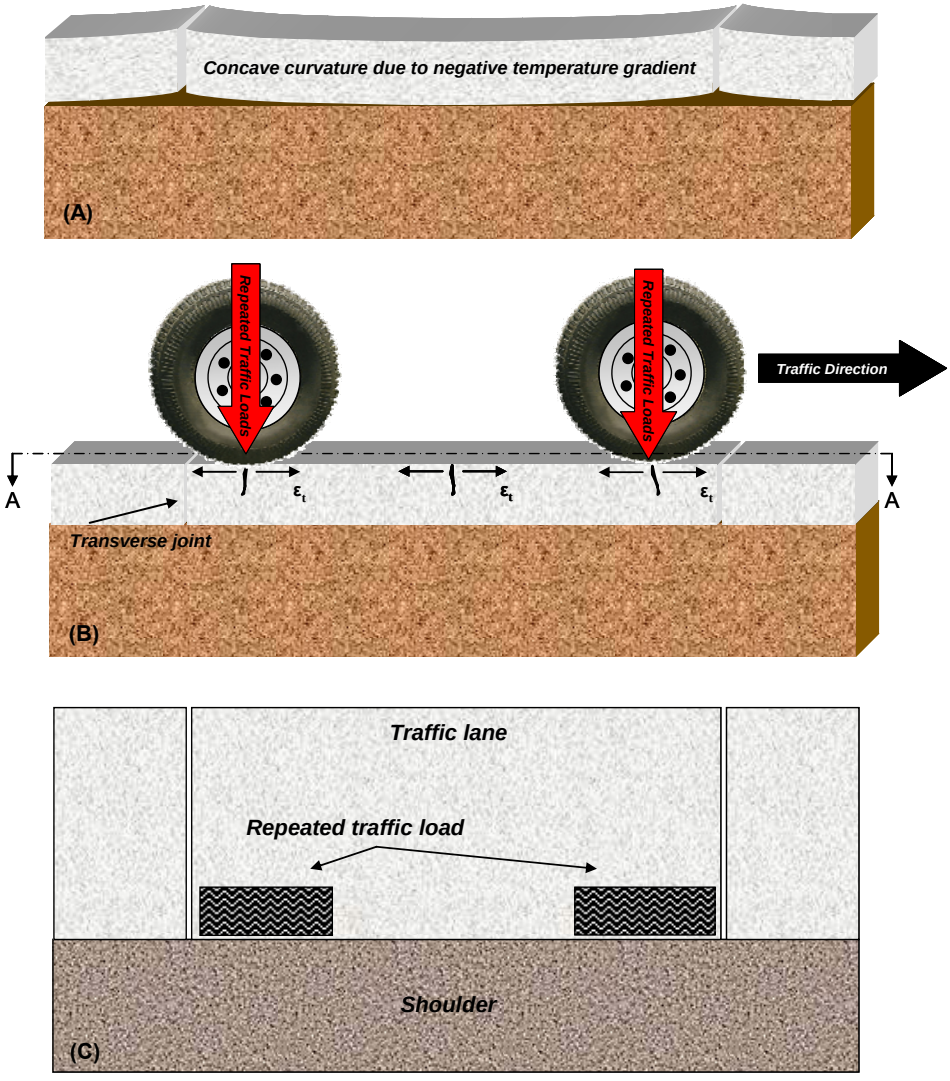

Figure 3-11. Illustration of top-down JPCP transverse cracking mechanics.

3.3.2 Joint Faulting

Repeated traffic loads across a transverse joint or corner edge with poor load transfer and a base prone to erosion can create the potential for joint faulting, or a differential in joint elevation as shown in Figure 3-12. As traffic loads progress from the approach slab to the leave slab, fines eroded from the base below the leave slab are pumped underneath the approach slab and out of the transverse joint as the leave slab rapidly deflects vertically. The pumping action creates a void below the leave slab that results in differential joint elevations as illustrated in Figure 3-13.

Figure 3-12. Photograph of JPCP faulting.

In order to evaluate faulting, traffic applications should be applied in a single direction only to simulate conditions necessary for pumping. The MEPDG calculates the mean transverse joint faulting on a monthly basis throughout the design life using the following model:

$$Fault_m = \sum_{i=1}^{m} \Delta fault_i$$

$$\Delta fault_i = C_{34} * \left(FAULTMAX_{i-1} - fault_i\right)^2 * DE_i$$

$$FAULTMAX_i = FAULTMAX_0 + C_7 * \sum_{j=1}^{m} DE * Log\left(1 + C_5 + 5^{EROD}\right)^{C6}$$

$$FAULTMAX_0 = C_{12} * \delta_{curling}\left[Log\left(1 + C_5 * 5^{EROD}\right) * \log\left(\frac{P_{200} * WetDays}{p_s}\right)\right]^{C6}$$

where $Fault_m$ = mean joint faulting at end of month m, in

$\Delta fault_i$ = incremental monthly change in mean transverse joint faulting during month i, in

$FAULTMAX_i$ = maximum mean transverse joint faulting for month i, in

$FAULTMAX_0$ = initial maximum mean transverse faulting, in

EROD = base erosion factor

DE_i = differential deformation energy accumulated during month i, function of modulus of subgrade reaction and slab deformation profile

$\delta_{curling}$ = maximum mean monthly slab corner upward deflection PCC due to temperature curling and moisture warping
P_s = overburden on subgrade, lbs
P_{200} = percent base material passing #200 sieve
WetDays = average annual number of wet days
C = calibration constants

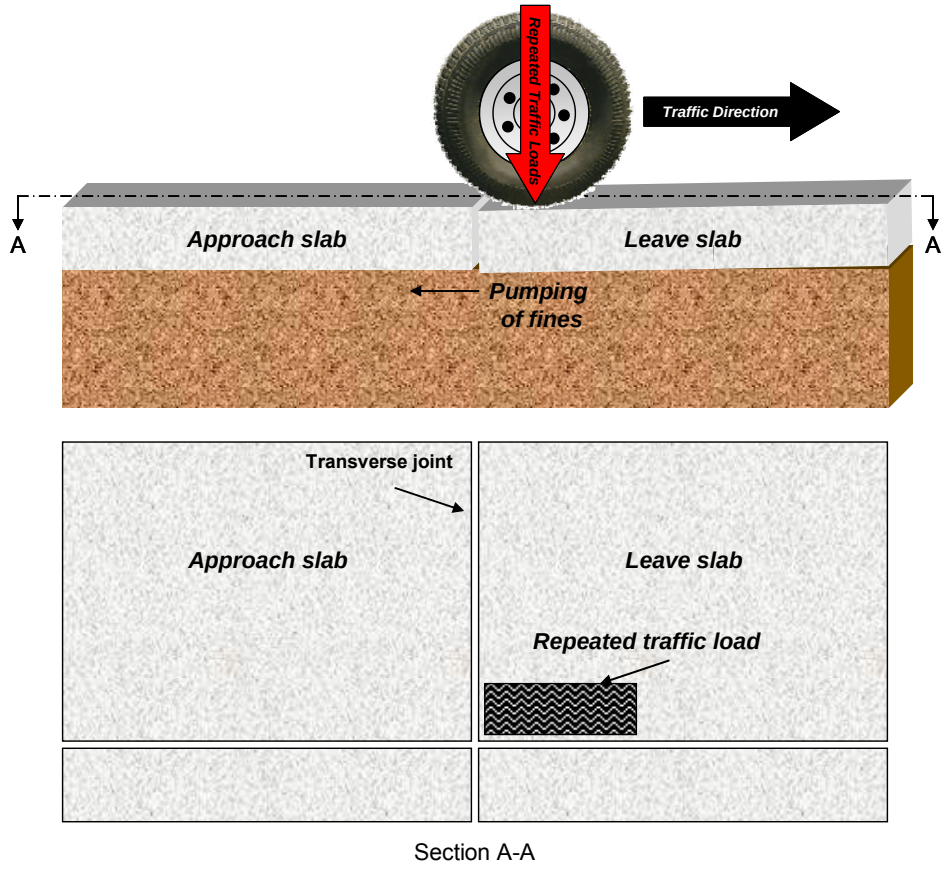

Figure 3-13. Illustration of JPCP faulting mechanics.

3.3.3 Punchouts

Punchouts are a form of cracking unique to CRCPs that develop when traffic loads are applied near the longitudinal edge of two closely spaced transverse cracks that have lost load transfer and/or support along the edge. Repeated traffic loads generate substantial tensile stress at the surface some distance from the longitudinal edge and eventually, a longitudinal crack forms between the transverse cracks and the broken piece of concrete punches into the base as shown in Figure 3-14. Punchouts may be limited by increasing the strength and thickness of the PCC, increasing the longitudinal steel content and placing reinforcement above mid-depth, incorporating a tied PCC shoulder, and reducing the PCC coefficient of thermal expansion. Figure 3-15 illustrates the mechanics of CRCP punchouts.

Figure 3-14. Photograph of CRCP punchouts.

Allowable load repetitions for fatigue cracking may be calculated using the following equation:

$$\log(N) = c_1 \left(MR / \sigma \right)^{c_2}$$

where N = allowable number of load applications
MR = modulus of rupture, psi
σ = applied stress at critical location
$c_{1,2}$ = calibration constants

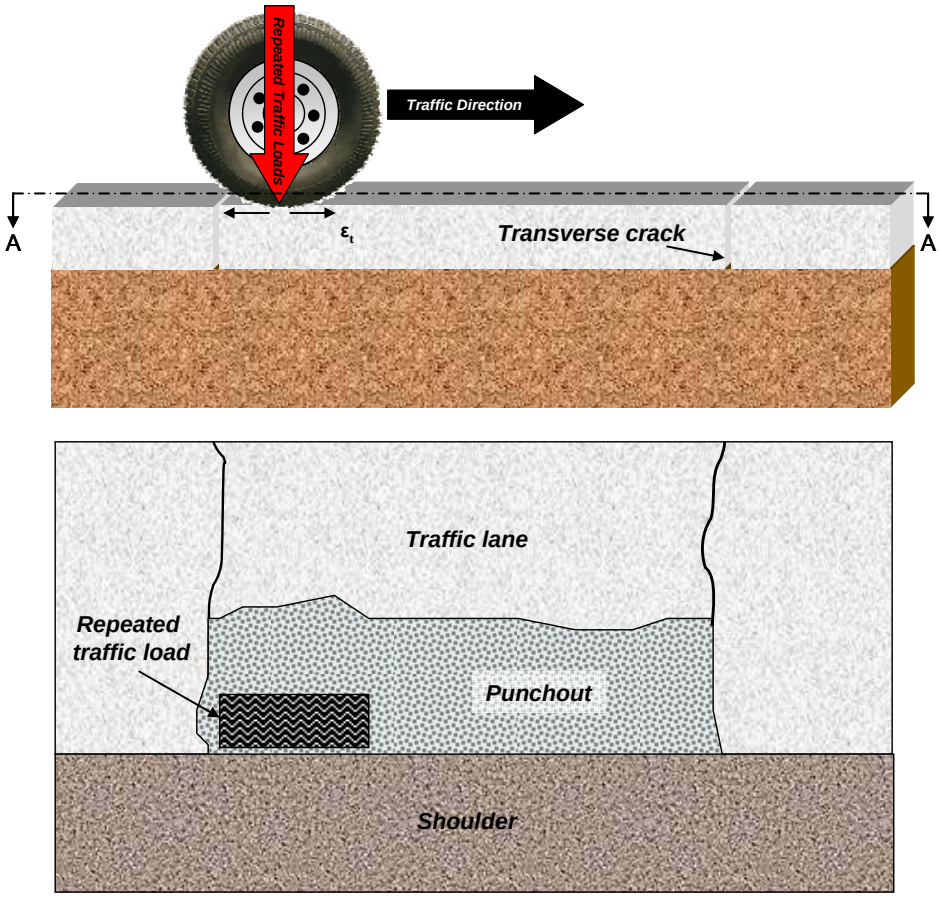

Figure 3-15. Illustration of CRCP punchout mechanics.

3.4 Mechanistic-Based Sensor Selection

Several factors dictate the selection of sensors for accelerated pavement testing. First, the sensors must be available and within funding limits. Personnel must also be trained and familiar with how to perform necessary calibrations, place the sensors, acquire the raw data, and process the acquired information into relevant data. Most importantly; however, appropriate sensors must be selected based upon the purpose of the test. For the most part, accelerated pavement tests can be classified as either material comparison or structural evaluation. A comparison of materials will rely on all other factors, except for the material in question, to remain constant. However, if one wishes to evaluate a structural model, then additional factors relevant to the model predictions must be measured as well.

3.4.1 Flexible Pavement Sensor Selection

It is common for accelerated pavement testing to focus only on the HMA layer for performance comparisons such as the rutting or cracking potential of the HMA layer. In these cases, it is often advantageous to construct the supporting pavement layers using typical materials and specifications with varying HMA mixtures. It is still important to characterize the supporting layers, but detailed instrumentation may not be warranted.

The performance of support layers may be evaluated with limited instrumentation or through nondestructive means throughout the test. Table 3-5 summarizes the instrumentation required for HMA comparison tests.

Table 3-5. Sensors for HMA evaluation.

Distress Type	Required Measurements	Optional Measurements	Considerations
HMA rutting	Vertical deformation using a vertical strain gauge at mid-depth of HMA layer of interest. Temperature at the surface, mid-depth, and bottom of HMA	Horizontal strain at bottom of HMA (Many models attempt to correlate horizontal strain and vertical deformation) Vertical deformation of supporting layers through stress/strain correlation. Place pressure gauges at top and mid-depth of unbound layers and 6 inches below embankment surface Vertical deformation of supporting layers using multi-depth deflectometers Moisture at mid-depth of base layer	Stiffness of HMA strain gauges should be compatible with expected strain Ambient/elevated temperatures Saturated/unsaturated
HMA bottom-up cracking	Horizontal strain at the bottom of the HMA layer Temperature at the surface, mid-depth, and bottom of the HMA	Base response using pressure gauges at surface, mid-depth, and bottom of layer Moisture of base layer	Stiffness of HMA strain gauges should be compatible with expected strain Accelerated temperature aging prior to testing Saturated/unsaturated
HMA top-down cracking	Horizontal strain at the surface of the HMA layer Horizontal strain at the bottom of the HMA layer Temperature at the surface, mid-depth, and bottom of the HMA		Stiffness of HMA strain gauges should be compatible with expected strain Accelerated temperature aging prior to testing

Additional instrumentation will often be required for structural model verification tests. In order to make the most accurate performance prediction, most structural models attempt to account for as many variables as possible. For instance, the most accurate prediction of a flexible pavement systems rutting potential will include not only the estimation of HMA rutting but also the deformation contribution of all pavement layers. Table 3-6 shows the instrumentation required for verification of the MEPDG distress models for flexible pavements.

Table 3-6. Sensors for model verification of flexible systems.

Distress Model	Required Measurements	Optional Measurements	Considerations
HMA rutting	Vertical deformation using a vertical strain gauge at mid-depth of HMA layer of interest. Temperature at the surface, mid-depth, and bottom of HMA Vertical deformation of supporting layers through stress/strain correlation. Place pressure gauges at top and mid-depth of unbound layers and 6 inches below embankment surface	Horizontal strain at bottom of HMA (Many models attempt to correlate horizontal strain and vertical deformation) Moisture at mid-depth of base layer Vertical deformation of supporting layers using multi-depth deflectometers	Stiffness of HMA strain gauges should be compatible with expected strain Ambient/elevated temperatures Saturated/unsaturated
HMA bottom-up cracking	Horizontal strain at the bottom of the HMA layer Temperature at the surface, mid-depth, and bottom of the HMA	Base response using pressure gauges at surface, mid-depth, and bottom of layer Moisture of base layer	Stiffness of HMA strain gauges should be compatible with expected strain Accelerated temperature aging prior to testing Saturated/Unsaturated
HMA top-down cracking	Horizontal strain at the surface of the HMA layer Horizontal strain at the bottom of the HMA layer Temperature at the surface, mid-depth, and bottom of the HMA		Stiffness of HMA strain gauges should be compatible with expected strain Accelerated temperature aging prior to testing

Figure 3-16 illustrates a typical Florida pavement instrumented to measure critical and supplemental responses required for mechanistic models.

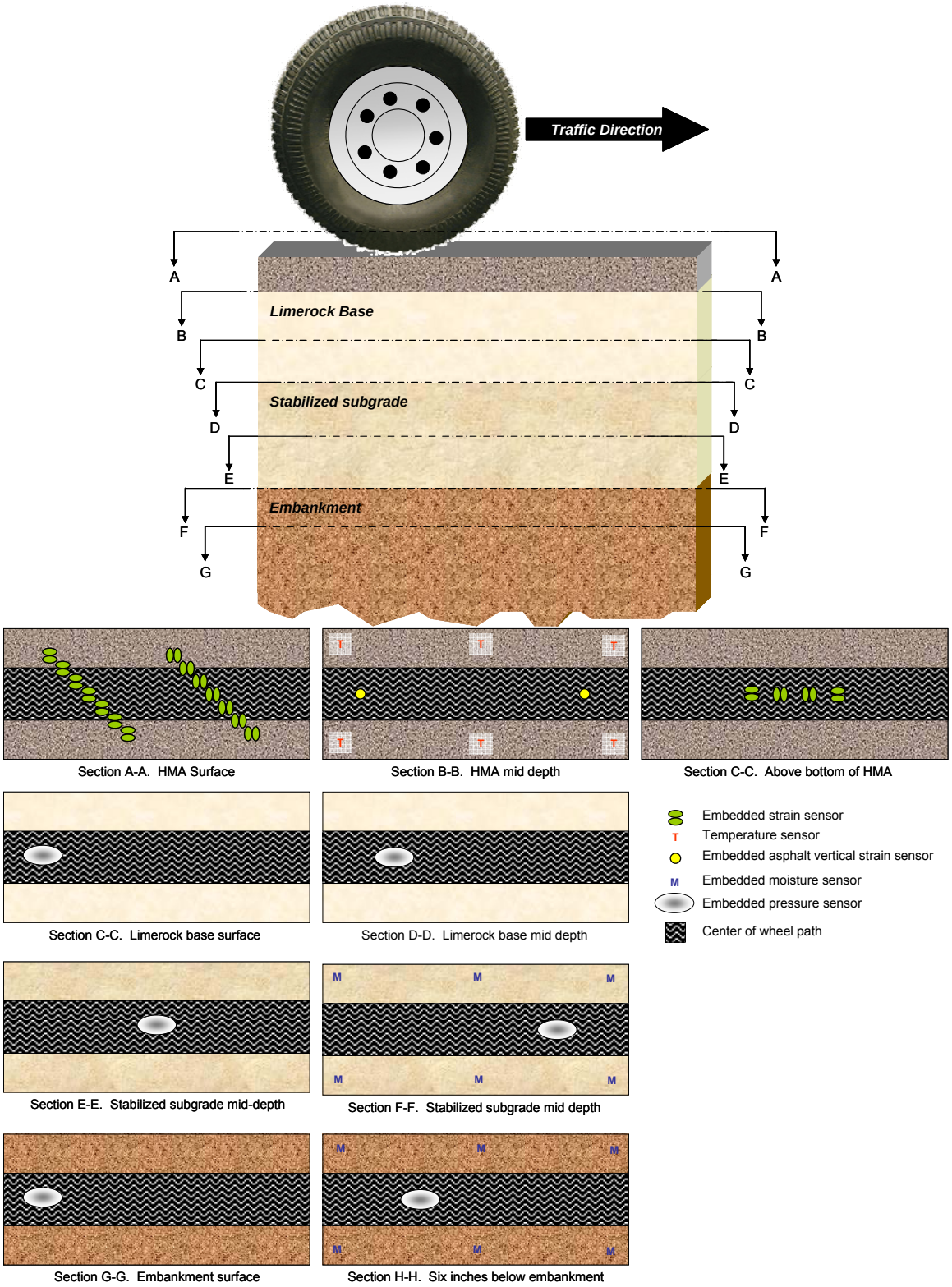

Figure 3-16. Illustration of an instrumented typical Florida flexible pavement.

3.4.2 Rigid Pavement Sensor Selection

Performance comparison and model verification tests are also common uses of accelerated testing of rigid pavements. Performance comparisons may evaluate the cracking potential of a PCC layer by varying the concrete mix design, mix additives, or thickness. Again, in order to evaluate the PCC layer and eliminate confounding test factors, the supporting layers should be constructed similarly while varying the PCC layer. The MEPDG models for rigid pavements do not directly consider the foundation support so the instrumentation required for both types of test are similar and is shown in Table 3-7. However, more emphasis on characterizing the foundation response is well founded when conducting model verification tests.

Figure 3-17 illustrates a typical Florida pavement instrumented to measure critical and supplemental responses required for mechanistic models.

Table 3-7. Sensors for rigid pavements.

Distress Type	Required Measurements	Optional Measurements	Considerations
JPCP bottom-up cracking	Horizontal strain at slab bottom near longitudinal edge, midway between transverse joints Temperature throughout slab depth	Horizontal strain at top and bottom of slab center due to thermal curvature Base surface response at mid slab using a pressure gauge	Critical stress greatest when traffic loading occurs during extreme positive temperature gradient
JPCP top-down cracking	Horizontal strain at slab surface near longitudinal edge, midway between transverse joints Temperature throughout slab depth	Thermal induced curvature at slab corner using a vertical JMDD Horizontal strain at top and bottom of slab corner due to thermal curvature Instrumented dowel bar to measure shear and strain Base surface response at slab corners using pressure gauges	Critical stress greatest when traffic loading occurs during extreme negative temperature gradient Top-down cracking requires an axle configuration that loads each slab edge simultaneously (impossible to reproduce with single wheel tests)
JPCP faulting	Deflection at joint edges due to faulting and thermal induced curvature using a MDD or vertical JMDD Temperature throughout slab depth	Thermal induced curvature at slab corner using a vertical JMDD Horizontal strain at top and bottom of slab corner due to thermal curvature Instrumented dowel bar to measure shear and strain Moisture of supporting layer Base surface response at slab corners using pressure gauges	Faulting is highly dependent on support conditions, presence of moisture, and pumping potential Saturated/unsaturated
CRCP punchout	Horizontal strain on leave side of transverse crack at slab surface some distance from longitudinal edge	Temperature throughout slab depth Moisture at mid-depth of base layer Base surface response below punchout using a pressure gauge	Cracks must form before surface strain gauges can be placed Saturated/unsaturated

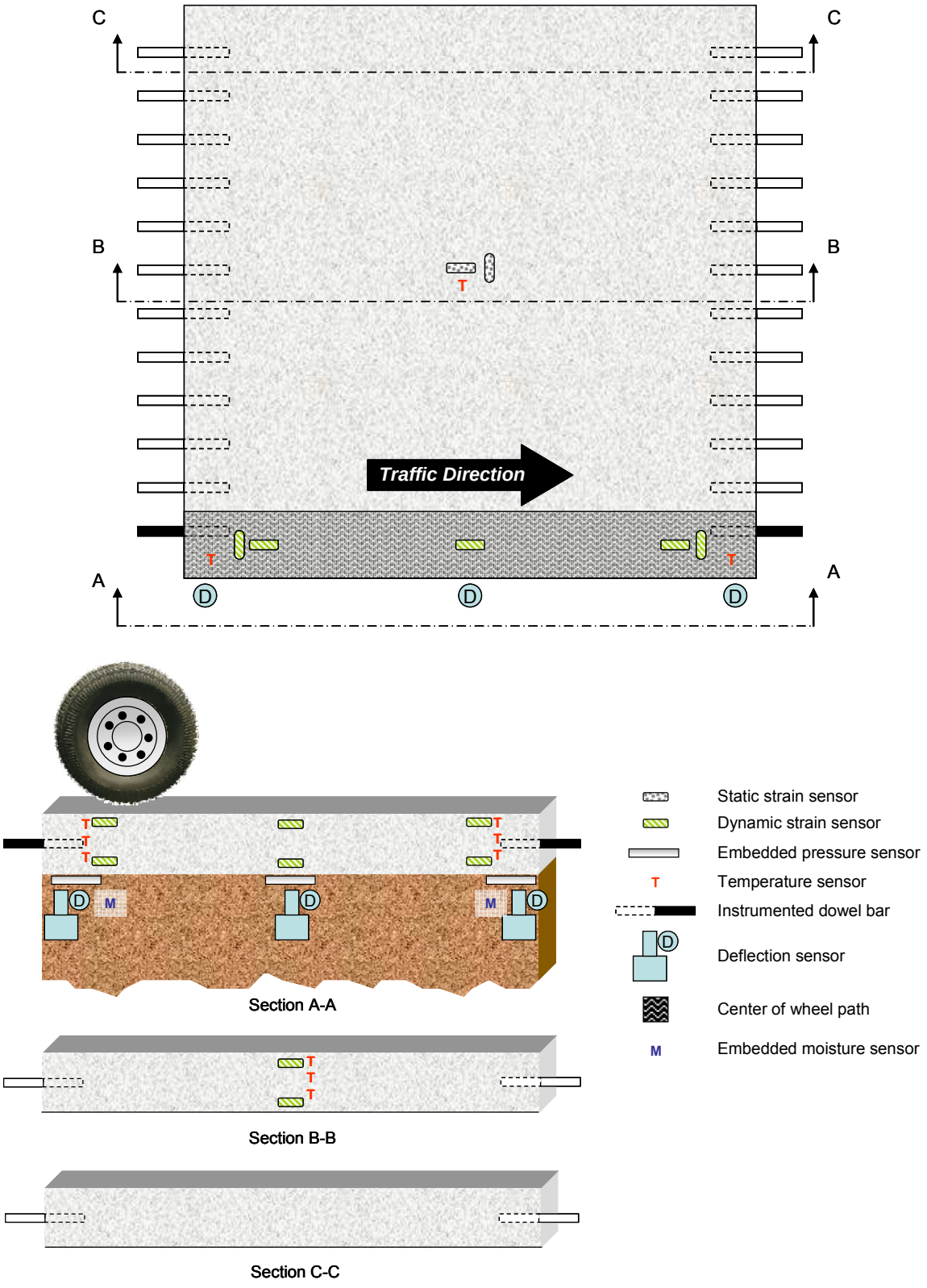

Figure 3-17. Illustration of an instrumented typical rigid pavement.

4 INTRUMENTATION BEST PRACTICES

4.1 Instrumentation Concepts

The use of embedded pavement instrumentation has been an important technology in the advancement of pavement engineering. Responses measured at critical locations in the structure enable engineers to develop a fundamental understanding of the interaction between pavement response and pavement performance. Virtually every road test or accelerated pavement test facility (APT), with the exception of the WesTrack experiment (Epps et al., 2002), has utilized embedded instrumentation to gain valuable mechanistic-empirical information.

While instrumentation has been used successfully, as demonstrated by the literature, there are some rudimentary concepts and steps needed for the success of the project that are not typically documented but are necessary. The point of these concepts and steps is to establish a gauge-tracking system that will ensure data veracity when a project reaches the analysis stage. These activities can be broken into four areas:

1. Pre-Installation
2. Construction
3. Post-Construction/Pre-Traffic
4. Under Traffic

The following sections are meant to provide procedural guidance through each of the four areas. While it is impossible to anticipate every gauge, and what should be done in a particular experimental setting, specific examples will be provided throughout this document to demonstrate concepts. Figure 4-1 provides an overall view of the process that will be detailed in the following sections.

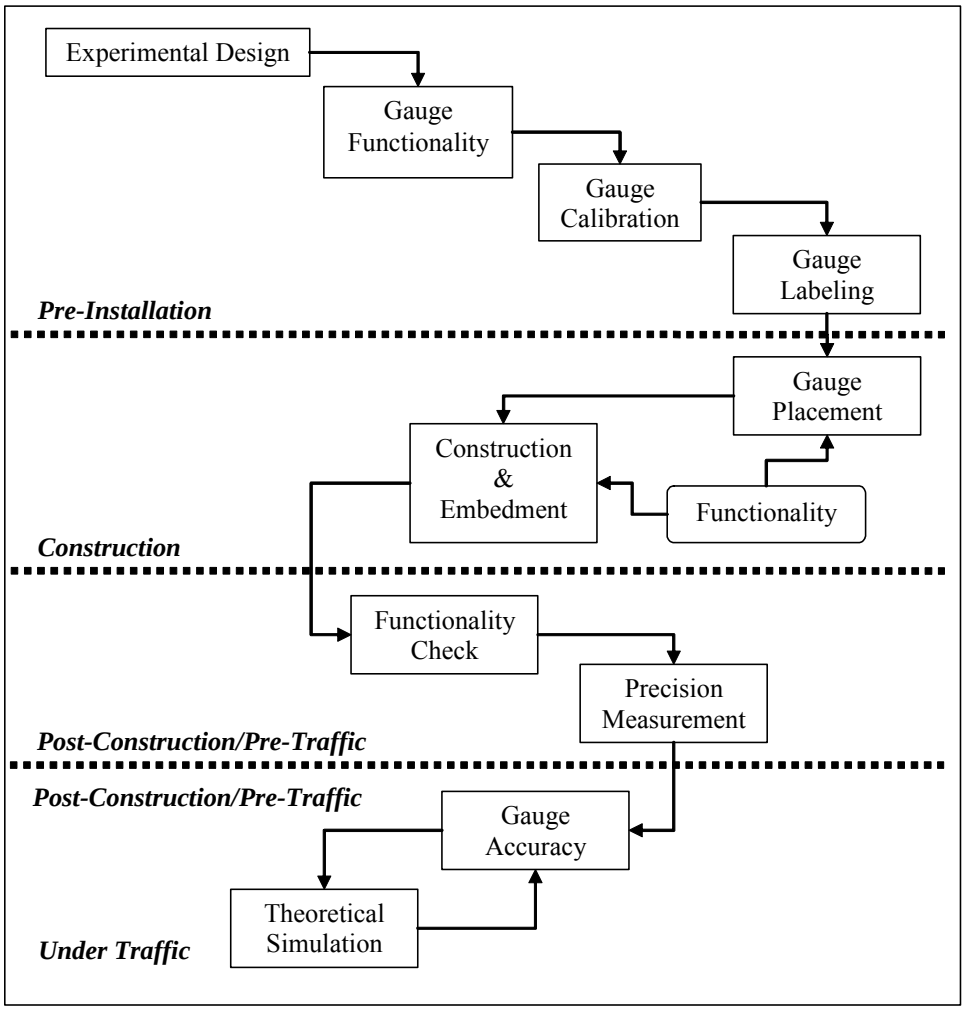

Figure 4-1. Procedure overview for demonstrating gauge veracity.

4.2 Pre-installation

As illustrated in Figure 4-1, pre-installation activities consists of experimental design, gauge functionality checks, gauge calibration and gauge labeling. This stage lays the critical groundwork for a successful experiment by assuring that only "good" gauges are installed and establishing a gauge tracking system.

4.2.1 Experimental Design

In experimental design, the research team must answer two critical questions. First, what are the important variables that should be measured in the experiment? Second, where should the measurements be made? These will be answered by the overall objective of the experiment. For example, if the objective is to develop fatigue transfer functions for asphalt mixtures, then asphalt strain gauges placed at the bottom of the asphalt layer would be appropriate. Other instrumentation, such as temperature probes, may also be required to link temperature effects to pavement response and performance. The research team must also consider the survivability rates of the selected gauges so that appropriate

redundancy can be planned. In any case, the number and types of gauges must be selected and the gauge configuration established. Figure 4-2 and Figure 4-3 illustrate example schematics used at the FDOT HVS facility. Key components of the figures include dimensions such as pavement geometry, layer identification, gauge labeling, gauge spacing and depth of embedment.

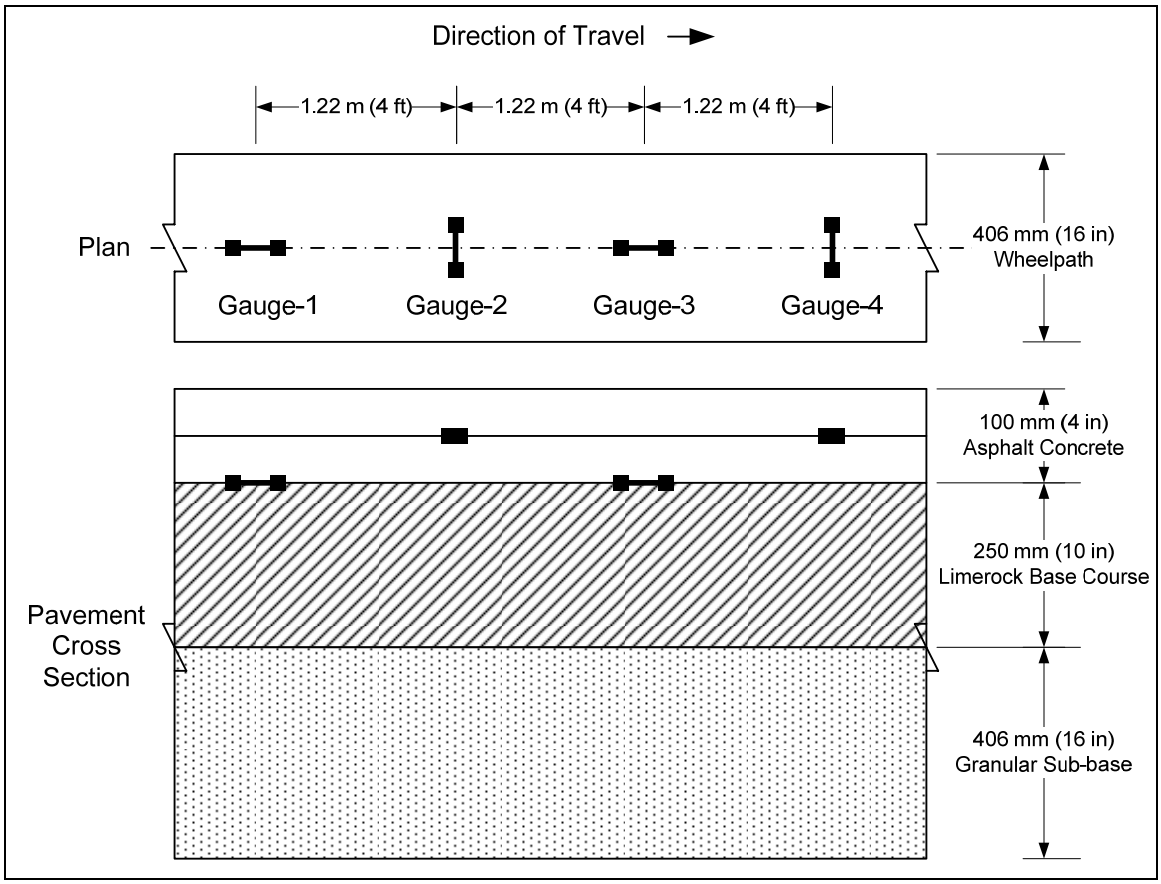

Figure 4-2. HMA experiment gauge layout.

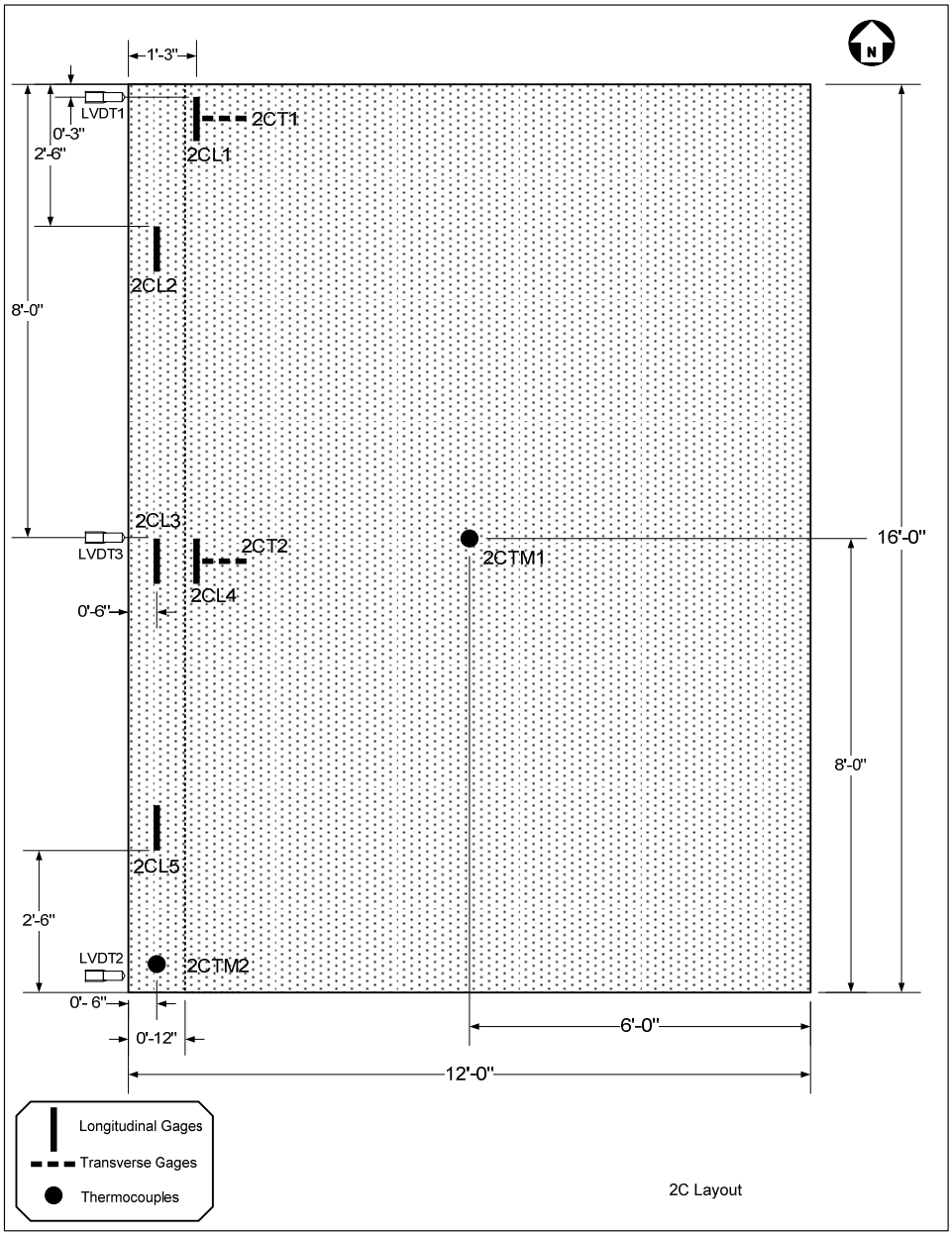

Figure 4-3. Concrete experiment gauge layout.

4.2.2 Gauge Functionality

Upon receipt of instrumentation from the vendor, each gauge should first be checked for functionality. Specifically, the following checks should be made:

- Gauge produces an output signal
- Baseline (unloaded) response is stable
- Gauge responds as expected to stimulus
- Gauge baseline (unloaded) signal is in acceptable range

To check the gauge functionality, each gauge should be connected to the data acquisition system that will be used in the experiment and a baseline reading should be obtained. In addition to compiling tabular data, a small amount (i.e., a few seconds) of data should be recorded for the baseline stability check. Figure 4-4 illustrates connecting asphalt strain gauges for functionality checks.

Figure 4-4. Connecting of asphalt strain gauges for functionality checks.

After the gauge has been verified to produce an output signal and the baseline reading is recorded, an external load or stimulus should be applied to check that the gauge responds as expected. This is important since gauges may have been wired incorrectly by the manufacturer and produce a response opposite to what is expected when loaded. Figure 4-5 illustrates checking an asphalt strain gauge and verifying the response on the data acquisition software.

Figure 4-5. Gauge response check.

The final functionality check ensures that the baseline signal is in an acceptable range. This is important since most gauges will drift with time and age and, although gauges can often be readjusted with resistors, it is best to start an experiment with baseline readings near zero. Figure 4-6 highlights this concept. In this example, four asphalt strain gauges were tested for functionality with a full-scale range of ±5 volts. All four gauges have relatively stable baseline readings and produce the expected output (tension results in positive voltage). However, gauges 1 and 2 have relatively high initial baselines with gauge 1 measuring off scale when put into tension. Though gauge 1 is functioning, it would be best to replace it with a gauge with an offset closer to zero.

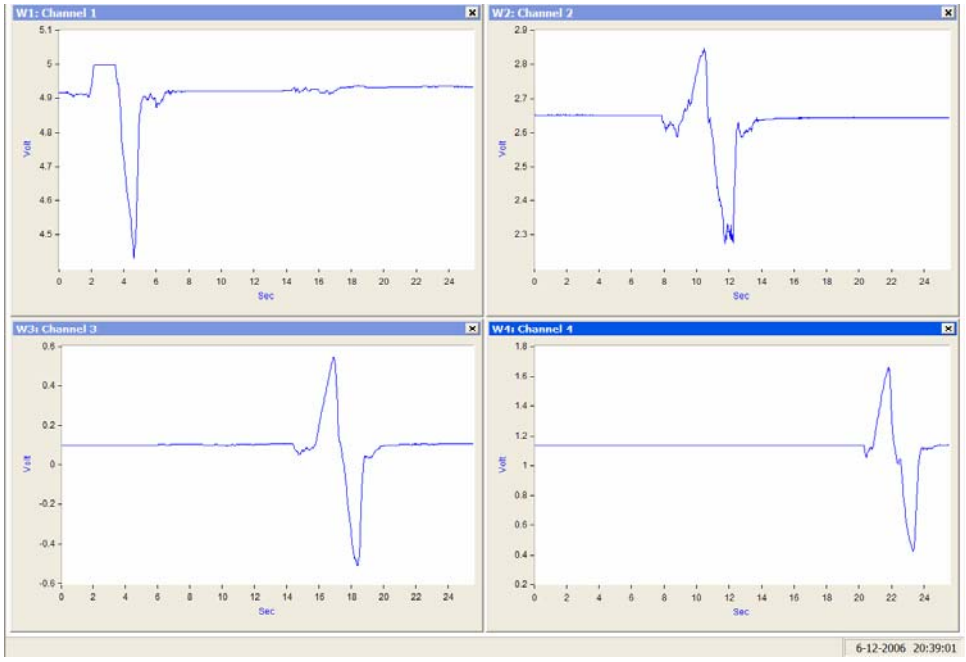

Figure 4-6. Asphalt strain gauge signals during functionality check.

When deciding whether to replace gauges prior to construction, all of the gauges should be considered together in the context of how many gauges are needed for initial construction. As an example, Figure 4-7 illustrates a distribution of baseline voltages compiled from 90 asphalt strain gauges, of which 18 were to be surplus, recently tested at the NCAT Test Track. The data indicate that nearly 90 percent of the gauges were within ±2 volts of zero. Since there were enough surplus gauges, only gauges with an initial offset between ±2 volts were used. Had there been fewer gauges, the gauges with higher offsets would have been evenly distributed amongst the planned test sections such that one would not have an overrepresentation of high-offset gauges.

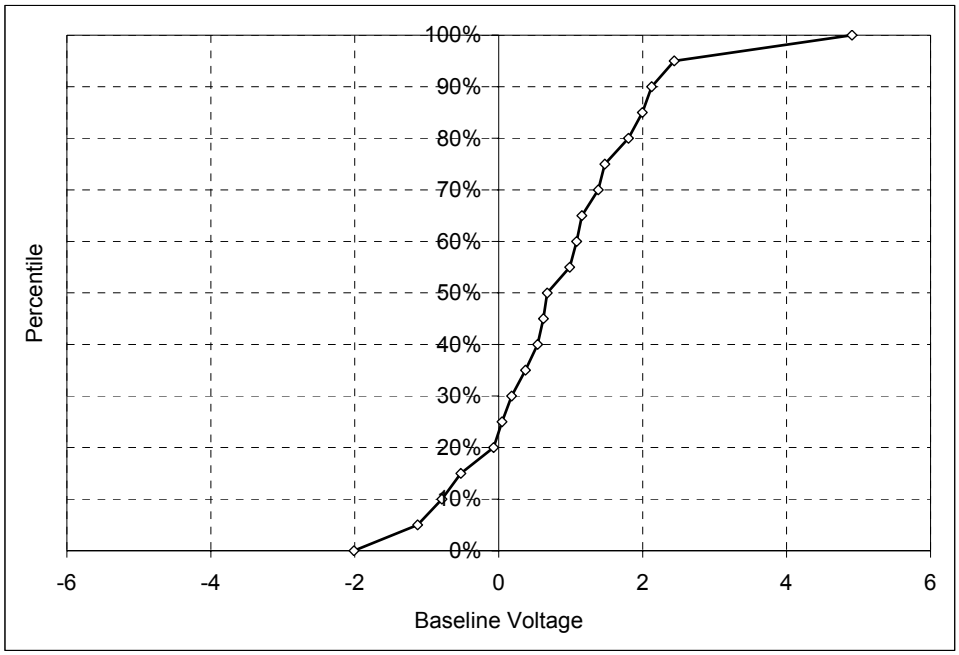

Figure 4-7. NCAT Test track baseline voltage statistical summary.

4.2.3 Gauge Calibration

Gauge calibration is an important part of the instrumentation process, because calibration factors are used to convert an electrical response (i.e., voltage) to an engineering response (i.e., stress or strain). While it would be ideal to locally calibrate each gauge, it may not be necessary, since many manufacturers provide gauge calibration factors that have been determined under laboratory conditions. A recent study by Hornyak et al. (2007) conducted extensive calibration studies of asphalt strain gauges, soil moisture probes and earth pressure cells. They concluded that their own calibration factors were in reasonable agreement with those provided by the manufacturer. However, in cases where gauge calibration factors are not provided, or when local calibration is needed, it is best to follow the manufacturer's recommended procedure. To highlight some gauge calibration practices for a number of instrumentation categories, the following sub-sections provide examples of calibration efforts for temperature, moisture, strain and pressure gauges.

4.2.3.1 Temperature

Temperature probes, in the form of thermistors or thermocouples, have a long and well-established history in pavement research. Manufacturers such as Campbell-Scientific provide ample documentation regarding the calibration of their gauges and can generally be relied upon to provide good results. For example, the Campbell-Scientific Model 108 thermistor has a reported accuracy of ±0.3ºC over a range of -3ºC to 90ºC (Campbell-Scientific, 2004). However, before installing the gauges, it is prudent to verify that each gauge matches the manufacturer-provided calibration. This is more of an effort to be sure the gauge is functioning properly as opposed to determining a new calibration coefficient.

Each temperature probe should be individually checked at several temperatures in the range of expected temperatures it will encounter once installed. Placing a probe in an ice-bath is a simple way to check 32ºF. Probes can also be checked for room temperature using a separate and accurate temperature device. The same can be done in a hot-water bath.

4.2.3.2 Moisture

Moisture probes, because they are measuring electrical properties of soil, typically require local calibration with the materials in which they will be embedded. The local calibration will account for the effects of specific mineralogy and density of the material.

It is important when calibrating moisture probes to prepare samples covering the range of expected moisture contents and at or near the expected in-place density of the material. Campbell-Scientific recommends that three moisture contents be used during calibration to accurately characterize the typically quadratic relationship between the gauge output and the actual moisture content (Campbell-Scientific, 2006). Based on this recommendation, it can be recommended that calibration samples should include a dry sample (0%), a sample near the optimum moisture content of the material and a sample at least double the optimum moisture content. This should adequately cover the in-service moisture contents the gauge will encounter.

As mentioned above, the density of the calibration samples should approximate expected in-service densities. It is also important to be sure the calibration sample is large enough so that the probe is truly measuring the moisture content of the material, rather than its container. Campbell-Scientific (2006) recommends at least 2.5 inches of soil surround their time domain reflectometer (TDR) probes during calibration. Similarly, a study by Hornyak et al. (2007) found that less than 2 inches of cover material resulted in significant changes in moisture contents for a capacitance-based moisture probe.

Recent calibration efforts as part of the 2003 NCAT Test Track found that 5-gallon buckets worked well for the Campbell-Scientific CS616 TDR probes. They were large enough to facilitate compaction and eliminate the edge effect of the bucket. They were small enough that large amounts of soil were not required. As shown in Figure 4-8, samples were prepared at three moisture contents. For each gauge, two sets of two moisture content readings were obtained, with the probe rotated 90º between sets. The data were plotted and evaluated using best fit linear and quadratic functions. Figure 4-8 summarizes the data for all gauges, though plots were also created for each gauge individually. Note that the linear function appeared to provide sufficient accuracy when compared to the quadratic function. Therefore, it was decided to use the linear function for each gauge. This was consistent with Campbell-Scientific's recommendation of using a linear function, if possible. The resulting calibration coefficients for each gauge are tabulated in Table 1 and were entered into the data acquisition system to obtain gravimetric moisture contents from the TDR probes.

a) Soil samples in sealed containers

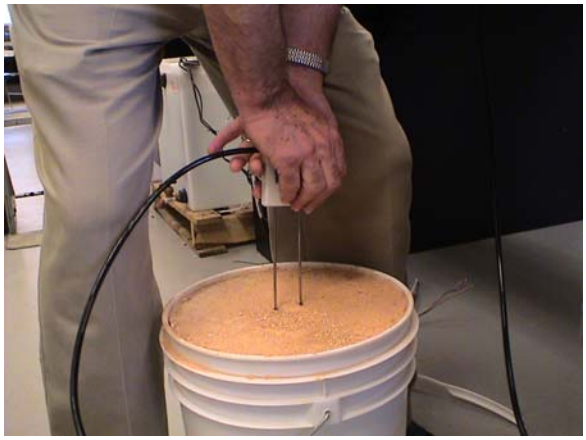

b) Inserting TDR probe

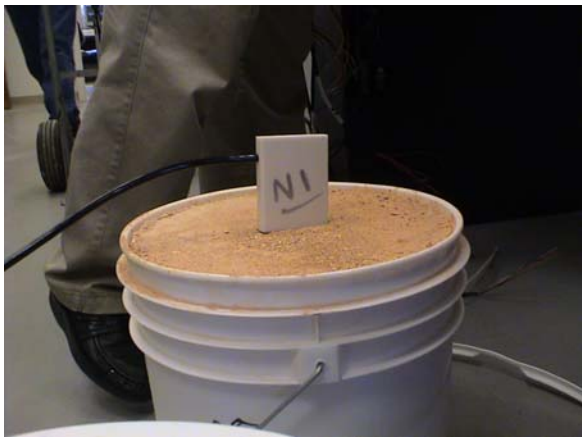

c) TDR probe while taking readings

Figure 4-8. Calibration of moisture probes (Timm et al., 2003)

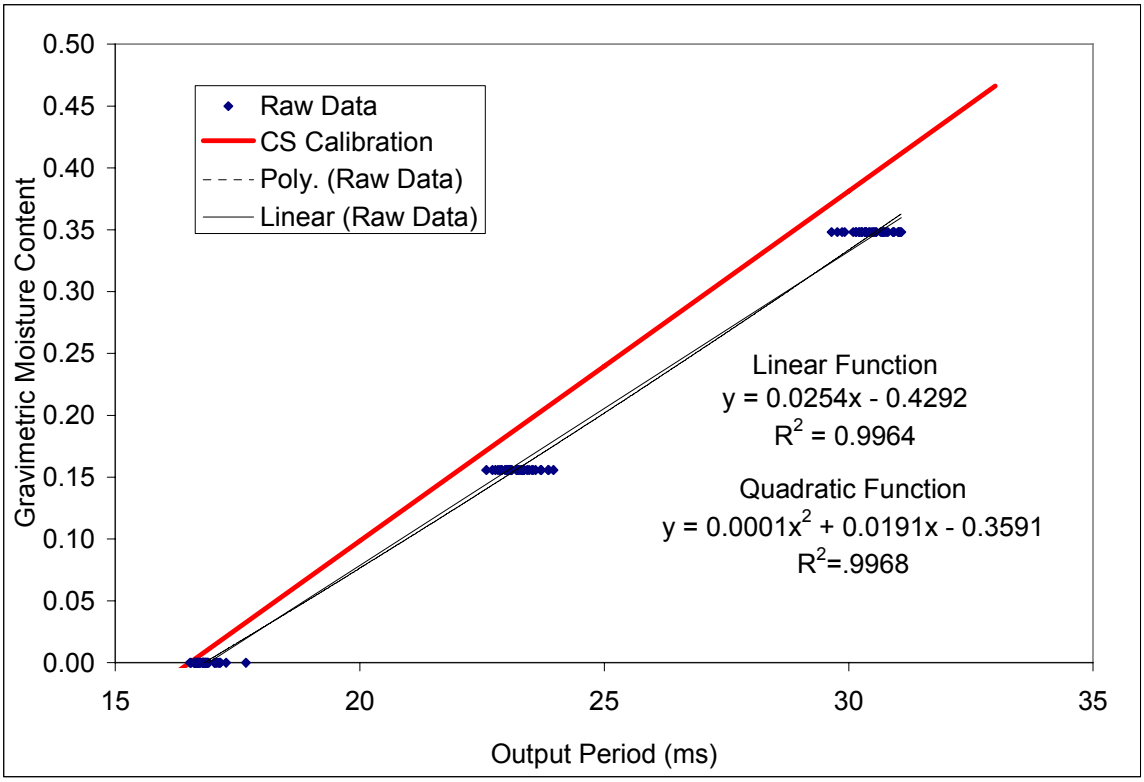

Figure 4-9. TDR calibration data – all gauges (Timm et al., 2003).

Table 4-1. Example TDR probe calibration coefficients (Timm et al., 2003).

Sensor	Slope Moisture Content / Period (ms)	Intercept Moisture Content	R^2
N1	0.0253	-0.4286	0.9980
N2	0.0246	-0.4174	0.9972
N3	0.0261	-0.4401	0.9985
N4	0.0264	-0.4481	0.9975
N5A	0.0252	-0.4255	0.9969
N5B	0.0261	-0.4456	0.9937
N5C	0.0249	-0.4187	0.9987
N6	0.0244	-0.4079	0.9986
N7	0.0260	-0.4419	0.9962
N8	0.0253	-0.4277	0.9991

4.2.3.3 Strain Gauges

Strain gauges are routinely provided with a calibration data sheet from the manufacturer. A search of scientific literature yielded little information regarding local calibration of these gauges for pavement studies. Personal inquiries to some of the major U.S. pavement test facilities and research projects (i.e., Mn/ROAD, SISSI, NAPTF, SmartRoad) revealed that little, if any, local calibration is performed. Tom Burnham of

Mn/ROAD stated (Burnham, 2006), "The only 'calibration' of sensors that we have done are what we call 'pre-installation quality checks'. We essentially check that the sensor we received from the manufacture is functioning properly. This typically involves checking voltage or resistance change to small manually applied forces to the sensors (in the laboratory)."

While it is generally unnecessary to provide local calibration for strain gauges, it can be done. A research group at Marquette University (Hornyak et al., 2007) recently conducted extensive calibration of strain gauges as part of a field instrumentation project on I-43 in Milwaukee, WI.

In their calibration of CTL asphalt strain gauges, the Marquette group (Hornyak et al., 2007) attached a precision extensometer to the nylon shaft of the strain gauge as pictured in Figure 4-10. A metal bracket was attached to the bottom of the asphalt strain gauge flange so that weights could be hung from the gauge. Strain measurements were obtained from both the precision extensometer and the asphalt strain gauge. The precision extensometer was assumed to be "truth" in their experiments. In the course of their experiments, they found that slight misalignments of the metal flange would cause seemingly erroneous readings. To counter this, they performed two sets of calibrations and averaged the results. The first calibration was performed as pictured in Figure 4-10. The second calibration consisted of rotating the precision extensometer 180º around the center of the shaft. Typical results, shown in Figure 4-11, illustrate that the effects of misalignment or bending can be significant and must be addressed in the calibration process.

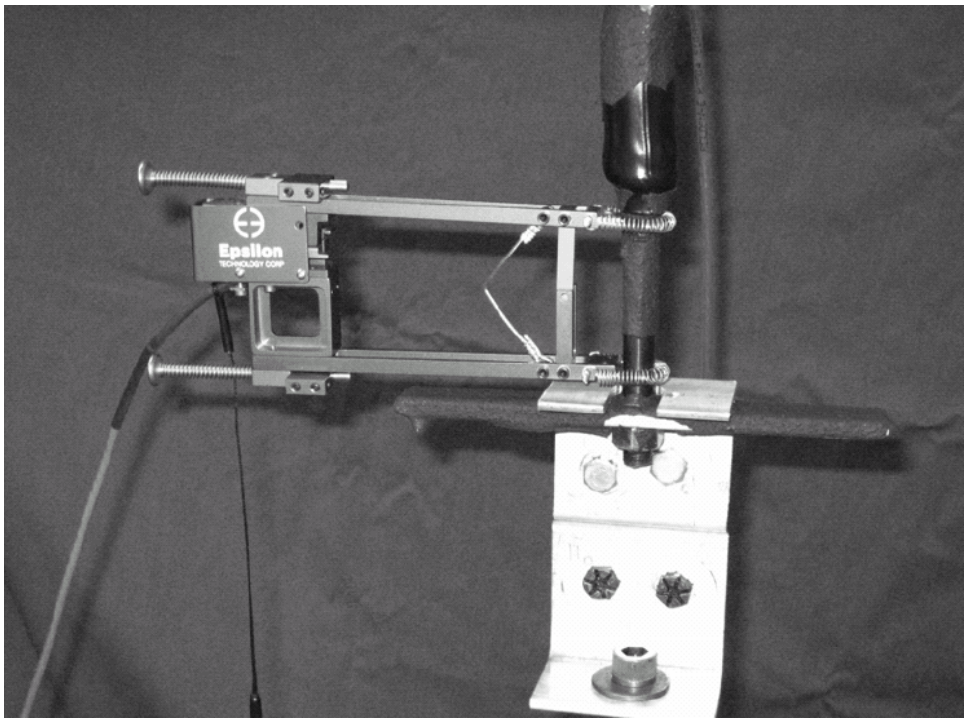

Figure 4-10. Calibration of CTL asphalt strain gauge (Hornyak et al., 2007)

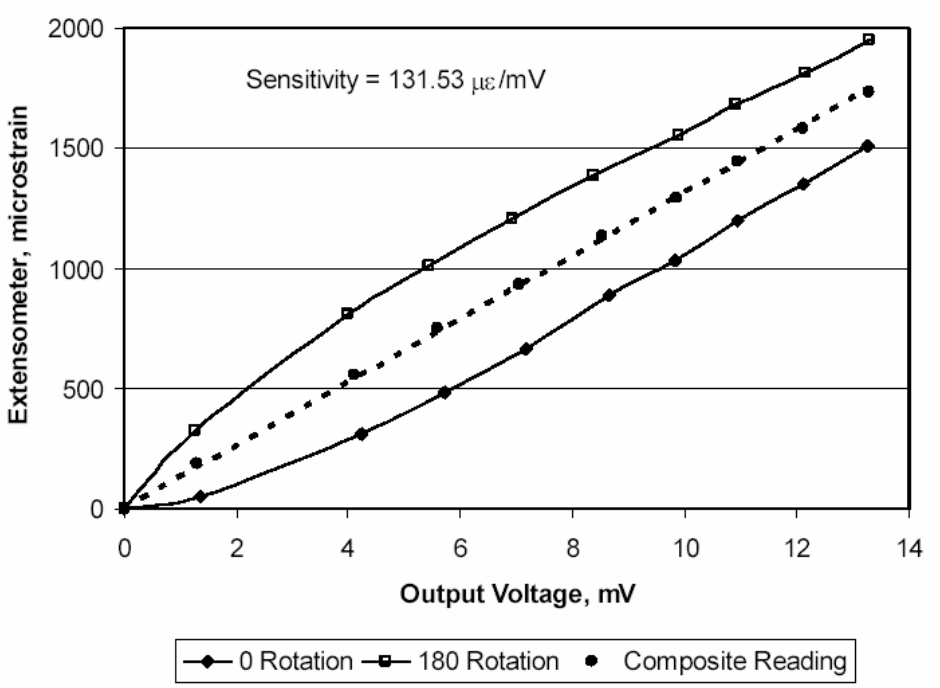

Figure 4-11. Typical CTL asphalt strain gauge calibration results (Hornyak et al., 2007)

A summary of the calibration results are shown in Figure 4-12. The black and gray bars correspond to Marquette and CTL-derived calibration coefficients, respectively. The white bars represent the ratio of the Marquette coefficient divided by the CTL coefficient. Ideally, the ratio would be 1.0 representing a perfect match. However, in reality, the Marquette coefficients were somewhat lower with an average ratio of 0.93 with a range of 0.83 to 1.10. Hornyak et al. (2007) stated that differences between gauges or even the mounting of the external calibration hardware could account for these differences.

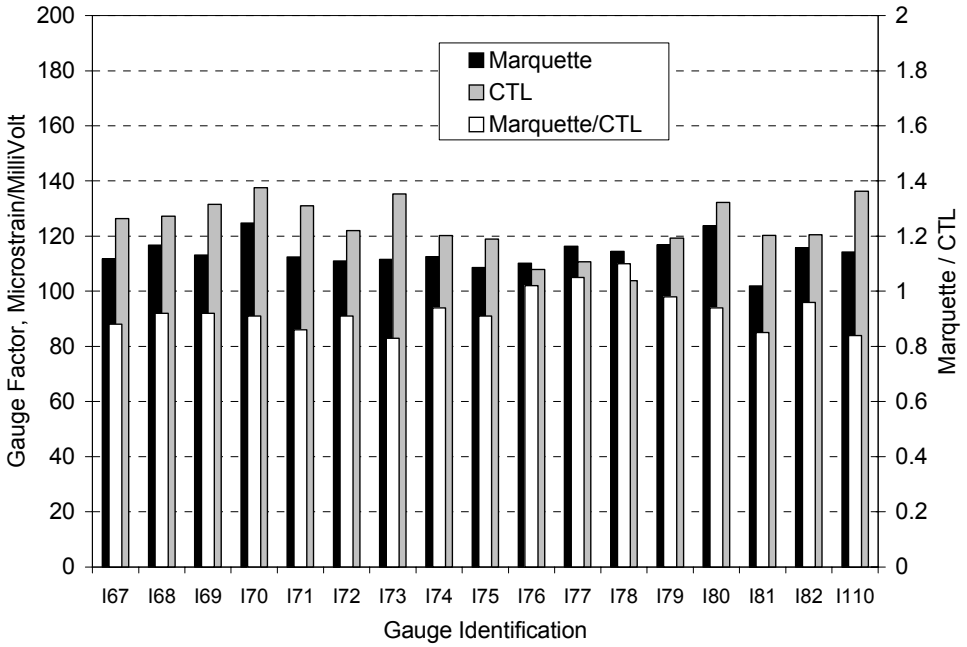

Figure 4-12. Summary of Marquette versus CTL calibration (after Hornyak et al., 2007).

4.2.3.4 Pressure

Like strain gauges, very little has been documented regarding local calibration of pressure cells used in pavement studies. Also similar to strain gauges, pressure cells typically are delivered with manufacturer-provided calibration factors. However, there have been two recent calibration efforts worth noting. The two efforts have in common earth pressure cells placed inside a water-filled pressurized chamber capable of reaching the full-scale pressure of the gauges. In both cases, the local calibration was reasonably close to the manufacturer calibration. Each is described below.

At Marquette University, as part of the project mentioned above in the strain gauge section, earth pressure cells were suspended inside a water-filled pressurized cylinder. Pressures were applied incrementally and measured both with the earth pressure cell and an external precise (±0.5% full scale) pressure gauge (Hornyak et al., 2007). Figure 4-13 summarizes their results where there is nearly an identical match between the local and manufacturer calibrations. It was concluded that the calibration factors fell within the manufacturer's recommended range, and the local calibration coefficients were just slightly (0.1% to 0.2%) higher (Hornyak et al., 2007).

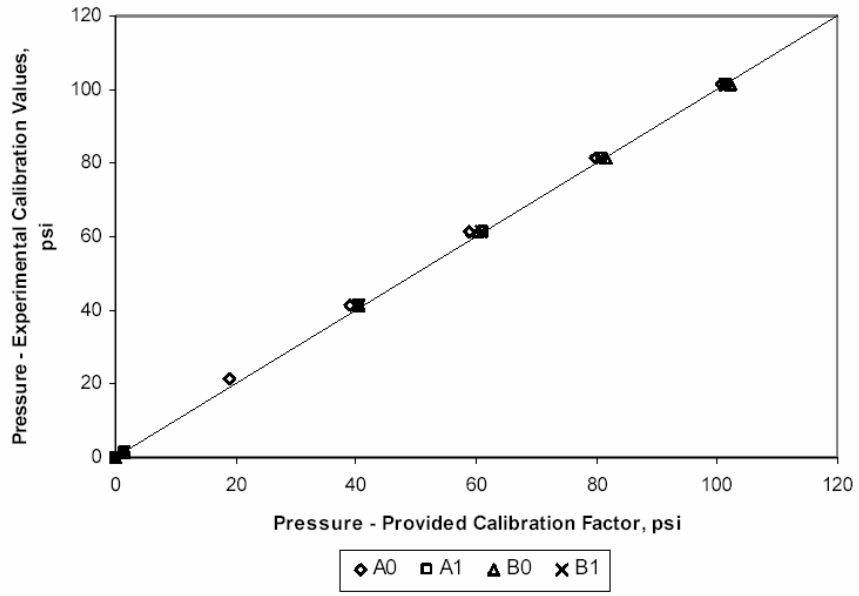

Figure 4-13. Summary of pressure cell calibration (Hornyak et al., 2007).

A similar effort was undertaken as part of the 2006 NCAT Test Track structural study. For this work, a custom steel calibration chamber was fabricated. Figure 4-14 illustrates different aspects of the calibration chamber. Since the 2006 NCAT Test Track research effort utilized 18 pressure cells, it was desirable to have a chamber capable of calibrating multiple gauges simultaneously. Given the materials on hand, the chamber was built to accommodate 6 gauges at one time. A rubber gasket and 17 bolts were used to seal the chamber during testing. External measurements were made by the Omega gauge pictured in Figure 4-14(d) while internal measurements were obtained directly from the pressure plates connected to an external data acquisition system.

During calibration, readings were taken at approximately 5 psi increments, from 0 psi to near the full scale of the gauge at 30 psi. The pressure was increased and decreased, over the 30 psi range, three times for repeatability and to ensure that the gauges were reading the same way when either increasing or decreasing the pressure. Figure 4-15 illustrates the results for two pressure plates relative to the Geokon-provided calibration. These results are representative of all the pressure plates that were calibrated. Clearly, the local and manufacturer calibrations are very similar and one could argue that the local calibration was not needed. However, the local calibration does provide valuable information regarding the accuracy of the gauge prior to installation in addition to a slightly more precise, gauge specific, calibration. Table 4-2 lists the individual calibration coefficients obtained at NCAT.

a) Chamber Fabrication b) Finished Chamber

c) Pressure Cells in Chamber d) Precision Pressure Gauge

Figure 4-14. NCAT pressure cell calibration chamber.

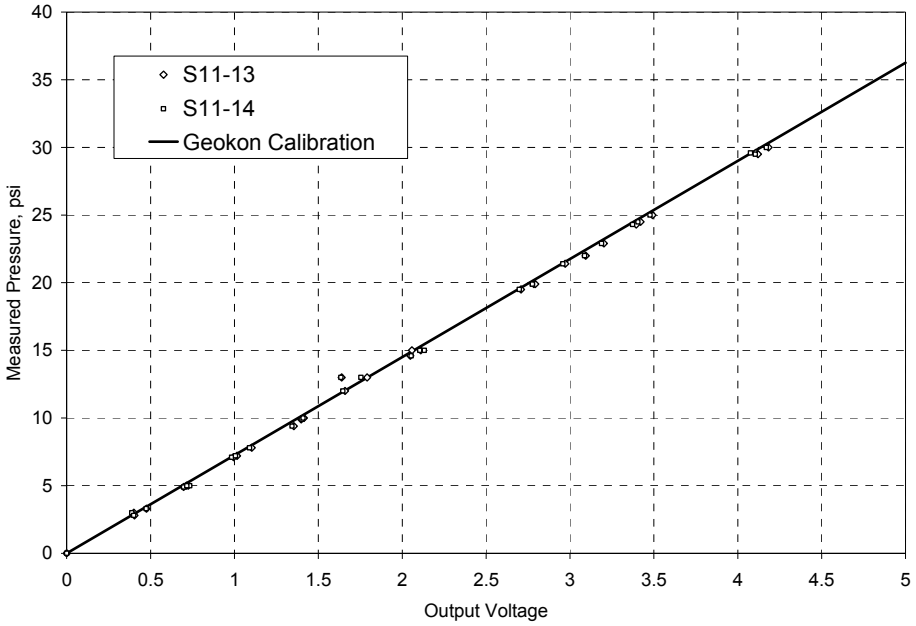

Figure 4-15. NCAT earth pressure cell calibration data.

Table 4-2. NCAT earth pressure cell calibration coefficients.

Section	Gauge	Slope	Intercept	R^2
1	1-13	7.295	-0.2670	0.9996
1	1-14	7.382	-0.3800	0.9989
2	2-13	7.309	-0.2970	0.9970
2	2-14	7.302	-0.2460	0.9987
8	8-13	7.197	0.0420	0.9970
8	8-14	7.173	0.0690	0.9980
9	9-13	7.177	0.0680	0.9980
9	9-14	7.188	0.0840	0.9970
10	10-13	7.247	-0.2400	0.9990
10	10-14	7.324	-0.3060	0.9996
11	11-13	7.181	-0.0230	0.9990
11	11-14	7.211	-0.0320	0.9989

4.2.3.5 Summary

Gauge calibration is an important part of any instrumented pavement research project. Previous studies seem to support using manufacturer-supplied calibration factors rather than performing calibration studies locally. Soil moisture probes, however, are a notable exception. These should be calibrated with the soils in which they will be embedded. The need to calibrate other classes of instrumentation should be judged on a case-by-case basis. While performing a local calibration may not provide entirely different calibration coefficients, it can provide confidence that the gauge is working properly when it is received at the project site. This could potentially help avoid installing a gauge that would pass a functionality check but not provide accurate pavement response measurements.

4.2.4 Gauge Labeling

After a gauge has passed the functionality and calibration checks, it can be assigned to a location within the experiment. It is important to maintain a database of the manufacturers' identification code in addition to the experimental section/location assignment. This will allow for efficient tracking through project or manufacturer records in the event that there is a problem with a gauge. It is also appropriate at this point to build a gauge calibration factor database. Finally, labels should be placed at either end of each cable to facilitate identification during installation (Figure 4-16).

Figure 4-16. Gauge labeling.

4.3 Construction

Gauge installation during construction is often the most critical element to project success. Typically, if gauges survive the harsh construction environment, they will continue to perform satisfactorily over the duration of the experiment. Most gauges will be provided by the manufacturer with some basic guidance regarding installation. As a general rule, it is recommended that the manufacturer's recommendations be followed. However, some installation procedures are so complex, time consuming or restrictive that deviations are sometimes necessary. For example, the installation guide for the Geokon Model 3500 earth pressure cell, a device used in many full-scale pavement test facilities, states (Geokon, 2004), "…no vibratory rollers should be permitted across the lens until it is protected by a compacted thickness of at least 1 meter (≈3 ft)." This forces a difficult decision between having adequate compaction and gauge survivability. In these kinds of situations, some trials may be warranted to determine the best balance between construction practice and gauge survivability. If adequate construction must be sacrificed at the cost of gauge survivability, it may be best to consider using another type of instrumentation. It should be noted that Geokon is by no means the only manufacturer with restrictive installation procedures.

Generally speaking, the gauge installation procedure can be divided into two stages; gauge placement and construction/embedment. In each stage, gauges should be monitored for functionality as will be explained below.

4.3.1 Gauge Placement

Gauge placement pertains to physically placing gauges in their respective locations prior to paving. In this stage, the best arrangement of cabling can be determined, typically

running cables together when possible, to minimize the effect of cabling on the pavement structure. Various methods can be used to locate the gauges from precise surveying techniques to simple string lines. Regardless of the method, it is important to have precise measurements of the final location. This includes station (longitudinal location), offset (transverse location) and depth. Figure 4-17 highlights the placement process.

Figure 4-17. Marking and placing of gauges.

Since the gauges experience a lot of handling during placement, and some may be damaged, it is recommended that functionality checks be performed once all gauges have been placed. This is a final check to ensure all gauges are operational prior to paving and any last minute changes can be made if necessary. Figure 4-18 illustrates this process where an oscilloscope had been connected to check signal waveforms. Ideally, the data acquisition system that will be utilized during experimentation should be used, and baselines recorded to detect significant changes from the pre-installation check.

Figure 4-18. Functionality check of gauges prior to paving.

4.3.2 Construction/Embedment

As discussed above, gauge survival during the construction process is critical to project success. During construction, it is important to monitor gauges to evaluate the construction process in terms of gauge functionality and gauge survivability. This should be done for every project so that a knowledge-base can be developed to guide future construction efforts.

Using the data-acquisition system, gauges can be watched for signal loss, over-ranging and erratic behavior throughout the construction process. This includes the hand-placement portion (Figure 4-19) in addition to the mechanized paving process (Figure 4-20).

Figure 4-19. Gauge hand placement process.

Figure 4-20. Paving over gauges.

Figure 4-21 illustrates data collected from an array of 12 asphalt strain gauges (windows 1-12) and one earth pressure cell (window 13) during construction. The roller passes are clearly evident by the short spikes in the signals and the baseline (unloaded) signals look relatively stable for most of the gauges. Gauge 10; however, appears to have an excessive noise problem that should be investigated. Application of a moving average, as demonstrated in Figure 4-22, indicates that the roller passes were evident but difficult to see due to signal noise. This gauge should be watched for further erratic behavior and it may be necessary to exclude data obtained from this gauge from analysis. Another problem arises from the fact that the gauge was frequently over ranged by roller passes. The extent that this could have damaged the gauge is impossible to tell at this point, but should definitely be evaluated in the future.

It is also interesting to note from Figure 4-21 that every gauge in at least one or more roller passes exceeded its full scale range. This is an indication that the construction practice may need to change in the future. However, a full analysis after construction is needed to assess what damage may have occurred. It is encouraging though that gauges were over-ranged and still appear functional. For example, Gauge 13 (an earth pressure cell) experienced two overloaded cycles (Figure 4-23) but exhibited approximately the same response before and after the over-ranging occurred.

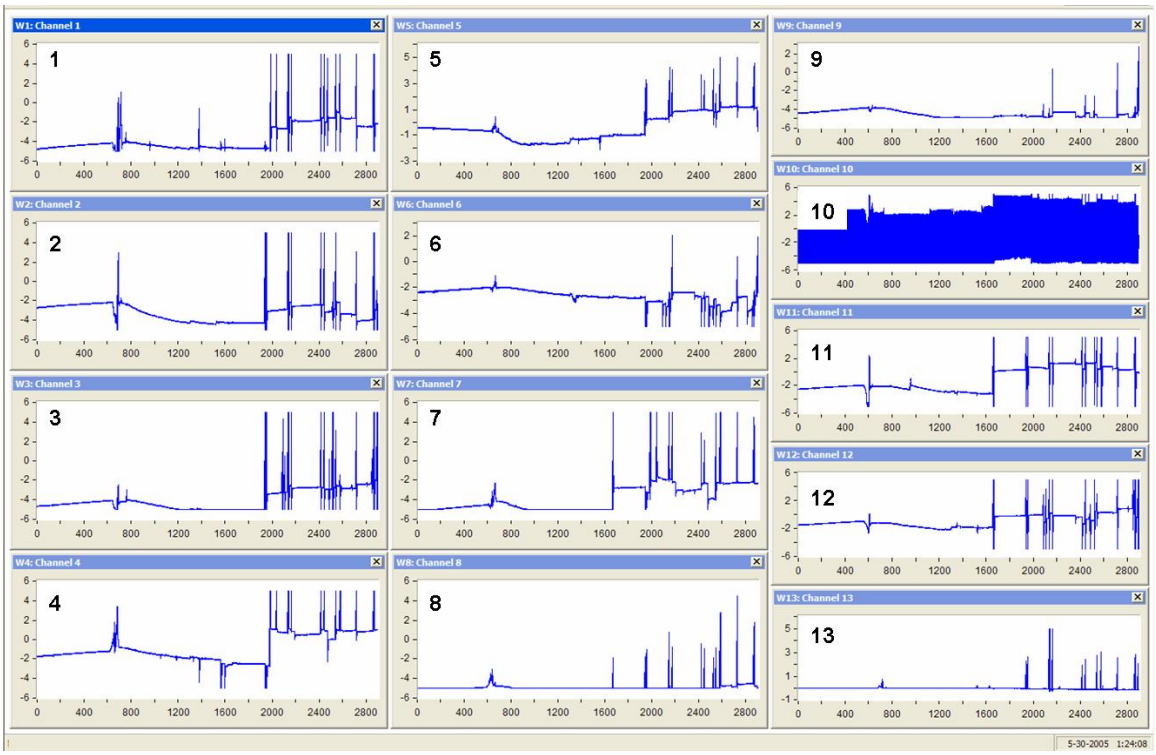

Figure 4-21. Gauge response during construction.

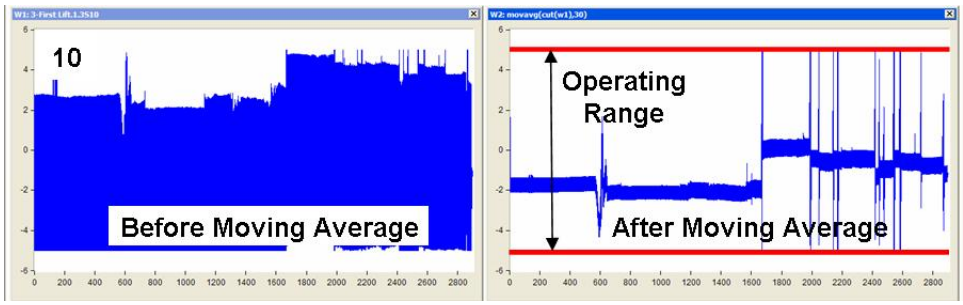

Figure 4-22. Application of a moving average to Gauge 10 in Figure 4-21.

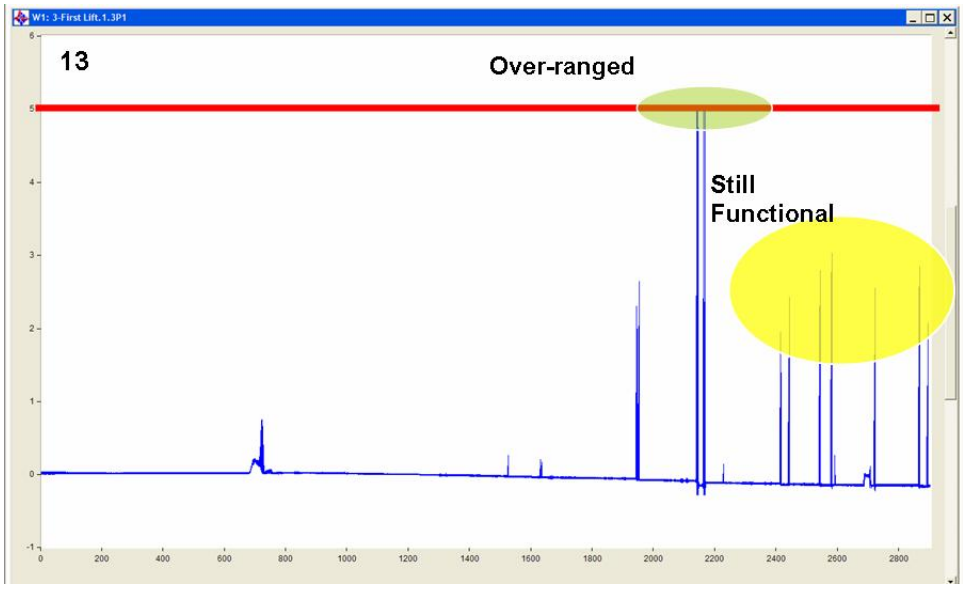

Figure 4-23. Over ranged cycle of gauge 13 in Figure 4-21.

4.4 Post-construction/Pre-Traffic

After construction, but before traffic applications begin, the instrumentation system should be assessed. Specifically, gauges should be identified that are:

1. No longer functioning
2. Off scale
3. behaving erratically

This can be accomplished by examining baseline (unloaded) traces and comparing them against what was observed during pre-installation. Significant changes should be noted so that erroneous data do not enter the project database. Gauges that are off scale can often be brought on-line by adding resistance on the circuit without compromising measurement capabilities.

Gauge precision should also be established at this point. Once the experiment begins and confounding factors such as pavement age, temperature, moisture and distress begin to affect the experiment, it will be difficult to distinguish between measurement error and effects of these factors. Therefore, it is important to establish gauge precision at the start of the experiment. Both within gauge and between gauge precision should be established. Within gauge refers to the precision of a single gauge under repeated, unchanging, stimulus. Between gauge refers to precision within an array of gauges designed to measure the same response under the same stimulus (e.g., vertical deflection at the top of the base material).

Within gauge precision can be determined in a straightforward manner by applying the same stimulus over a short period of time. It is recommended that this testing be done under representative conditions (e.g., middle of the expected temperature range). Take, for example, a deflection sensor to measure vertical displacement at the top of a base layer. The gauge precision can be determined by dropping a known load at the gauge location multiple times and determining the gauge response standard deviation. This value can be used when further precision testing is done later in the experiment to determine if a gauge is still working properly.

Precision obtained from multiple gauges in an array meant to measure the same quantity can be used to identify faulty gauges at the start of the experiment. Take, for example, the deflection data summarized in Table 4-3 for four redundant deflection sensors. Clearly, Sensor 4 provides less precise data and should be viewed with caution when analyzing data. It must also be understood that the higher standard deviation may not be a sensor problem, but an installation problem or local segregation of material. Regardless, it is important to know that data obtained from Sensor 4 will likely have more variability than the other three sensors.

Table 4-3. Deflection data for four redundant sensors.

Sensor	Deflection Standard Deviation, milli-inches
1	6
2	7
3	5
4	12

4.5 Under Traffic

Gauge accuracy is the foremost concern once a project is under traffic. It is critical that pre-traffic activities be executed as one component of gauge accuracy assurance. This will save time and resources by ensuring that only functioning gauges are included in the accuracy assessment. However, by themselves, these activities do not necessarily guarantee gauge accuracy. There must be a final check to determine the accuracy of the gauge response to some external stimuli. Since the gauge is now embedded within the structure, one must rely upon theoretical modeling to quantify the accuracy of the gauge.

When conducting a theoretical versus measured response study, it is important to realize the limitations of both approaches. Theoretical models consist of simplifying assumptions and the accuracy is therefore a function of the assumptions. For example, layered elastic models, as depicted in Figure 4-24, to predict flexible pavement responses typically include the following assumptions (Huang, 1993):

1. Each layer is homogeneous, isotropic, and linearly elastic with an elastic modulus *E* and a Poisson ratio ν.
2. The material is weightless and infinite in horizontal direction.
3. Each layer has a finite thickness *h*, but the lowest layer is infinite in thickness.
4. A uniform pressure *q* is applied on the surface over a circular area of radius *a*.
5. Continuity conditions are satisfied at the layer interfaces, as indicated by the same vertical stress, shear stress, vertical displacement, and radial displacement. For frictionless interface, the continuity of shear stress and radial displacement is replaced by zero shear stress at each side of the interface.

While these assumptions are generally accepted and used in practice, they can often be gross oversimplifications of the actual pavement.

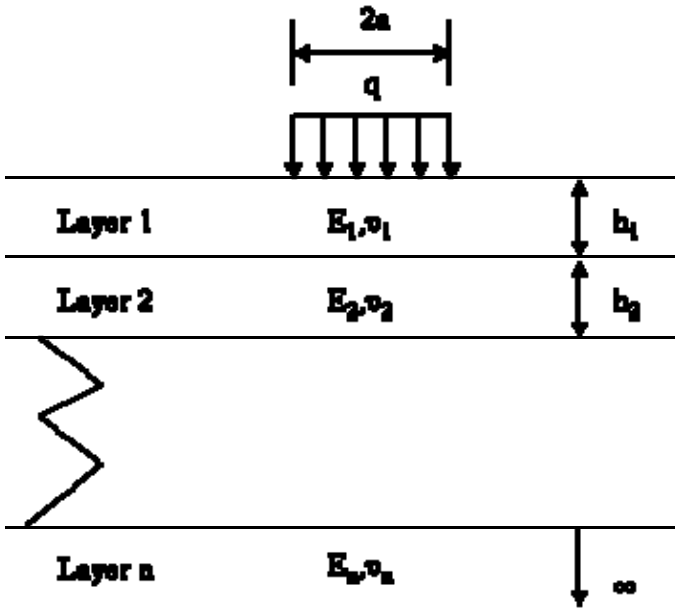

Figure 4-24. N-layer system subject to a circular load (Huang 1993).

Similarly, direct measurement of pavement responses also has its limitations. The very presence of a gauge can affect the pavement response by introducing a discontinuity in the structure. Further, slight misalignment or disorientation of a gauge could lead to seemingly inaccurate readings.

The point of this discussion is that "truth" is not necessarily perfectly represented by either theoretical modeling or direct measurement due to the limitations of both.

Therefore, a practical course of action is to use theoretical modeling to check the direct measurement and vice versa. Reasonable agreement between the two approaches gives confidence to the data in a given experiment. On a longer-term basis, through this recursive process, better theoretical models and direct measurement devices can be developed.

5 DYNAMIC DATA COLLECTION AND PROCESSING

5.1 Introduction

It is important to consider the specific objectives of a particular project when developing the data collection, processing and analysis scheme. One scheme does not exist that fits all experimental scenarios, so each scheme must be developed to accommodate the objectives of the given experiment. In addition, the available resources, in terms of personnel and software requirements must be considered since some schemes may be ideal from an experimental standpoint but impractical from an available resource standpoint. In this situation, compromises must be made to balance the research needs with the available resources. The following sections describe general principles that should be considered regardless of the experimental plan followed by illustrative examples using data from the FDOT HVS.

5.2 General Principles

There are some common issues that must be considered when working with dynamic pavement response data. Discussed in the following sub-sections, these include:

- Developing a data collection scheme to meet the experimental objectives.
- Separating actual pavement response from electronic noise in the signal.
- Identifying important features of dynamic response.
- Developing an efficient user-friendly system for processing and compiling data.

5.2.1 Developing a Data Collection Scheme

As noted above, it is critical to match the data collection and processing scheme to the experimental objectives. Thoughtful consideration should be given to planned uses for the data before the experiment begins since the data needs are directly related to the experimental objectives. Another important concept is that data collection does not necessarily mandate data processing and analysis. It would be possible, for example, to collect data continuously throughout an HVS experiment, but only process and analyze axle passes at key points during the experiment.

When developing a scheme it is important to answer the question, “How rapidly will conditions change during the experiment?” Under relatively stable conditions, the amount of data needed will generally be less than when experimental factors are more transient. Estimating the amount of data required can be based on experience, or by examining some actual data and determining the stability of the experimental conditions. The following examples highlight this process.

Take, for example, the data shown in Figure 5-1 obtained from FDOT HVS Experiment 3-2A after 350 load repetitions. Clearly the strain response is very consistent and though more data could have been collected, processed and analyzed, five repetitions appear to be sufficient to characterize the strain response at this point. Figure 5-2, derived from the raw data in Figure 5-1, illustrates more precisely how consistent the data are amongst passes with all the data within 3 microstrain for each respective series (Min, Max and Difference). One could argue that three passes would have sufficed.

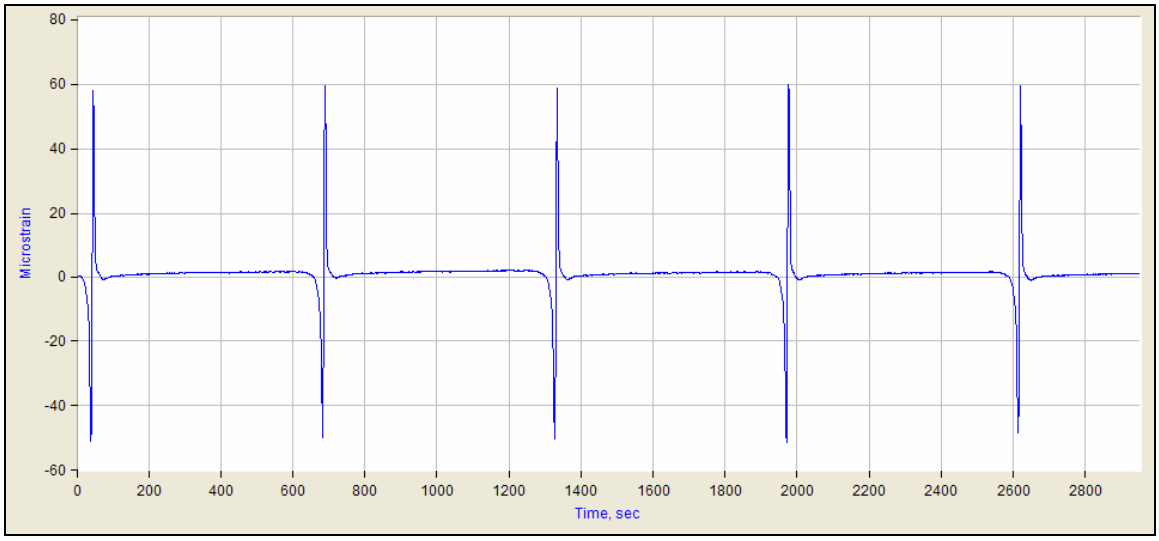

Figure 5-1. Raw strain data from Experiment 3-2A at 350 passes.

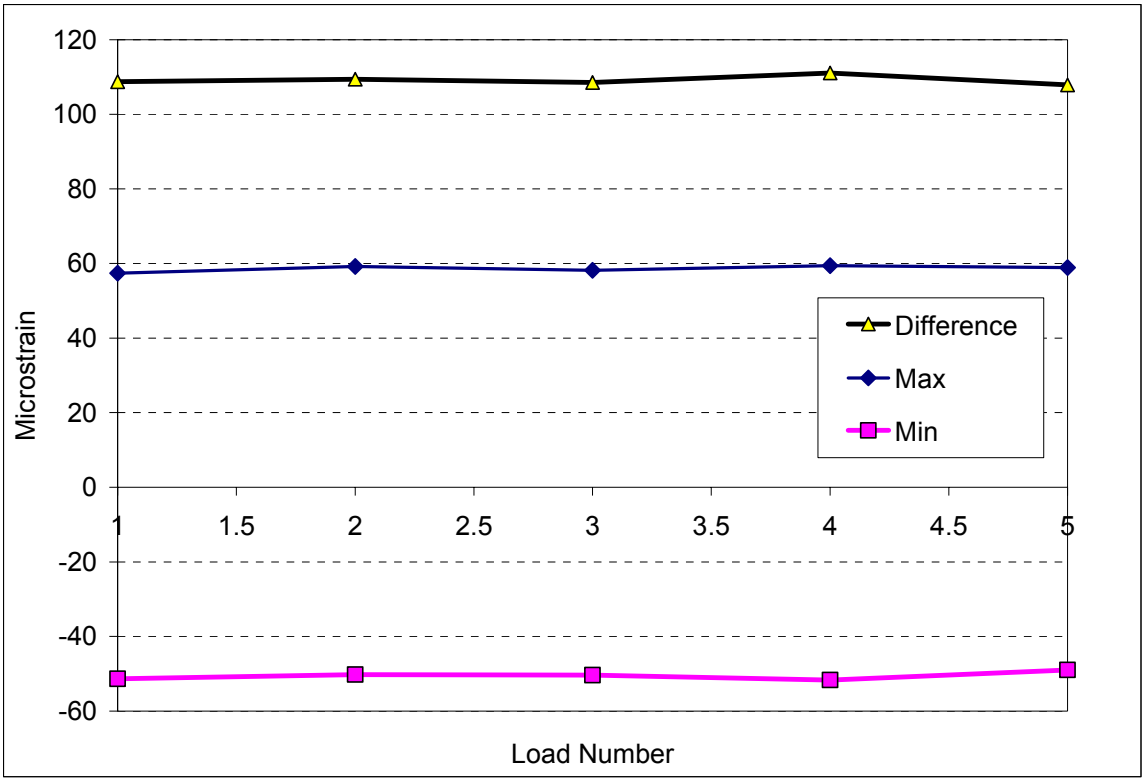

Figure 5-2. Summarized strain data from Experiment 3-2A at 350 passes.

In contrast, Figure 5-3 illustrates raw strain data collected from FDOT HVS Experiment 3-2B at 15,050 passes. Wheel wander was used during this experiment, as evidenced by the varying strain trace. Clearly, wheel wander introduces a great deal more variability in the strain response that needs to be captured with sampling relatively more axle passes when compared to Experiment 3-2A.

Figure 5-3. Raw strain data from Experiment 3-2B at 15,050 passes.

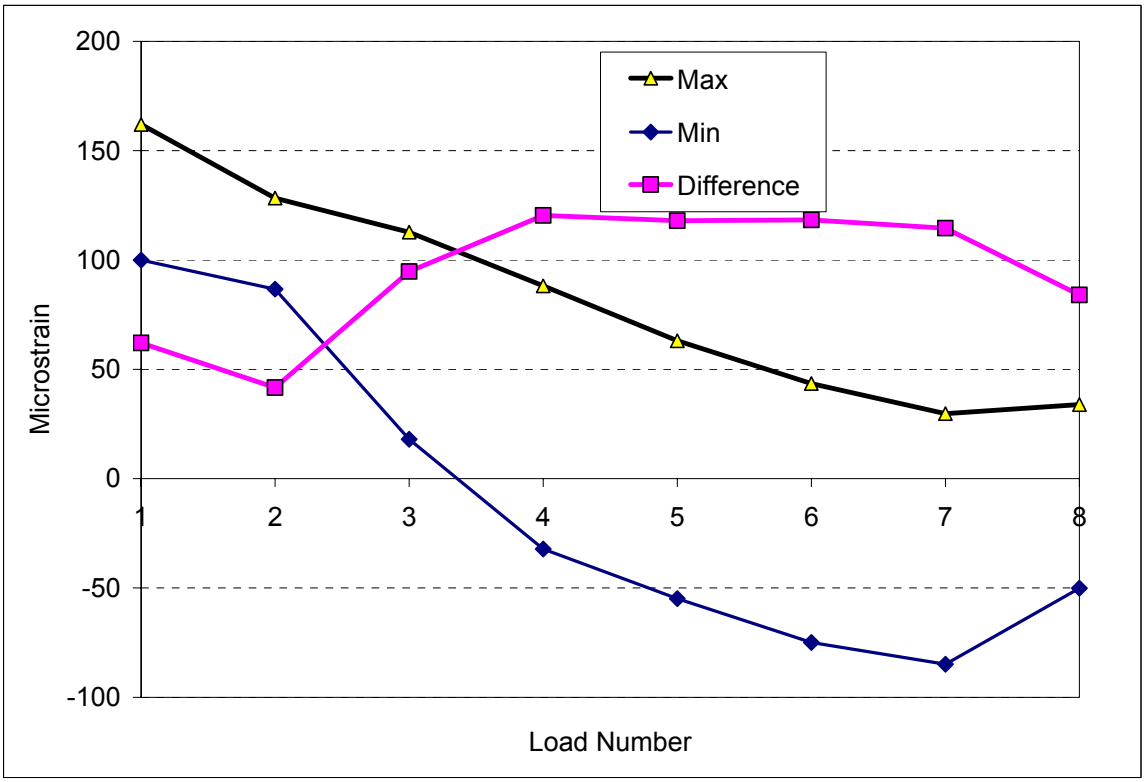

Figure 5-4. Summarized strain data from Experiment 3-2B at 15,050 passes.

5.2.2 Removing Noise from Signal

Electronic noise is a common problem that must be dealt with when examining dynamic pavement response data. To minimize the amount of noise, efforts should be made to minimize it at the power supply source, but it still can be a problem. Electronic noise can be effectively eliminated by simply computing a moving average of data points. Most data processing software contains this as a standard feature. It can also be done manually in Microsoft Excel®. Figure 5-5 illustrates the effect of a moving average on a noisy strain signal. As seen in the figure, care must be taken so that the moving average is not so large that the true engineering response is lost. In this example, the raw signal represents 2000 samples/sec with a 10 point moving average providing a sufficiently clean signal. Wider moving averages would significantly alter the true response measurement. In general, the ratio of moving average to sample rate should not exceed 1percent. If higher ratios are needed, then more complex methods of signal cleaning may need to be employed. For example, Figure 5-6 illustrates the effect of a single pole analog low pass filter at 40 Hz applied to another strain trace.

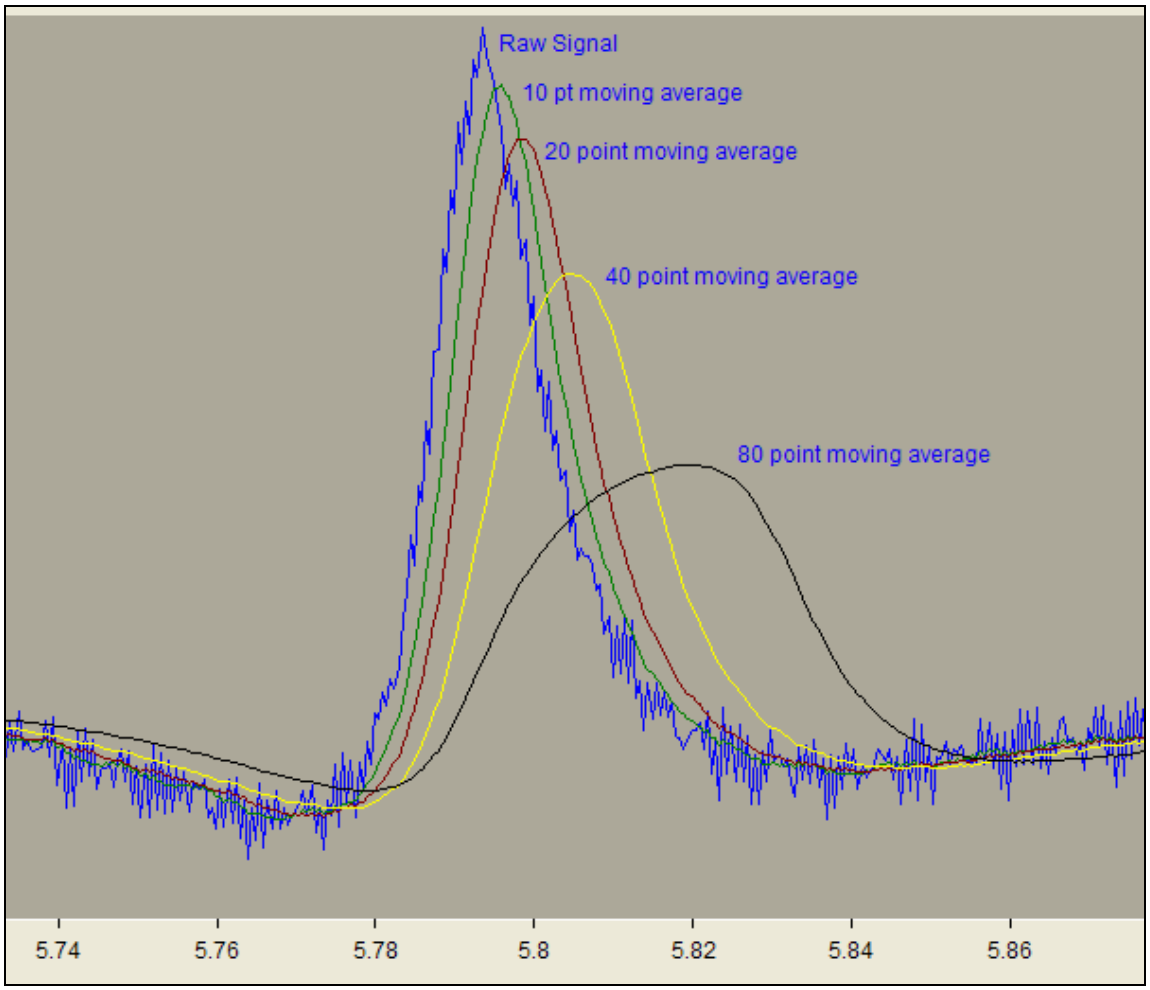

Figure 5-5. Effect of moving average on raw strain signal.

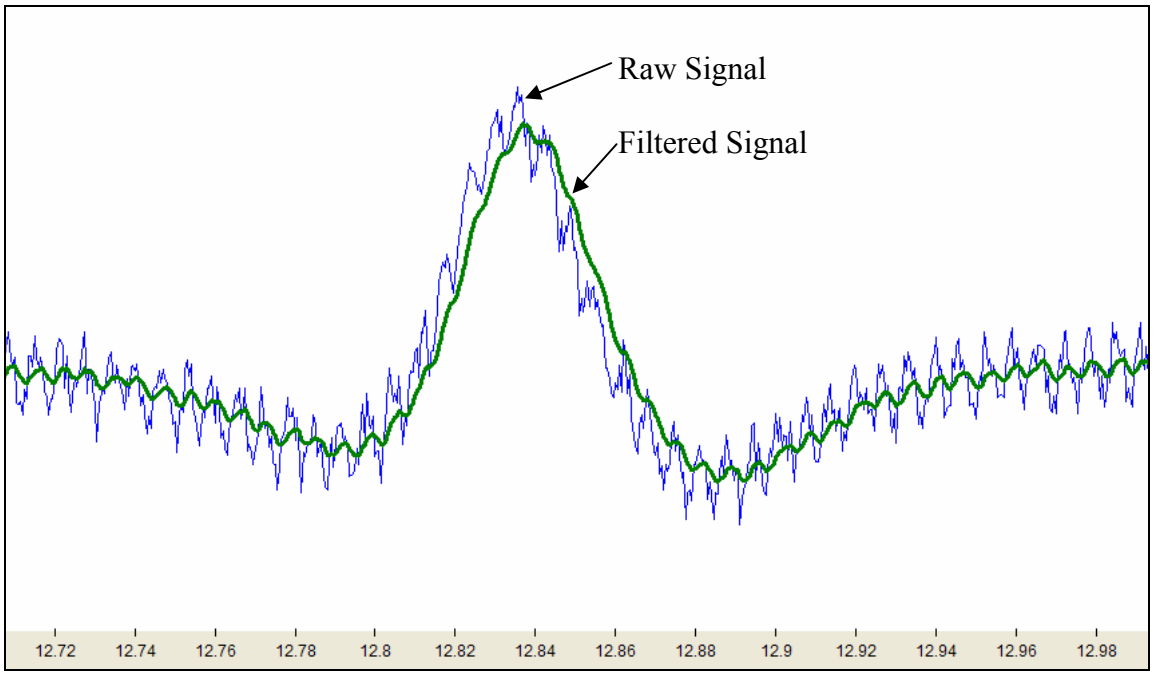

Figure 5-6. Effect of single pole analog low pass filter.

5.2.3 Identifying Important Features in the Dynamic Response

There are many approaches to defining the "pavement response" from a dynamic signal. Some researchers define strain as the peak response relative to a baseline reading. Others define it by subtracting the minimum from the maximum response. Regardless of the approach, from a data processing perspective, it is important to define strain for a particular experiment so that the data processing scheme can be tailored to acquire the necessary information from the response signal.

Consider the strain trace shown in Figure 5-7 obtained from the FDOT HVS program. From this relatively simple trace, strain could be defined in a variety of ways including subtracting point 1 from point 3 or subtracting point 2 from point 3. Alternatively, there may be useful information that can be obtained from the unloading portion of the curve (points 3 to 4 or 4 to 5). Since these would generate drastically different strain values, it is critical for the researchers under the guidance of experience and the experimental objectives to clearly define the strain response. From a data processing perspective, the issue is selecting the appropriate points from which strain can be computed.

The importance of visually reviewing data cannot be overemphasized with respect to identifying the key components of the dynamic response. Depending on the placement and orientation of gauges, drastically different responses can be observed. Therefore, careful review of the raw dynamic traces should be accomplished before beginning to develop a data processing scheme.

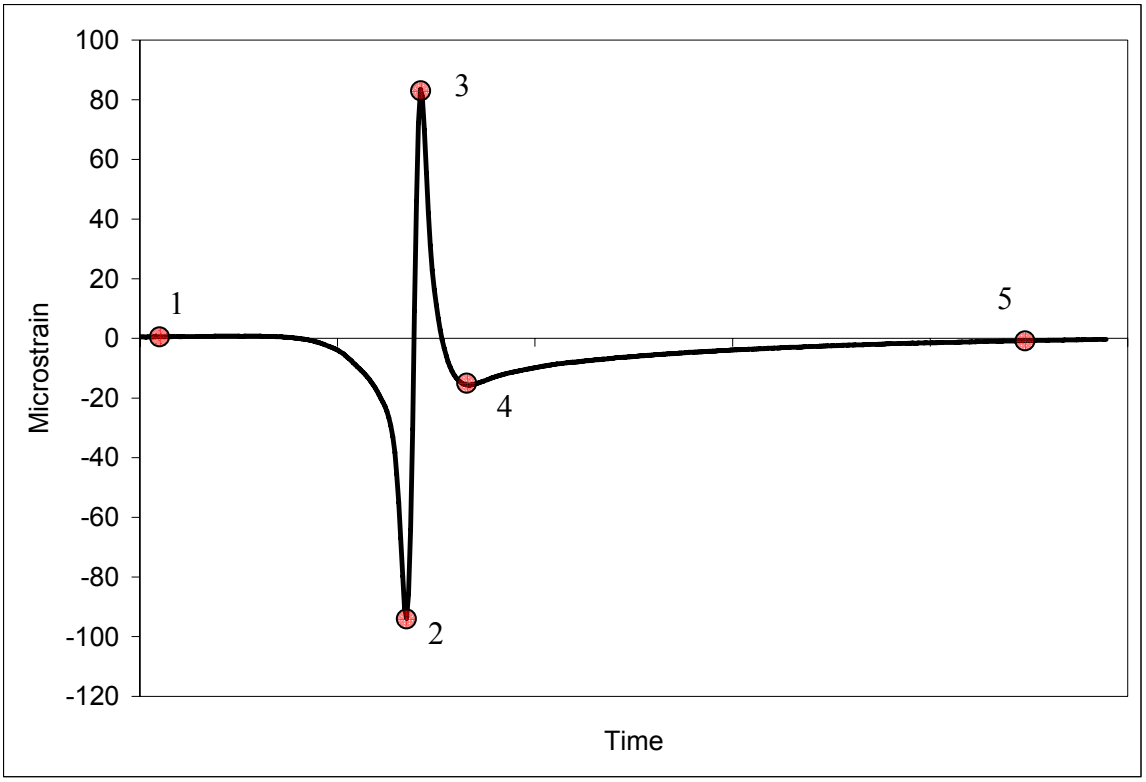

Figure 5-7. Dynamic strain trace.

5.2.4 Developing a Data Processing Scheme

Once decisions have been made regarding the volume of data to collect, signal filtering and the definition of pavement response, the data processing scheme can be developed. For the sake of efficiency, it is important to have a scheme that is as automated as possible. For the sake of quality, it is important to have some visual human interaction with the data. Effectively balancing these two components will ensure a scheme that provides useful information in a timely manner.

To maximize automation, consistency must be maintained in the data collection process. In a given experiment, maintaining consistent file naming and file formatting are critically important. Seemingly minor decisions such as whether a file is tab- or comma-delimited can wreak havoc on the ability to automatically upload data files into a processing template. It does not necessarily matter which format is chosen, so long as that format is maintained throughout the experiment.

It is important, when developing a processing scheme, to carefully consider how the data will be organized and compiled into a database. Identifying the important factors in the experiment, as they relate to the experimental objectives, will help define the database. These factors essentially become column headings within the database and the processing scheme should be designed to automatically create data for the database.

There are many proprietary software environments to choose from when building a processing scheme. Programs such as Microsoft Excel®, National Instrument's LabVIEW, MathWorks MATLAB® and DSP DADiSP® are just a few examples of the numerous software packages available. Each package has its own advantages and disadvantages in terms of handling large data files, user-friendliness, built-in computational capabilities and cost. For example, Excel® is readily available and most engineers are very comfortable working in this environment. However, there are file size limitations, there are not many built-in signal processing features and computations can be somewhat slow compared to other programs available. Deciding upon a particular package is an agency decision and should be based on the factors mentioned above. It is important to point out, however, that a particular processing scheme can be implemented in most software packages.

5.3 Case Study – FDOT HVS Experiment 3-2A

HVS experiment 3-2A, conducted by FDOT, was used as a case study to demonstrate the concepts described above. As shown in Figure 5-8, experiment 3-2A was part of the larger experiment 3 which involved 15 sub-experiments. Experiment 3-2A, highlighted in Figure 5-9, consisted of four asphalt strain gauges and one pressure cell embedded at the bottom of the HMA.

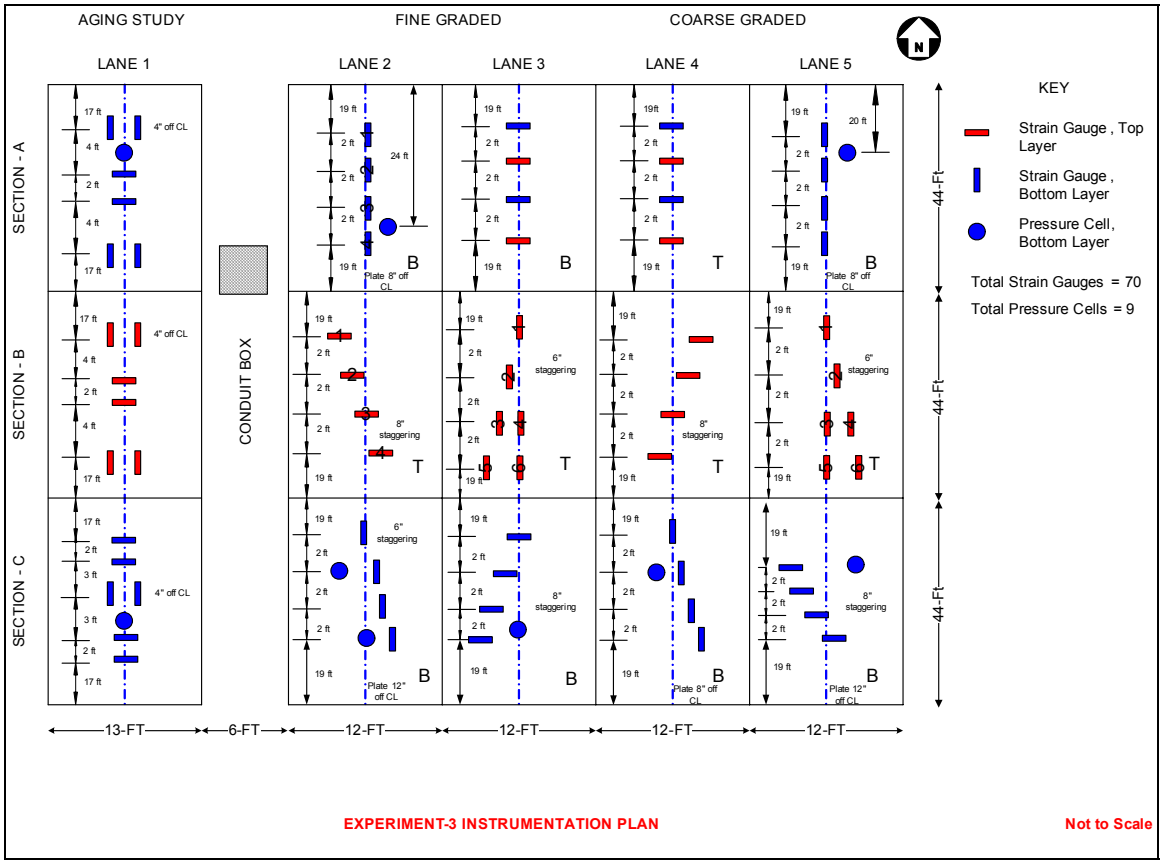

Figure 5-8. FDOT HVS Experiment 3.

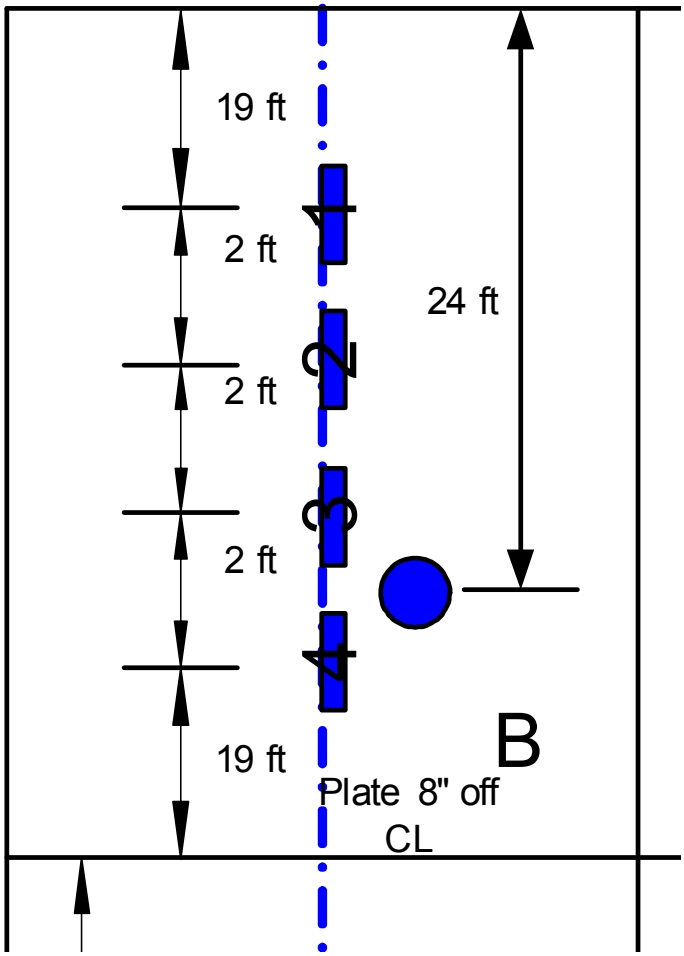

Figure 5-9. FDOT HVS Experiment 3-2A

5.3.1 Data Collection

Data collected by FDOT from the asphalt strain gauges were provided for this project. Almost 90,000 load repetitions were applied during the experiment. Periodically throughout the experiment, groups of four or five axle passes were recorded by the data acquisition system. Initially, data were collected once every 50 passes. After 1,000 load repetitions, data were collected once every 100 passes. In total, there were 804 individual files containing data from the four asphalt strain gauges collected for this project. It is important to emphasize that the data had been collected prior to this project and therefore the data collection scheme was developed independently of this project. However, after reviewing the data, it appears that the data collection scheme was sound.

5.3.2 Signal Filtering

Figure 5-10 illustrates five axle passes collected at 78,050 load repetitions. Each load pass is clearly visible, signifying a very good signal-to-noise ratio for each gauge. A closer look at the first load pass is provided in Figure 5-11. The time lag between gauges, due to spatial arrangement, is evident. Also, the signals appear extremely clean requiring

no further filtering. This may be due to pre-processing signal filtering built into the data acquisition hardware and software, very stable power sources or both.

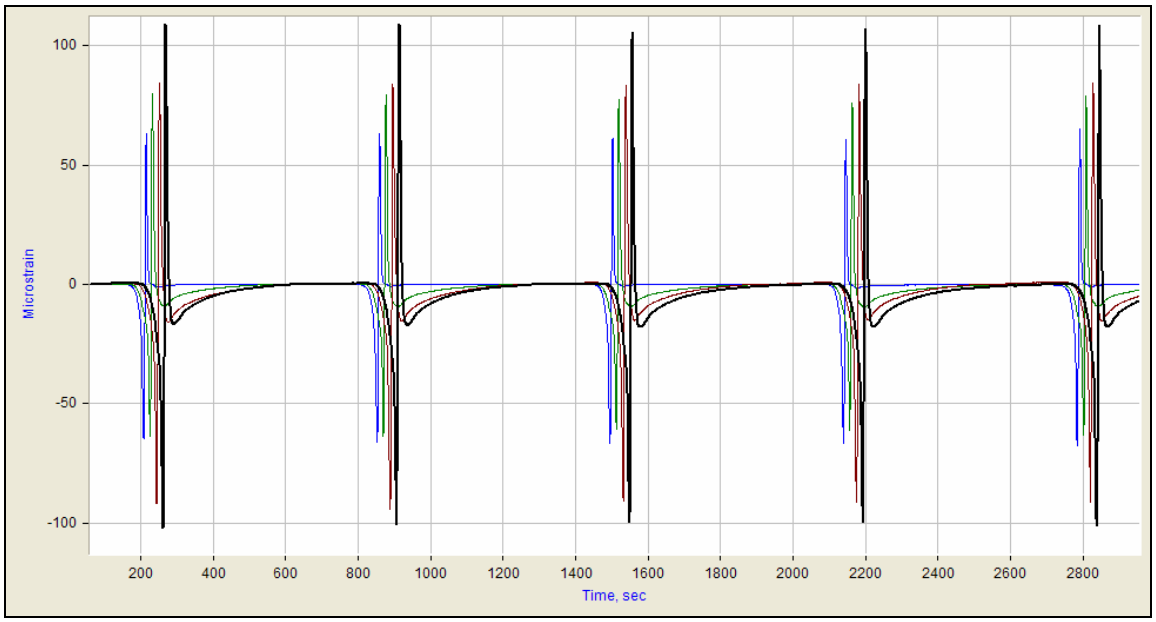

Figure 5-10. Raw strain data at 78,050 load repetitions.

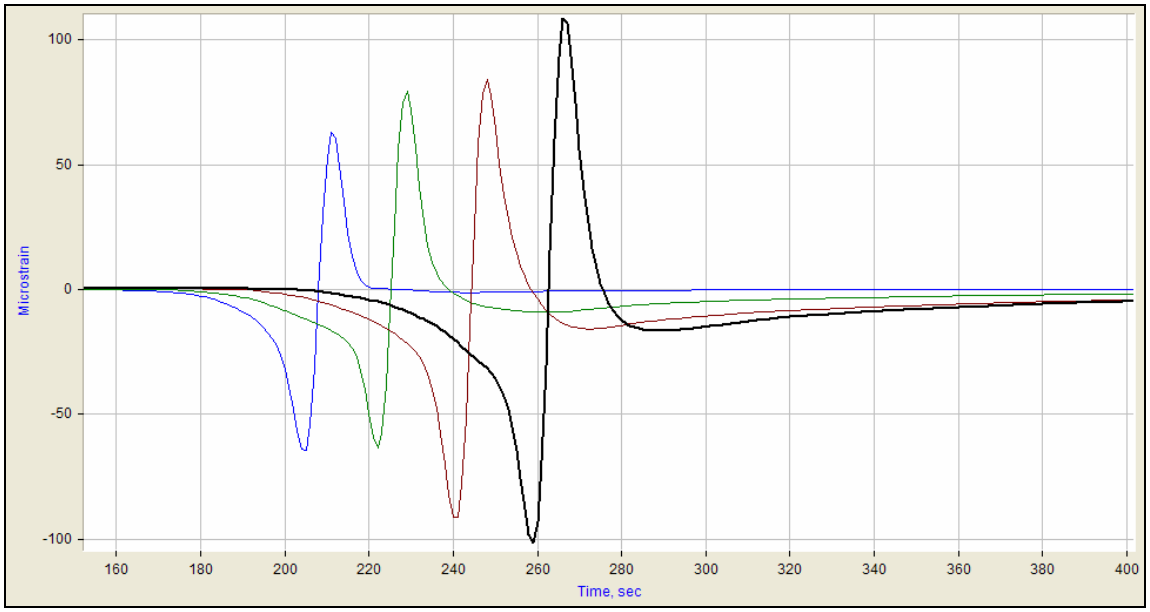

Figure 5-11. Raw strain data from first load pass at 78,050 repetitions.

Most of the signals collected in experiment 3-2A were similar in shape and signal quality to those in Figure 5-10. Occasionally, however, traces such as that shown in Figure 5-12, collected at 250 passes, were observed. According to FDOT personnel, loads were definitely applied during this data collection interval, so the system must have malfunctioned in some way. In the larger scope of the experiment, this does not pose a problem since the vast majority of the data were excellent.

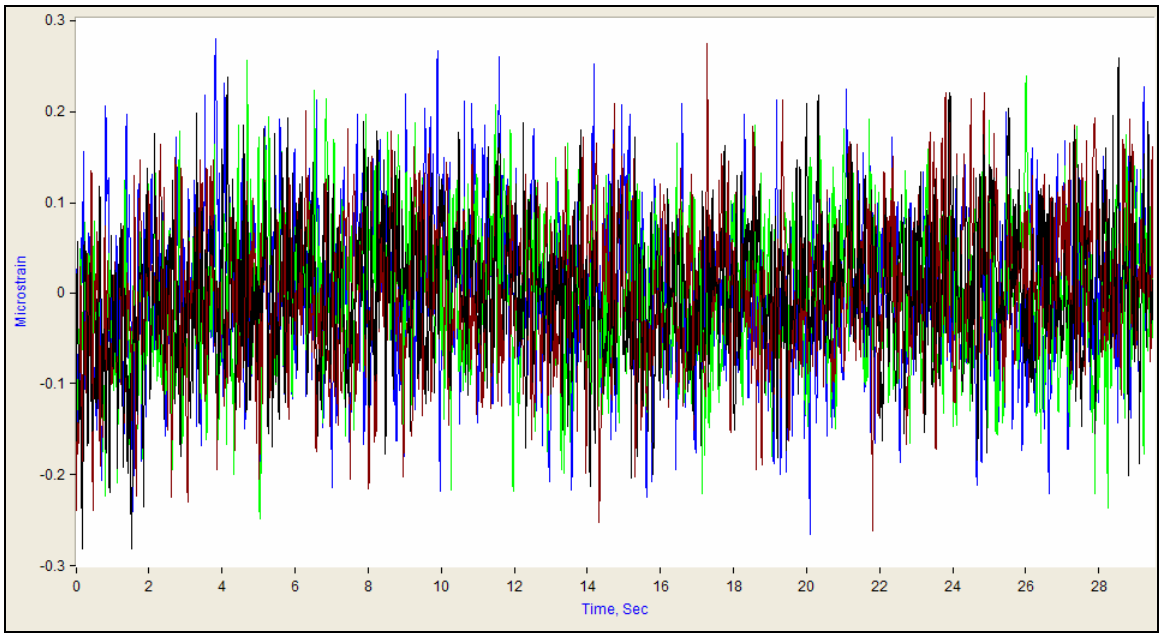

Figure 5-12. Raw strain data at 250 load repetitions.

5.3.3 Important Features of Dynamic Response

For the purposes of this report, strain will be defined as the amplitude between the maximum and minimum strain recorded for each axle pass. Figure 5-13 illustrates this definition that captures both the compressive and tensile pavement response as the load approaches, is directly over, and moves away the strain gauge. In terms of processing, the minimum and maximum had to be determined, from which the amplitude was computed.

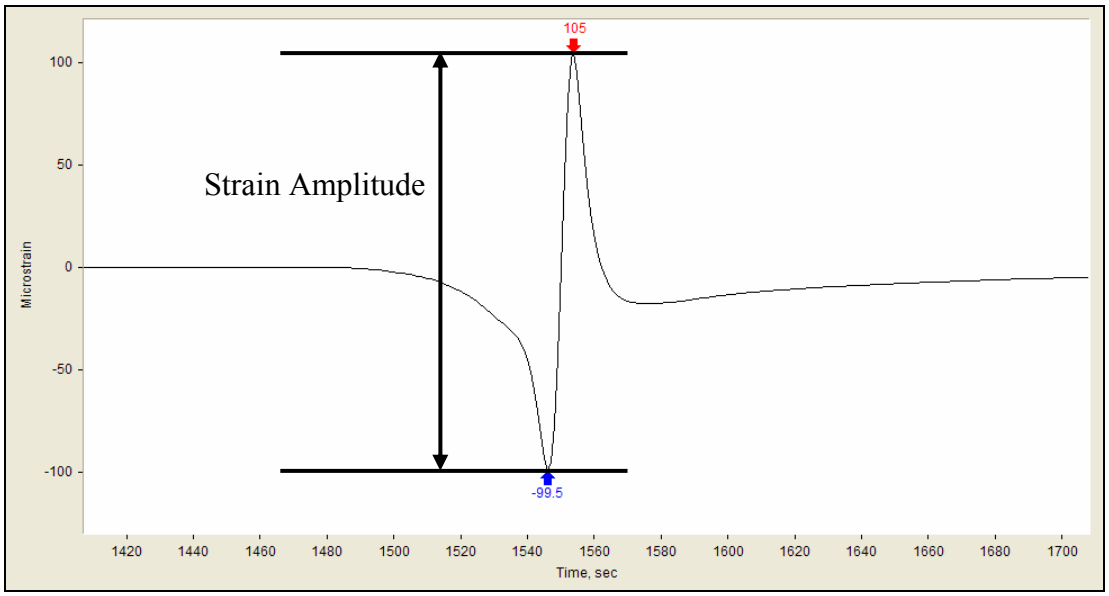

Figure 5-13. Strain definition.

5.3.4 Data Processing Scheme

For the purposes of this project, the data processing scheme was developed in the computer program DADiSP® 2002. This commercially-available software package is intended for the type of signal processing required by dynamic pavement response measurements. It has a number of built-in functions but allows the user to develop custom algorithms to meet particular data processing needs. It should be noted that the concepts implemented within DADiSP® are not unique to the program and can be applied to other software packages.

The data processing template developed for this project is shown in Figure 5-14. In the upper left corner of Figure 5-14, Window 1 contains the raw data collected by the datalogger during the experiment. These data files are loaded into the template using a user-friendly dialog box. Window 2 shows the raw data, in this case 5 load events on four gauges. Window 8 contains the algorithm to find the peak and valley values on a gauge-by-gauge basis. After entering the gauge number in Window 8, a graph is created (Window 7) showing the raw signal in addition to the peaks and valleys. This plot allows the processor to quickly assess the quality of the data. Finally, Window 4 contains an algorithm that computes the differences between the peak and valley responses, per load event, and summarizes the data according to maximum value, minimum value, average and standard deviation. Each of these windows and accompanying algorithms are described in more detail below.

5.3.4.1 Importing Data – W1

Importing data into the template can be accomplished using the DADiSP® ASCII import dialog box (Figure 5-15). Aside from selecting the appropriate file and which columns of data to upload, it is also important to define how the file is delimited.

5.3.4.2 Display Raw Data – W2

After importing the raw data to W1, a graph is automatically generated in W2. The initial baseline for each strain is subtracted, using the average of the first ten data points from the signal, so that each gauge is zeroed. Viewing the data allows the processor to verify that the data look normal or as expected. After checking the data, the processor zooms in on the first axle pass, centering the load in the middle of the window as shown in Figure 5-16. This step is critical to the processing template as will be explained in the next sub-section.

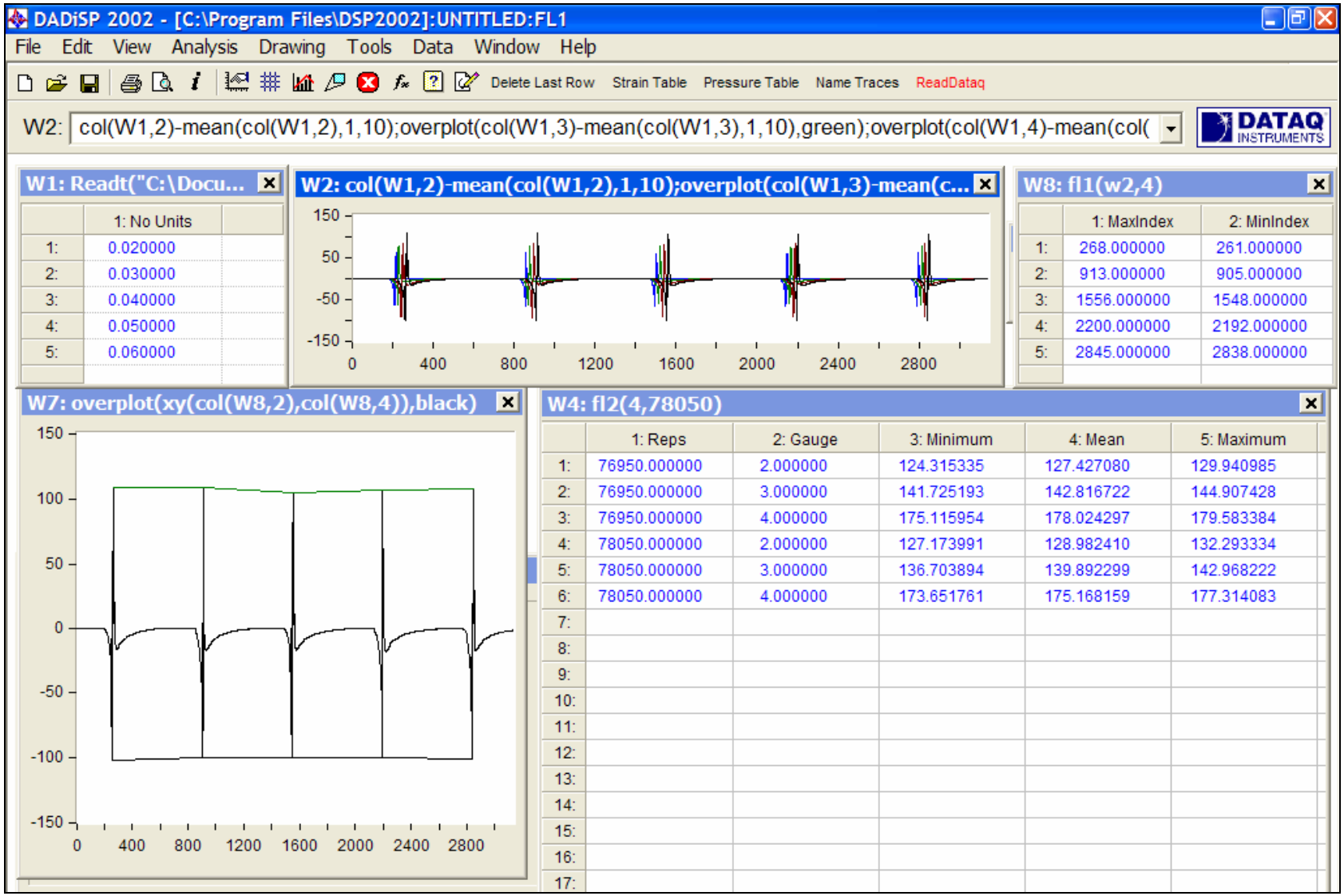

Figure 5-14. DADiSP® processing template.

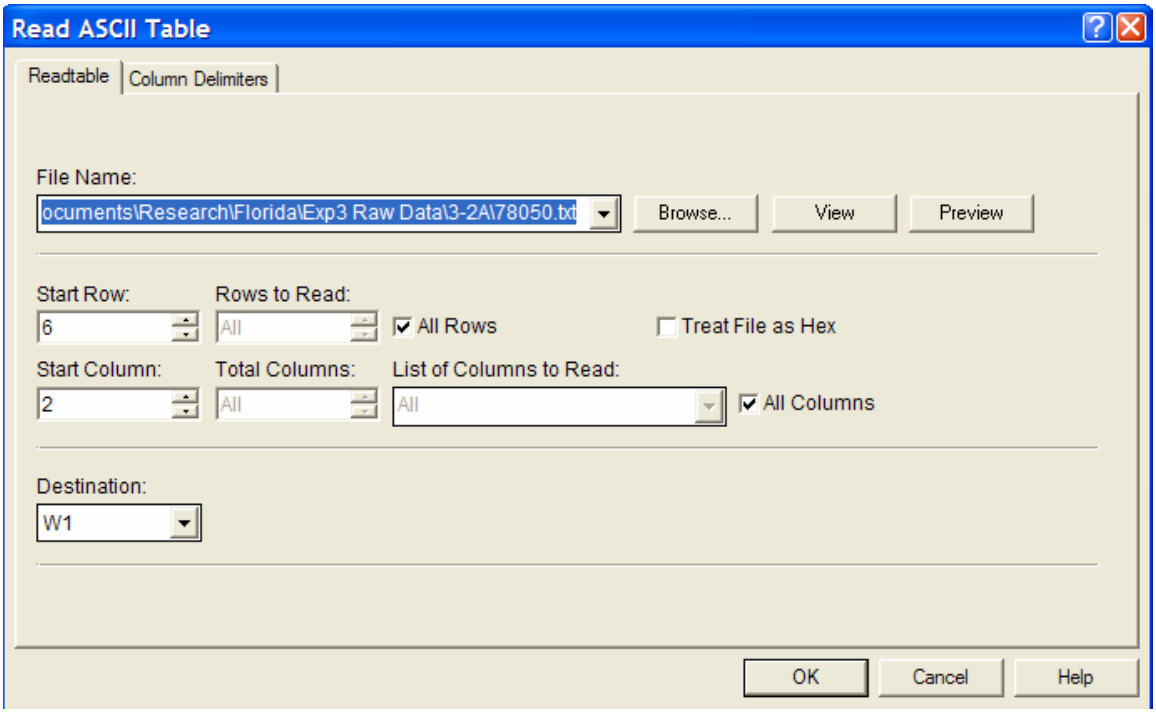

Figure 5-15. DADiSP® ASCII import dialog box.

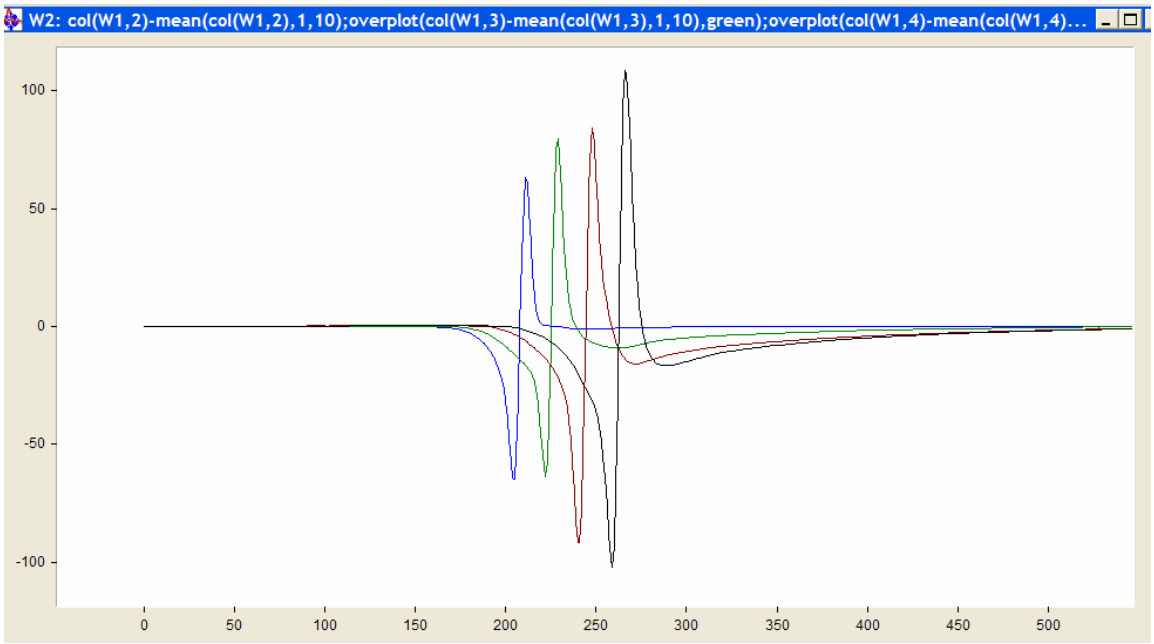

Figure 5-16. First load repetition centered in W2.

5.3.4.3 Execute FL1 Algorithm – W4

After the data have been centered as shown in Figure 5-16, the algorithm FL1 can be executed to determine the minimum, maximum and amplitude of each axle pass. The concept is relatively simple, as illustrated in the flow diagram in Figure 5-17. Basically, the algorithm isolates each axle pass and searches for the local minimum and maximum

during the given axle pass time interval. After it has found these values, it computes the difference (amplitude) and then jumps ahead to the next axle pass. It continues this process until the strain from all axles has been computed. A table is created containing the timestamps and strain values in addition to a graphical output the processor can check for quality. The graph includes the raw strain trace in addition to a plot of the minimums and maximums. It is important to note that this processing algorithm takes advantage of the regular time intervals between passes imparted by the HVS. If the interval were more erratic, a different approach would be required. The actual code for FL1 is contained in Appendix A.

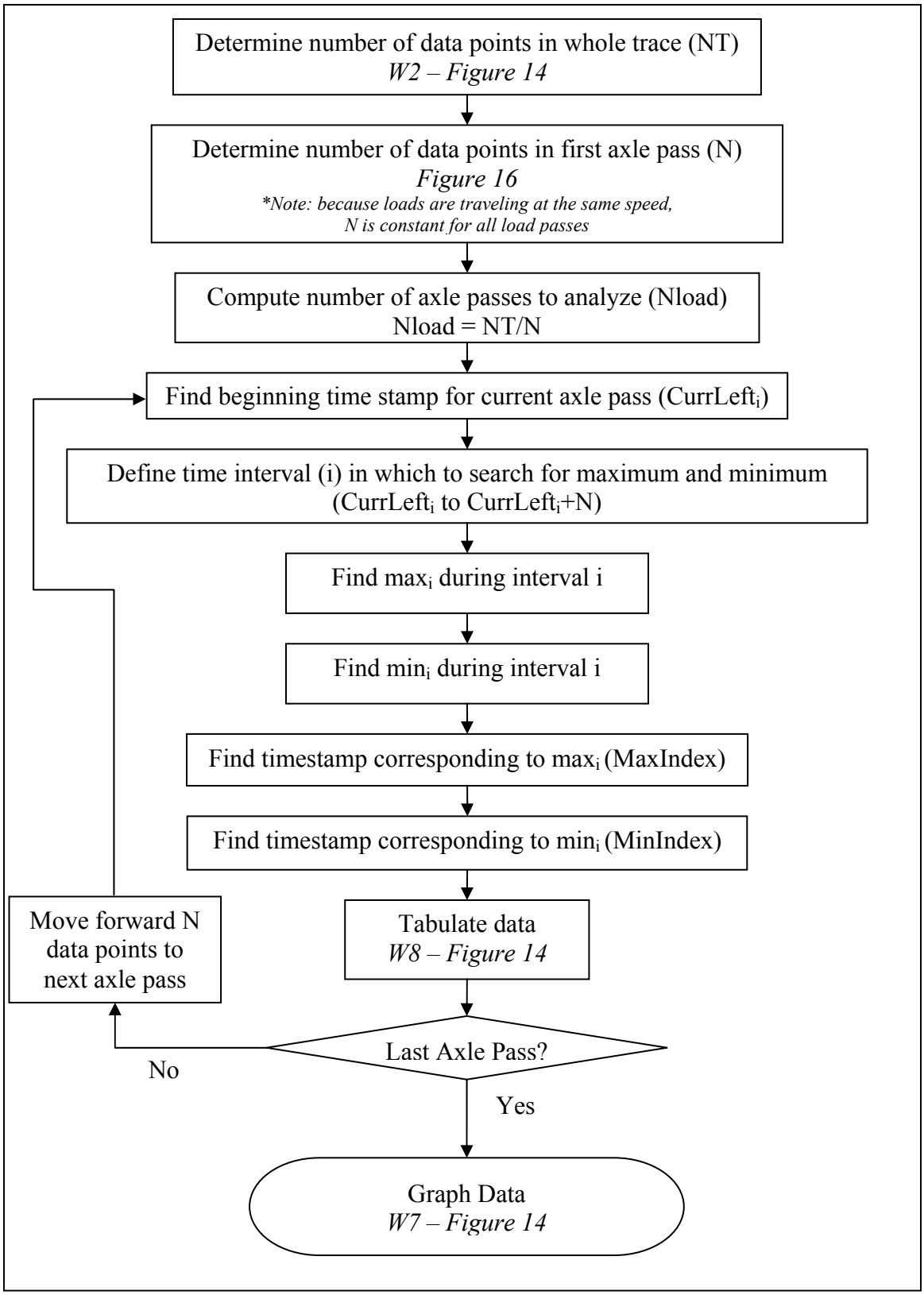

Figure 5-17. FL1 flowchart.

To demonstrate the versatility of this algorithm, Figure 5-18 through Figure 5-21 illustrate the variety of strain traces processed with the FL1 algorithm. Figure 5-18 is the simplest of cases and was previously shown as part of Figure 5-14. Figure 5-19 illustrates a strain trace obtained from an experiment including wheel wander and a larger number of axle passes. Note that the processing algorithm accurately captures the minimums and maximums despite a baseline that is continually shifting during the data capture. This highlights the need to isolate each axle pass and determine minimums and maximums from a local baseline rather than a global baseline.

Figure 5-20 and Figure 5-21 are from another experiment where a loaded axle was moved in one direction after which most of the load was then removed and backed back over the gauge array to begin the next pass. The resulting trace shows the alternating large and small pavement response. Figure 5-20 was processed like Figure 5-18 and Figure 5-19 resulting in capturing the minimum and maximum of each axle pass. Figure 5-21 shows the same raw data but with the small axle hits ignored. This was done by simply centering the first large strain response in W2 which enable FL2 to effectively ignore the small strain responses. No modifications of the code were required.

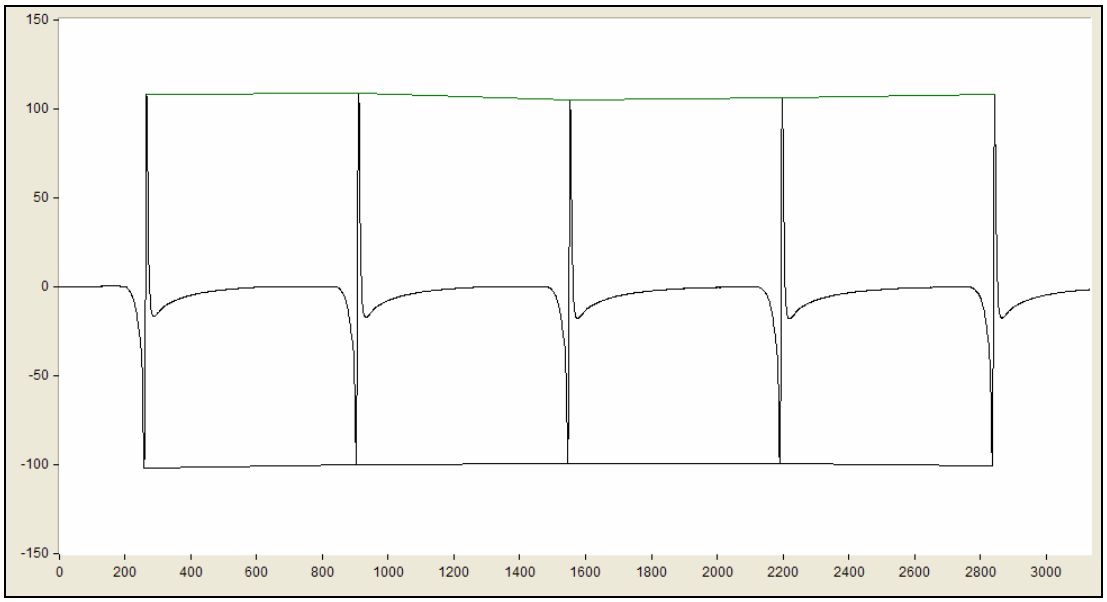

Figure 5-18. Strain trace from experiment 3-2A.

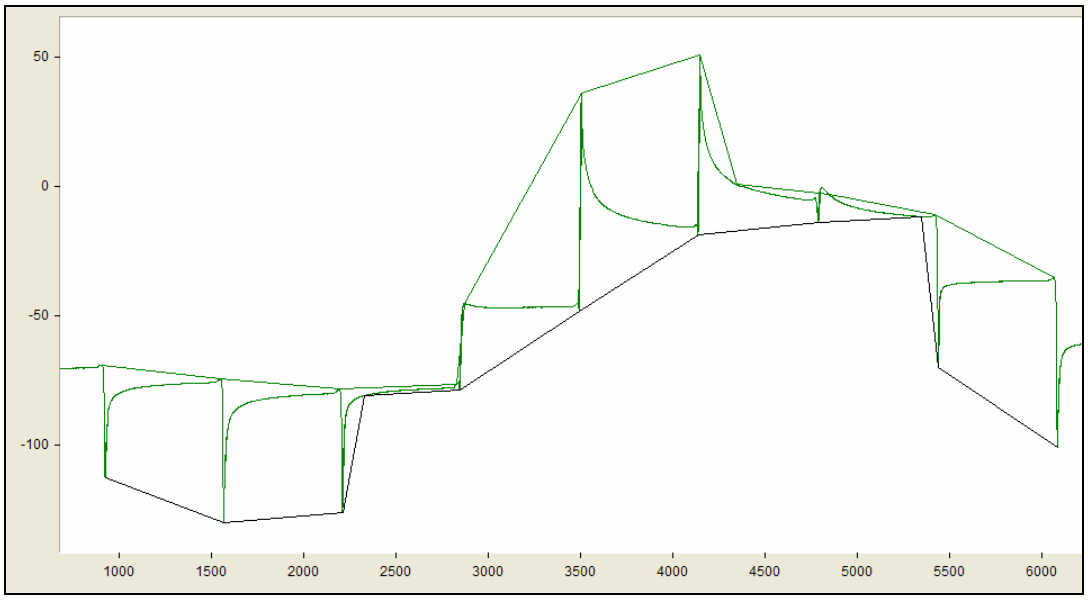

Figure 5-19. Strain trace with wheel wander.

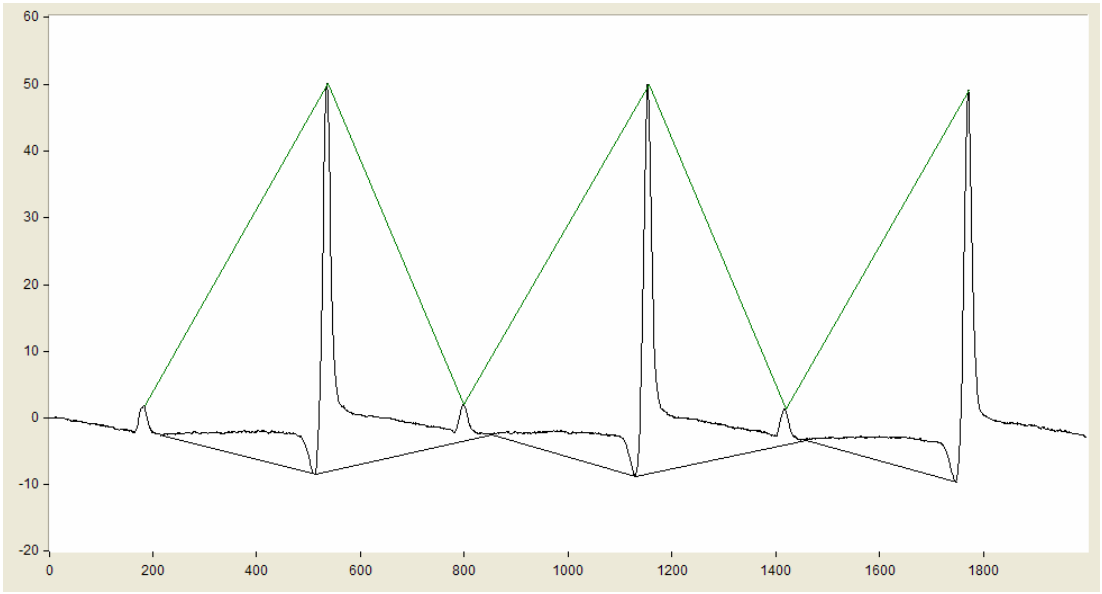

Figure 5-20. Strain trace with all axle hits recorded.

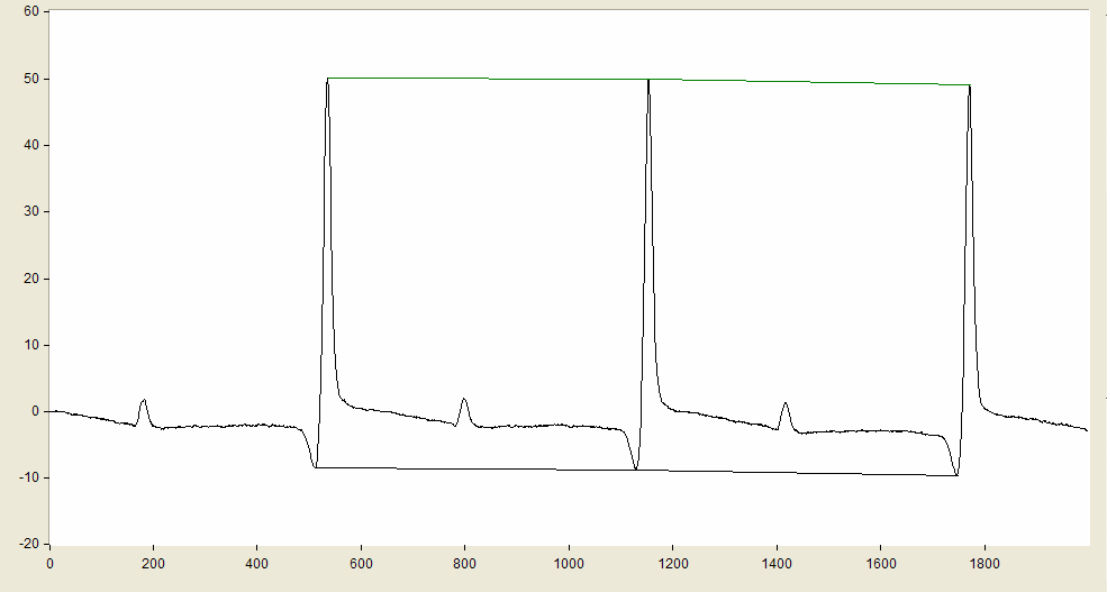

Figure 5-21. Strain trace with small axle hits ignored.

5.3.4.4 Summarize Data

After the minimums, maximums and amplitudes are computed and the processor has visually checked the data for quality, another algorithm (FL2) can be executed to build a table that summarizes the strain data from the individual axle passes. Using built-in DaDisp functions, the FL2 algorithm computes and tabulates the following in W4:

- Minimum amplitude
- Average amplitude
- Maximum amplitude
- Amplitude standard deviation

This table can then be copied into Excel® or other applications as needed. It should be noted that other parameters can easily be tabulated as well by modifying the FL2 code. The FL2 code is provided in Appendix B.

5.3.5 Experiment 3-2A Summary

The data processing template depicted in Figure 5-14 was employed to process data from experiment 3-2A. Figure 5-22 summarizes the data. Note that not all of the 804 files were processed. In fact, only 17 were included in this analysis. More frequent sampling was done at the beginning of the experiment and at the end where there appeared to be more changes in strain with increasing number of repetitions. However, over the middle portion of the experiment, very little change in strain response was observed and sampling at a greater interval was not required. Overall, the gauges exhibited similar trends, though there appeared to be increasing strain in the direction of moving traffic (Gauge 1 < Gauge 2 < Gauge 3 < Gauge 4). The reason for this is not immediately evident, but could be related to imperfections in the HMA due to the presence of the gauges themselves. Gauge 1 could have read the lowest since there was nothing in front of it as the axle approached.

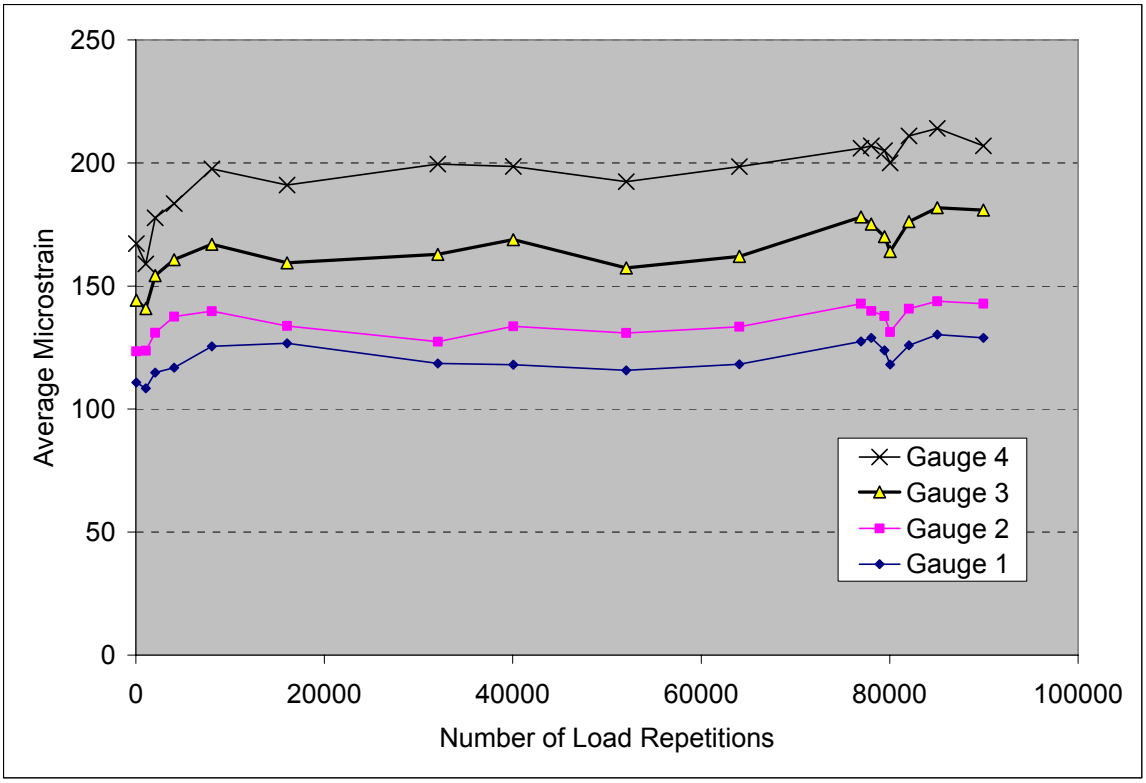

Figure 5-22. Average strain response from experiment 3-2A.

6 CONCLUSIONS AND RECOMMENDATIONS

6.1 General

FDOT uses its HVS to apply wheel loadings to investigate pavements and to produce controlled, accelerated accumulation of damage. Instrumentation systems are employed during these experiments to measure responses at critical locations. While it is impossible to anticipate every possible sensor or experimental setting, certain concepts apply to all instrumentation projects. The project can be divided into six logical phases that must be performed: pre-installation; construction; post-installation/pre-traffic; under traffic; and data processing and analysis.

6.1.1 Pre-installation

6.1.1.1 Conclusions

Careful selection and installation of sensors are prerequisites for a successful instrumentation project. This research identified at least 64 commercially-available sensors as well as several custom sensors developed for specific purposes. The selection of sensors depends upon the type of pavement and the objectives of the experiment. The following criteria may be used to evaluate pavement instrumentation:

1. Ability to measure the desired responses
2. Cost
3. Availability (i.e., delivery times)
4. Reputation for good reliability
5. Continuity with previous research efforts.

Past studies have shown that manufacturer-provided calibration factors can be used with a good level of confidence. Most commercially-available sensors are calibrated in the factory under carefully controlled conditions and do not routinely require site calibration. However, the calibration of certain sensors, such as soil moisture probes, is dependent upon the properties of the medium in which they are embedded. These sensors should always be calibrated under conditions as close as possible to those anticipated in service. When working with a new gauge type or gauge vendor, it is important to establish a level of confidence in their calibration procedures. This can be done through within-agency calibration.

Mechanistic concepts were used to develop guidelines for sensor locations for both flexible and rigid pavement systems. For flexible pavements, the primary distress mechanisms include fatigue cracking (both top-down and bottom up) and rutting. For rigid pavements, the distress mechanisms include top down cracking, bottom-up cracking, joint faulting, and punchouts (for CRCP).

6.1.1.2 Recommendations

As a general rule, we do not recommend that FDOT calibrate sensors with factory-supplied calibration factors. However, in cases where gauge calibration factors are not provided, or when local calibration is needed, it is best to follow the manufacturer's recommended procedure.

Manufacturer's installation recommendations should be followed whenever possible. However, some installation procedures are so complex, time consuming or restrictive that deviations are sometimes necessary.

Instrumentation of HVS experiments can be costly and time-consuming; therefore, the sensor location plan should be thoughtfully considered during the experimental planning stage. The location of sensors should be based upon the objectives of the experiment, the anticipated distress types, and the mechanistic concepts described in Chapter 0 of this report. Table 6-1 provides a matrix of possible experimental objectives and special considerations and directs the user to the proper list of sensors that should be considered. The expected distress types will dictate the sensors required; therefore, not all of the sensors listed in Table 3-5, Table 3-6, or Table 3-7 may be required depending upon the experiment objectives and expected outcome.

6.1.2 Construction

6.1.2.1 Conclusions

Sensor installation during construction is often the most critical to project success. Typically, if sensors survive the harsh construction environment, they will continue to perform satisfactorily over the duration of the experiment. Most sensor manufacturers provide basic guidance regarding installation. However, some installation procedures are so complex, time consuming or restrictive that deviations are sometimes necessary.

Various methods can be used to locate the sensors from precise surveying techniques to simple string lines. Regardless of the method, it is important to have precise measurements of the final location. This includes station (longitudinal location), offset (transverse location) and depth. During construction, it is important to monitor sensors to establish sensor functionality and sensor survivability. Using the data-acquisition system, sensors can be watched for signal loss, over-ranging and erratic behavior throughout the construction process.

6.1.2.2 Recommendations

Gauges that have been used before, and have a large degree of confidence with their measurement capabilities, should be checked for functionality during pre-installation, construction, post-construction and under-traffic conditions.

Table 6-1. Recommended sensors based upon experiment objective and special considerations.

	Case 1	Case 2	Case 3	Case 4	Case 5
Experiment Objective	Evaluation of asphalt concrete structural layer or friction course	Evaluation of asphalt concrete structural layer or friction course	Calibration or validation of mechanistic model or design procedure for a flexible pavement system	Evaluation of Portland cement concrete structural layer	Calibration or validation of mechanistic model or design procedure for a rigid pavement system
Special Considerations	Supporting layers (base, subbase, embankment) are not a variable in the experiment	One or more of the supporting layers or a variable in the experiment	All layers of the pavement structure are important	Supporting layers (base, subbase, embankment) are not a variable in the experiment	All layers of the pavement structure are important
Recommended Sensors	Consider sensors listed in Table 3-5	Consider sensors listed in Table 3-5	Consider sensors listed in Table 3-5	Consider sensors listed in Table 3-7	Consider sensors listed in Table 3-7

6.1.3 Post-construction/Pre-Traffic

6.1.3.1 Conclusions

After construction, but before traffic applications begin, the instrumentation system should be assessed. Specifically, sensors should be identified that are no longer functioning, off scale, or behaving erratically. This can be accomplished by examining baseline (unloaded) traces and comparing them against what was observed during pre-installation. Significant changes should be noted so that erroneous data do not enter the project database. Sensors that are off scale can often be brought on-line by adding resistance on the circuit without compromising measurement capabilities.

6.1.3.2 Recommendations

Within gauge precision can be determined in a straightforward manner by applying the same stimulus over a short period of time. It is recommended that this testing be done under representative conditions (e.g., middle of the expected temperature range). Take,

for example, a deflection sensor to measure vertical displacement at the top of a base layer. The gauge precision can be determined by dropping a known load at the gauge location multiple times and determining the gauge response standard deviation. This value can be used when further precision testing is done later in the experiment to determine if a gauge is still working properly.

6.1.4 Under Traffic

6.1.4.1 Conclusions

Sensor accuracy is the foremost concern once a project is under traffic. It is critical that pre-traffic activities be executed as one component of sensor accuracy assurance. This will save time and resources by ensuring that only functioning sensors are included in the accuracy assessment.

6.1.4.2 Recommendations

Consistency in data collection should be maintained throughout a given experiment to enable maximum automation in data post-processing.

6.1.5 Data Processing and Analysis

6.1.5.1 Conclusions

The two most important data processing concepts are to link the data processing scheme to the experimental objectives and to develop the definition of dynamic pavement response for the given experiment. From these two ideas flows the data processing scheme for a given experiment. Every new experiment will require a customized data processing scheme. No one universal scheme will fit every possible testing scenario. Finally, from a data collection standpoint, it is important to realize that not all the data that has been collected necessarily requires processing.

A visually-based interactive processing scheme was developed that determined strain amplitude under repetitive loading. The data processing concepts were implemented in DSDiSP® but could be applied in most signal processing software. The processing scheme was shown to be robust, handling a variety of complex strain cases, while enabling the processor to visually check the quality of the data.

When conducting a theoretical versus measured response study, it is important to realize the limitations of both approaches, i.e., “truth” is not necessarily perfectly represented by either due to their respective limitations. Therefore, a practical course of action is to use theoretical modeling to check the direct measurement and vice versa. Reasonable agreement between the two approaches increases confidence in the data in a given experiment. On a longer-term basis, through this recursive process, better theoretical models and direct measurement devices can be developed.

6.1.5.2 Recommendations

The data processing scheme developed for a particular experiment should be linked to the specific objectives of that experiment. Every new experiment will require a unique data processing scheme. No one scheme that fits all experimental plans can be developed.

It is important to have researchers carefully review a sample of raw data prior to developing a data processing scheme. It is important to emphasize that not all data collected must be post-processed. Rather, the research team should collect sufficient data from which a sample can be post-processed to describe the experiment

Sensor accuracy can be evaluated relative to theoretical models. After reviewing a large number of studies, it appears that reasonable agreement between measured and theoretical responses is on the order of ± 20 percent.

7 REFERENCES

Almohn, Izzaldin M., Zhongjie Zhang, and Murad Abu-Farsahk. 2005. "Pressure Distributions Within Different Embankment Materials Under Traffic Loading," 2005 Annual Meeting CD, Transportation Research Board, National Research Council, Washington, DC.

Al-Qadi, Imad L. and Marwa M. Hassan, and Mostafa A. Esleifi. 2005. "Field and Theoretical Evaluation of Thermal Fatigue Cracking in Flexible Pavements," *Transportation Research Record: Journal of The Transportation Research Board, No. 1919,* Transportation Research Board, National Research Council, Washington, DC.

Aston University. 2006. "Fiber Bragg Grating Sensing," www.ee.aston.ac.uk/research/prg/fbg-sensing.html, accessed April 27, 2006.

Barker, W. R., and Gonzales, C. R. (1991). "Pavement Design by Elastic Layer Method," *Aircraft/Pavement Interaction, An Integrated System*, P. T. Foxworthy, Ed., American Society of Civil Engineers, New York, NY.

Boussinesq, J. 1885. Application des potentiels à l'étude de l'équilibre et du mouvement des solides élastiques, Gauthier-Villars, Paris, France.

Burmister, D. M. 1943. "The Theory of Stresses and Displacements in Layered Systems and Application to the Design of Airport Runways," *Proceedings, Highway Research Board*.

Burnham, Thomas R. 1999. "Concrete Embedment Strain Sensors at the Mn/ROAD Project: As-Built Orientation and Retrofit," Accelerated Pavement Testing 1999 International Conference, Reno, NV, October 18-20, 1999.

Burnham, Thomas R. 2006. Personal e-mail correspondence, November 30, 2006.

Campbell-Scientific. 2004. *Model 108 Temperature Probe Instruction Manual*.

Campbell-Scientific. 2006. *CS616 and CS625 Water Content Reflectometers Instruction Manual*.

Christenson, Donald W. 2004. *Revised Interim Report: Top-Down Fatigue Cracking of Hot-Mix Asphalt Layers – Phase 1*, NCHRP Report 1-42, Transportation Research Board, National Research Council.

Epps, J.A., A. Hand, S. Seeds, T. Schulz, S. Alavi, C. Ashmore, C.L. Monismith, J.A. Deacon, J.T. Harvey, R. Leahy, 2002. *Recommended Performance-Related Specification*

for Hot-Mix Asphalt Construction: Results of the Westrack Project, NCHRP Report 455, Transportation Research Board, National Research Council.

Freeman, Reed B., H. Tommy Carr, Tom McEwen, and R. Buzz Powell. 2001. *Instrumentation at the National Center for Asphalt Technology Test Track*, ERDC TR-01-9, Engineer Research and Development Center, Vicksburg, MS.

Garg, Naveet and Gordon F. Hayhoe. 2001. "Asphalt Concrete Strain Responses at High Loads and Low Speeds at the National Airport Pavement Test Facility," *Advancing Airfield Pavements, Proceedings of the 2001 Airfield Pavement Specialty Conference*, American Society of Civil Engineers.

Geokon, "Instrumentation Manual Model 3500/3510 Earth Pressure Cells," 2004.

Ghanderhari, Masoud and Cristain Vimer. 2005. "In-Situ Monitoring of Moisture in Pavement Materials," 2005 Annual Meeting CD, Transportation Research Board, National Research Council, Washington, DC.

Harvey, J. L. Du Plesis, and J. Roesler. 2004. "Accelerated Pavement Testing on Concrete Pavements: A Review of Some Lessons Learned," Second International Conference on Accelerated Pavement Testing.

Hilderbrand, Gregers. 2002. V*erification of Flexible Pavement Response for a Field Test*, Report 121, Danish Road Institute, Roskilde, Denmark.

Hornyak, N., J.A. Crovetti, D.E. Newman and J. Schabelski. 2007. "Asphalt Pavement Instrumentations: The Quest for Truth," Transportation Research Board PrePrint CD.

Huang, Y.H., *Pavement Analysis and Design*, Prentice-Hall, Inc., 1993.

Hudson, W. Ronald and Ronald P. White. 2003. *Draft Manuals and Procedures for MLS Data Collection and Equipment Operation Including Plans for MLS Shakedown Test,* Report No. FHWA/TX/05/5-1924-01-1, Center for Transportation Research, University of Texas at Austin, Austin, TX.

Hugo, Frederick and Amy Epps Martin. 2004. *NCHRP Synthesis 325: Significant Findings from Full-Scale Accelerated Pavement Testing*, Transportation Research Board, Washington, DC.

Hussain, Mustaque and Zhong Wu. 2003. *Pilot Instrumentation of A Superpave Test Section at the Kansas Accelerated Testing Laboratory*, Report K-TRAN:KSU-98-2, Kansas State University, Manhattan, Kansas.

Janoo, Vincent, Lynne Irwin, Krut Knuth, Andrew Dawson, Robert Eaton. 1999. "Use of Inductive Coils to Measure Dynamic and Permanent Pavement Strains," Accelerated Pavement Testing 1999 International Conference, Reno, NV, October 18-20, 1999.

Jeong, Jin-Hoon and Dan G. Zollenger. 2004. "Insights on Early-Age Curling and Warping Behavior from a Fully Instrumented Test Slab System," 2004 Annual Meeting CD, Transportation Research Board, National Research Council, Washington, DC.

Khazanovich, L. and Ioannides, A.M. (1995). "DIPLOMAT: an Analysis Program for Both Bituminous and Concrete Pavements," *Transportation Research Record No. 1482*, Transportation Research Board, National Research Council, Washington, pp. 62-60.

Kopperman, S., Tiller, G., and Tseng, M. (1989). "*ELSYM5, Interactive Microcomputer Version, Users Manual*," Report FHWA-RD-89-143.

Loulizi, Amara, Imad L. Al-Qadi, Samer Lahouar, and Thomas E. Freeman. 2001. "Data Collection and Management of Instrumented Smart Road Flexible Pavement Stections," *Transportation Research Record 1769*, Transportation Research Board, National Research Council, Washington, DC.

Losberg, A. 1960. "Structurally Reinforced Concrete Pavements," Doktorsavhandlingar Vid Chalmers Tekniska Högskola, Götegorg, Sweden.

Mateos, Angel and Mark B. Snyder. 2002. "Validation of Flexible Pavement Structural Response Models Using Mn/ROAD Data," Assessing *and Evaluating Pavements, Transportation Research Record No. 1806*. Transportation Research Board, National Research Council, Washington, DC.

Metcalf, John F. 1996. *NCHRP Synthesis of Highway Practice 235: Application of Full-Scale Accelerated Pavement Testing*, Transportation Research Board, National Research Council, Washington, D.C.

Michelow, J. 1963. "Analysis of Stresses and Displacements in an N-Layered Elastic System Under a Load Uniformly Distributed in a Circular Area," California Research Corporation, Richmond, CA.

Nam, Jeong-Hee, Seong-Min Kim, and Moon C. Won. 2006. "Measurement and Analysis of Early-Age Concrete Strains and Stresses in Continuously Reinforced Concrete Pavement under Environmental Loading," 2006 Annual Meeting CD, Transportation Research Board, National Research Council, Washington, DC.

Nassar, Walid. 2001. *Utilization of Instrument Response of SuperPave Mixes at the Virginia Smart Road to Calibarate Laboratory Developed Fatigue Equations*, Ph.D. Dissertation, Virginia Polytechnic Institute and State University, Blacksburg, VA.

Peutz, M. G. F, Van Kempen, H. P. M, and Jones, A. 1968. "Layered Systems under Normal Surface Loads," *Highway Research Record No. 228*, Highway Research Board, National Research Council, Washington, pp. 34-45.

Priest, A.L. 2005. "Calibration of Fatigue Transfer Functions for Mechanistic-Empirical Flexible Pavement Design," M.S. Thesis, Auburn University, Auburn, AL.

Rainwater, N. Randy, Wesley C. Wright, Eric C. Drumm, Gan Zou, and Ronald E. Yoder. 2006. "Evaluation of Instrumentation for Monitoring Seasonal Variations in Pavement Subgrade Water Content," 2006 Annual Meeting CD, Transportation Research Board, National Research Council, Washington, DC.

Rao, Shreenath and Jeffery R. Roesler. 2005. "Characterizing Effective Built-in Curling from Concrete Pavement Field Measurements," *Journal of Transportation Engineering,* Volume 131, Number 4, April 2005, pp. 320-327, American Society of Civil Engineers.

Romanoschi, Stefan A., Mustaque Hossain, Andrew Gisi, and Michael Heitzman. 2004. "Accelerated Pavement Testing Evaluation of the Structural Contribution of Full-Depth Reclamation of Material Stabilized with Foamed Asphalt," *Transportation Research Record: Journal of The Transportation Research Board, No. 1896*, Transportation Research Board, National Research Council, Washington, DC. Pp 199-207.

Saeed, Athar, Jim W. Hall, Jr. and Michael I. Hammons. 2000. *Whitetopping Instrumentation and Strain Response Analysis for the Savannah-Hardin County Airport Runway Rehabilitation*, ARA-TR-00-0095-1, Applied Research Associates, Vicksburg, MS.

Saeed, A. and J. W. Hall, Jr. 2003. *NCHRP Report 512: Accelerated Pavement Testing: Data Guidelines*, Transportation Research Board, National Research Council, Washington, DC.

Sargand, Shad. 1994. *Development of an Instrumentation Plan for the Ohio SPS Test Pavement (DEL-23-17.48.* Report No. FHWA/OH-94/019, Ohio University, Athens, OH.

Seeds, Stephen B. 2003. "Flexible Pavement Design Summary of the State of the Art." *Transportation in the New Millennium*. Transportation Research Board, National Research Council, Washington, DC.

Sheehan, Matthew J., Scott M. Tarr, and Shiraz Tayabji. (2004). *Instrumentation and Field Testing of Thin Whitetopping Pavement in Colorado and Revision of the Existing Colorado Whitetopping Procedure*, Report No. CDOT-DTD-R-2004-12, Colorado Department of Transportation.

Selig, Ernest T., Jian Zhang, and Willem Ebersohn. (1997). "Evaluation of Dynamic Earth Pressure Cells for Subgrade," *Transportation Research Record No. 1596,* Transportation Research Board, National Research Council, Washington, DC.

Sharp, Stephen R., Devin R. Cooper, Gerardo G. Clemena, and Mohamed K. Elfino. 2005. "Fiber Optic-Based Strain Sensor for Asphalt Pavements," 2005 Annual Meeting CD, Transportation Research Board, National Research Council, Washington, DC.

Steyn, Wjvdm, L du Plessis, and E Denneman. 2006. *Technical Memorandum: Instrumentation for APT and LTPP*. Contract Report CSIR/BE/IE/ER/2006/001/B, CSIR Built Environment, Pretoria, South Africa.

Sowacs.com (2006). *TDR (Time Domain Reflectometers): how they work, some literature on them, where to get them and how much they cost,* http://www.sowacs.com/sensors/tdr.html, accessed April 11, 2006.

Tabatabaee, Nadar, Peter Sebaaly. 1990. "State-of-the-Art Pavement Instrumentation," *Transportation Research Record 1260*, Transportation Research Board, National Research Council, Washington, DC.

Tabatabaee, Nadar, Imad L. Al-Qadi, and Peter B. Sebaaly. 1992. "Field Evaluation of Pavement Instrumentation Methods," *Journal of Testing and Evaluation*, Vol. 20, No. 2, March 1992, pp. 144-151.

Tia, Mang, Reynald Roque and Okan Sirin. 2001. *Evaluation of Superpave and Modified Superpave Mixtures by Means of Accelerated Pavement Testing (Planning and Design Phase),* Department of Civil and Coastal Engineering, University of Florida, Gainesville, FL.

Timm, D. H. and D.E. Newcomb. 2003. "Calibration of Flexible Pavement Performance Equations for Minnesota Road Research Project," *Transportation Research Record No. 1853, Pavement Management and Rigid and Flexible Pavement Design*, Transportation Research Board, National Research Council, Washington, DC.

Timm, David, Angela Priest, and Thomas V. McEwen. 2004. *Design and Instrumentation of the Structural Pavement Experiment at the NCAT Test Track*, NCAT Report 04-01, Auburn University, Auburn, AL.

Van Cauwelaert, F. J., Alexander, D. R., White, T. D, and Barker, W. R. (1989). "Multilayer Elastic Program for Backcalculating Layer Moduli in Pavement Evaluation," *Nondestructive Testing of Pavements and Backcalculation of Moduli*, ASTM STP 1026, Albert J. Bush, III and Gilbert Y. Baladi, Eds., American Society for Testing and Materials, Philadelphia, PA.

Vijayanath, Bhuvangiri K., Zhong Wu, Mustaque Hossain, Andrew J. Gisi. 1999. *Instrumentation of the Superpave Test Sections at the Kansas Accelerated Testing Laboratory*, International Conference on Accelerated Pavement Testing, Reno, Nevada, October 18-20, 1999.

Wang, J., B. Birgisson, and R. Roque. 2007. "Development of a Windows-Based Top-Down Cracking Design Tool for Florida Based on the Energy Ratio Concept," Transportation Research Board 86th Annual Meeting Compendium of Papers on CD-ROM, Transportation Research Board, National Research Council, Washington, DC.

Westergaard, H. M. 1926. “Stresses in Concrete Pavements Computed by Theoretical Analysis,” *Public Roads*, Vol. 7, No. 2, pp. 25-35.

Wright, W.C., R. E. Yoder, N.R. Rainwater, and E. C Drumm. 2001. “Calibration of Five-Segment Time Domain Reflectometry Probes for Water Content Measurement in High Density Materials,” *Geotechnical Testing Journal*, Vol. 24, No. 2, June 2001, pp. 172-184.

Wu, Chung-Lung, and Matthew J. Sheehan. 2002. “Testing and Performance Evaluation of Ultrathin Whitetopping Pavements at Spirit of St. Louis Airport.” *Design and Rehabilitation of Pavements, Transportation Research Record 1809*, Transportation Research Board, National Research Council, Washington, DC.

APPENDIX A: FL1 Code

```
FL1(a,Channel)
{
        /*This subroutine determines minimum and maximum values over entire strain trace*/
         /*a = window you want to evaluate*/

        /*Clear W8 and W7*/

        clear(w8,w7);

        /*Find the total length of the series*/
        NT=length(W1);

        /*Find the length of the cut window*/
        N = length(cut(a));

        /*Find the left most data point in window*/
        XLeft = getxl(a);

        /*Convert data point to index*/
        IndexLeft = XTOIDX(a,XLeft);

        /*Determine the number of loads that will be evaluated*/
        NLoads = int(NT/N);

        /*concat(curr, ravel({NT},{N},{XLeft},{IndexLeft}, {NLoads}));*/

        /*Build the Max and Min Table*/
        for(j=0; j<NLoads; j++)
        {
                /*Set current left index*/
                CurrLeft = IndexLeft + j*N;

                /*Find Maximum Value*/
                CurrMax = max(extract(col(a,Channel),CurrLeft,N));

                /*Find Minimum Value*/
                CurrMin = min(extract(col(a,Channel),CurrLeft,N));

                /*Find XIndex for Maximum Value*/
                MaxIndex = CurrLeft+MAXIDX(extract(col(a,Channel),CurrLeft,N));

                /*Find XIndex for Minimum Value*/
                MinIndex = CurrLeft+MINIDX(extract(col(a,Channel),CurrLeft,N));

                /*Find Strain Amplitude*/
                CurrAmp = CurrMax - CurrMin;

                concat(curr, ravel({MaxIndex},{MinIndex},{CurrMax},{CurrMin},{CurrAmp}));

        }
        w8:setcolheader("MaxIndex", 1);
        w8:setcolheader("MinIndex",2);
        w8:setcolheader("Maximum",3);
        w8:setcolheader("Minimum",4);
        w8:setcolheader("Amplitude",5);

        /*w7:yvals(w2);*/
        SETVARIABLE(dummy, channel);
        w7:col(w2,dummy);
        w7:overplot(xy(col(W8,1),col(W8,3)),green);
        w7:overplot(xy(col(W8,2),col(W8,4)),black);
        SETPLOTSTYLE(w7, 0);


}
```

APPENDIX B: FL2 Code

```
                                        FL2(Gauge,Reps)
{
        MinValue = min(col(w8,5));
        MeanValue = mean(col(w8,5));
        MaxValue = max(col(w8,5));
        StdevValue = STDEV(col(w8,5));
        concat(curr,
ravel({Reps},{Gauge},{MinValue},{MeanValue},{MaxValue},{StdevValue}));

        w4:setcolheader("Reps", 1);
        w4:setcolheader("Gauge", 2);
        w4:setcolheader("Minimum", 3);
        w4:setcolheader("Mean",4);
        w4:setcolheader("Maximum",5);
        w4:setcolheader("Stdev",6);
}
```